CONTROL OF THE QUASI-STEADY STATE

IN FED-BATCH FERMENTATION

by

Nicolas Kalogerakis

A thesis submitted to the

Faculty of Graduate Studies and Research

of McGill University

in partial fulfillment of the requirements for the

degree of Master of Engineering

Thesis supervisor: Prof. T.J. Boyle

Department of Chemical Engineering
McGill University
Montreal, Quebec

August 1979

ABSTRACT

Theoretical analysis and simulation runs have shown that fed-batch cultures can reach a quasi-steady state (QSS) where cell and substrate concentrations are constant as total volume increases. A control system, realized on the Interdata 7/16 minicomputer, driven by PROCON software package, has been used to force the system to different QSS operating points rapidly, measuring only cell concentration. Experiments have shown:

- Cell concentration transient response was reduced from approximately 25 hours to 2 1/2 hours, making possible observation of different QSS's in a single run, agreeing relatively well with computer simulation runs.
- The control system was found able to compensate rapidly different types of disturbances which excited cell concentration.
- The nonlinearities of the system were experimentally verified.
- Only limited data were obtained on glucose transients, not all in agreement with theory.
- Yields of 50 to 60% were obtained even at high substrate concentrations.

SOMMAIRE

L'analyse théorique et les essais de simulation ont démontré que les cultures en semi-continu peuvent atteindre un état de quasi-stabilité (QSS = Quasi-Steady State), lorsque les concentrations de cellules et de substrat restent constantes au fur et à mesure que le volume global augmente. Nous avons utilisé un système de contrôle réalisé sur mini-ordinateur Interdata 7/16 par un ensemble de logiciel PROCON afin de pousser le système rapidement vers divers points de fonctionnement en QSS, en mesurant uniquement la concentration cellulaire. Les résultats des expériences furent les suivants:

- La réponse transitoire de la concentration cellulaire a été ramenée d'environ 25 heures à 2.5 heures, permettant ainsi d'observer plusieurs QSS au cours d'une seule campagne de culture, la correspondance aux essais de simulation sur ordinateur étant relativement bonne.
- Le système de contrôle s'est révélé capable de compenser rapidement divers types de perturbations qui étaient venus exciter la concentration cellulaire.
- Les non linéarités du système ont été vérifiées expérimentalement.
- Les données obtenues sur les transitoires de glucose sont limitées et ne correspondent pas toutes aux données théoriques.
- Nous avons obtenu des rendements de 50 à 60% même aux concentrations de substrat élevées.

ACKNOWLEDGEMENTS

The author wishes to express his sincere appreciation and gratitude to:

Professor T.J. Boyle, supervisor of this project, for his valuable advice, guidance, support and encouragement throughout all facets of this work;

Professor B. Volesky, for kindly providing most of the utilized equipment;

The other staff members and fellow graduate students who have aided either directly or indirectly in the completion of this work;

Mrs. Linda Walter for typing this thesis in a very short time.

Last, but not least, I wish to thank my parents for their financial support and incessant encouragement.

TABLE OF CONTENTS

LIST OF FIGURES

LIST OF TABLES

NOTATION

a	$(\frac{\partial \sigma}{\partial s})_{QSS}$
b	$(\frac{\partial \mu}{\partial s})_{QSS}$
D	dilution factor, hr^{-1}
F	total feedrate to the fermentor, l/hr
F_A	flowrate of feed-A, l/hr
F_B	flowrate of feed-B, l/hr
F_W	water flowrate, l/hr
k_c	controller gain
k_1	kinetic parameter in Monod eq., hr^{-1}
k_2	kinetic parameter in Monod eq., g/l
m	maintenance energy coefficient, g sugar/g cells/hr
r_x	growth rate, $\frac{d\,x}{dt}$, g/hrl
r_s	uptake rate, $\frac{d\,s}{dt}$, g/hrl
s	substrate concentration in the fermentor, g/l
s_D	desired substrate concentration, g/l
S	total substrate fed to the fermentor, g
sl	substrate concentration in the feed, g/l
s_A	substrate concentration of the feed F_A, g/l
t	time, hr

V_L	volume of the liquid phase in the fermentor, l
x	cell concentration in the fermentor, g/l
x_D	desired cell concentration, g/l
X	total cells in the fermentor, g
Y	overall yield, g cells/g sugar
Y_a	true yield coefficient, g cells/g sugar

Greek Letters

μ	specific growth rate, hr^{-1}
σ	specific uptake rate, hr^{-1}
$\hat{\sigma}$	desired specific uptake rate, hr^{-1}
λ	eigenvalues of the linearized model
τ	time constants of the linearized model
ρ	density

Superscripts

-	the value of the variable at QSS
*	reduced quantities, $M/\bar{M}$

Subscripts

0	value of the variable at time t = 0
MIN	minimum value of the variable
MAX	maximum value of the variable

CHAPTER 1: INTRODUCTION

During the past century fed-batch culture (the Zulauf process) has been employed by the baker's yeast industry as it permits production of yeast biomass without simultaneous production of sizable quantities of ethanol. Fed-batch culture refers to a batch culture which is fed continuously with nutrient medium. The volume variation in a fed-batch culture distinguishes it from chemostat continuous flow culture where equal inlet and outlet volumetric flowrates maintain the culture volume constant. In batch culture the yield of yeast, based on the amount of available fermentable sugar, is low, often not more than 15%, while in fed-batch culture a yield of up to 60% can be obtained under appropriate growth conditions. The production of ethanol may occur where there is oxygen starvation (Pasteur effect) or high sugar concentration (Crabtree effect). The latter characterizes batch cultures where sugar concentration is high most of the fermentation time, resulting in a low overall yeild.

The term fed-batch culture was first used by Yoshida et al [22] (1973) who tried fed-batch culture of Candida tropicalis using n-hexadecane as the only carbon source. In 1970, Edwards et al [11] introduced the extended culture, a fed-batch culture in which the limiting substrate concentrations are kept constant by proper feed rate and feed composition control, using as measured variable the concentration of the limiting substrate in the fermentor.

A few years later various investigators, (Pirt [17], 1974) presented arguments to show that when the specific growth rate of organisms follows that of a Monod type, a fed-batch culture may reach a quasi-steady state (QSS) which is defined as the state where cell and substrate concentrations remain constant as the total volume of the liquid phase increases. The feeding schedule in a fed-batch culture under which both concentrations are kept constant is called QSS-fed-batch culture.

Dunn and Mor [10] (1975) developed equations which describe variable-volume cultivation, with emphasis on constantly fed semicontinuous cultures, and drew the analogy between the QSS in variable volume cultivation and a dynamic steady state in variable flow constant-volume chemostat bioreactors. Recently, Lim et al [14] (1977) showed that under certain conditions an extended culture is equivalent to an exponentially fed-batch culture and that an exponentially fed-batch culture may be mimicked by a continuous-flow culture with a constant dilution rate. Furthermore, they investigated operational conditions under which an exponentially fed-batch culture and an extended culture may be reduced to a QSS-fed-batch culture. However, due to the dynamic characteristics of the process the rate of approach to QSS, as recently examined by Boyle [4] (1978) is very slow, requiring a very large volume expansion such as to preclude observation of the QSS, at least in a laboratory fermentor. QSS-fed-batch cultures therefore, cannot be realized without a control system which would force the process to reach QSS rapidly.

Aiba et al [1] (1976) proposed a computer control scheme for baker's yeast fed-batch cultivation with the primary goal being the maximization of the overall yield. This was done by eliminating the glucose effect through manipulation of the feed rate with an ad hoc measurement of the respiratory quotient which was controlled from 1.0 to 1.2. Towards the same goal, yield maximization, Wang et al [20] (1977) proposed a control system to monitory yeast growth, measuring cell concentration indirectly through material balancing from measurements of the O_2 uptake rate, CO_2 production rate, gas flow rate and ammonia addition rate.

Boyle [3],[4] (1978) proposed a simple control system designed to force the process to reach any feasible QSS operating point rapidly, where both cell and substrate concentrations are independently specified. This is done by manipulation of the dilution factor and the feed composition, using cell concentration as the only measured variable. The proposed control system enables operation of QSS-fed-batch cultures, may be utilized to obtain kinetic data, and can potentially be used towards yield maximization as the substrate concentrations can be controlled to any desired low level where ethanol production is practically zero. Moreover, the control system may be used for a reliable investigation of the effects on cell growth of sudden changes in dissolved oxygen, temperatures, pH as well as in substrate concentration.

The above control system was implemented in this work to evaluate how well a control system based on a very simple process model can perform the above mentioned functions. As the control system uses cell concentration as the only measured variable in controlling both cell and substrate concentrations, it is crucial to have a reliable cell concentration measurement. Although a continuous measurement was not available sampling was used to enable implementation of the control system. The evaluation of the control system provides sufficient information on cell concentration transients and indicates possible difficulties in substrate concentration control.

The objectives of this work are:

(1) Implementation of the proposed control system.

(2) Evaluation of its performance.

CHAPTER 2: THEORETICAL BACKGROUND

2.1 THE PROCESS

2.1.1 FED-BATCH CULTURE

The overall mass balance for the liquid phase in terms of volumetric flow, liquid densities and volume, assuming well mixed stirred tank bioreactor is:

$$\frac{d\,(V\rho)}{dt} = F\rho_i$$

Normally the density changes are small giving:

$$\frac{dV}{dt} = F \qquad (2\text{-}1)$$

The balance on biomass in the liquid phase gives:

$$\frac{d(xV)}{dt} = r_x V \qquad (2\text{-}2)$$

Assuming the usual growth rate kinetics

$$r_x = \mu x$$

where μ is the specific growth rate, equation (2-2) yields to:

$$x\frac{dV}{dt} + V\frac{dx}{dt} = \mu x V$$

combining with equation (2-1)

$$\frac{dx}{dt} = (\mu - \frac{F}{V}) x \qquad \text{or}$$

$$\frac{dx}{dt} = (\mu - D) x \qquad (2\text{-}3)$$

where D is the dilution factor, $\frac{F}{V}$.

The balance on the limiting substrate is:

$$\frac{d(Vs)}{dt} = Fsl - r_s V \qquad (2\text{-}4)$$

Assuming $r_s = \sigma x$, σ being the specific substrate uptake rate, the above equation gives:

$$s \frac{dV}{dt} + V \frac{ds}{dt} = Fsl - \sigma x V \qquad \text{or}$$

$$\frac{ds}{dt} = D (sl-s) - \sigma x \qquad (2\text{-}5)$$

Equations (2-1), (2-3) and (2-5) describe the dynamics of the fed-batch culture, provided that the dependency of μ and σ on the limiting substrate concentration and cell age distribution is known. The common assumption that under constantly kept environmental conditions σ and μ are dependent only on the limiting substrate concentration will be adopted from now on.

More specifically, μ is normally considered dependent on substrate concentration according to the Monod kinetic

relation:

$$\mu = \frac{k_1 s}{k_2 + s} \qquad (2\text{-}6)$$

The above equation implies that the specific growth rate reaches asymptotically its maximum value, k_1, as s increases.

The specific substrate uptake rate, σ, is considered to be related to the specific growth rate as follows:

$$\sigma = \frac{\mu}{Y} \qquad (2\text{-}7)$$

where Y is the overall yield coefficient. Since the limiting substrate is the energy source as well, part of it will be used to supply energy for the synthesis of biomass and part will be used for the maintenance of the biomass. This implies:

$$\sigma x V = \frac{\mu}{Y_G} x V + m x V \qquad (2\text{-}8)$$

where Y_G is the "true growth yield" and m is the "maintenance coefficient" [17]. Introducing the overall yield coefficient, equation (2-8) yields to:

$$\frac{1}{Y} = \frac{1}{Y_G} + \frac{m}{\mu} \qquad (2\text{-}9)$$

It should be noted here that the previous equations are not valid under all transient situations because the Monod equation has been found to apply only under steady or

slow changing conditions, that is, in a state where balanced growth will usually occur. Balanced growth conditions identify a biological state during which the intracellular metabolic reaction network is operating at essentially steady state conditions [10].

2.1.2 QUASI-STEADY STATE

The quasi-steady state, QSS, in fed-batch culture is defined as the state where the concentration of cells and limiting substrate remain constant with time while the volume of the liquid phase increases.

Setting $\frac{dx}{dt} = \frac{ds}{dt} = 0$, equations (2-3) and (2-5) give:

$$\mu = D \qquad (2\text{-}10)$$

$$x = \frac{\mu}{\sigma} (s1 - s) \qquad (2\text{-}11)$$

Since μ and σ are functions of s, equation (2-10) defines the value of s in the QSS and equation (2-11) defines the value of x given that of s. The physical constraints $s>0$ and $x>0$ yield to an upper limit for D so that a QSS can exist.

$$0 < D < \mu(s1) \qquad (2\text{-}12)$$

For dilution factor values higher than the upper limit, the reaction volume increases faster than the cell growth rate and the cell concentration drops towards zero. This is analogous to wash-out in a chemostat.

Equations (2-10) and (2-11) constitute two simultaneous nonlinear equations for the values of s and x in the QSS. Dilution factor, D, and substrate concentration in the feed, s1, constitute the external conditions which can be set. For any given pair of D and s1, a QSS operating point exists provided that the dilution factor obeys the previous constraint.

Assuming Monod type kinetics explicit formulas for x and s in the QSS can be obtained:

$$s = \frac{k_2}{\frac{k_1}{D} - 1} \qquad (2\text{-}13)$$

$$x = Y\left(s1 - \frac{k_2}{\frac{k_1}{D} - 1}\right) \qquad (2\text{-}14)$$

$$\frac{1}{Y} = \frac{1}{Y_G} + \frac{m}{D} \qquad (2\text{-}15)$$

with the range of D being:

$$0 < D < \frac{k_1 s1}{k_2 + s1}$$

Note that constant dilution factor implies exponential feeding:

$$\left.\begin{aligned} \frac{F}{V} &= D \\ \frac{dV}{dt} &= F \end{aligned}\right\} \rightarrow \frac{dF}{F} = D\,dt \rightarrow$$

$$F = F_o\, e^{Dt}$$

with F_o satisfying the initial condition $\frac{F_o}{V_o} = D$.

Following the previous analysis, the plausible question what the rate of approach to QSS is, arises. The following numerical examples give a good picture of the process dynamics. All the process parameters used in the simulation are shown in table (2-I).

TABLE 2-I

x_o	s_o	V_o	k_1	k_2	Y
6 g/l	.005 g/l	5 l	.30 hr^{-1}	.15 g/l	.50

TABLE 2-II

	x	s	D	s1
Qss (1)	6 g/l	.075 g/l	.1 hr^{-1}	12.075 g/l
QSS (2)	7 g/l	.075 g/l	.1 hr^{-1}	14.075 g/l

In fig. (2-1) the transient response of the process is shown to applied constant inputs D = .1 hr^{-1} and s1 = 12.075 g/l, corresponding to the QSS point given first in table (2-II). Substrate concentration moves up fast, slightly overpassing the final value (by 1.5%) and then drops very slowly to its equilibrium value. Cell concentration

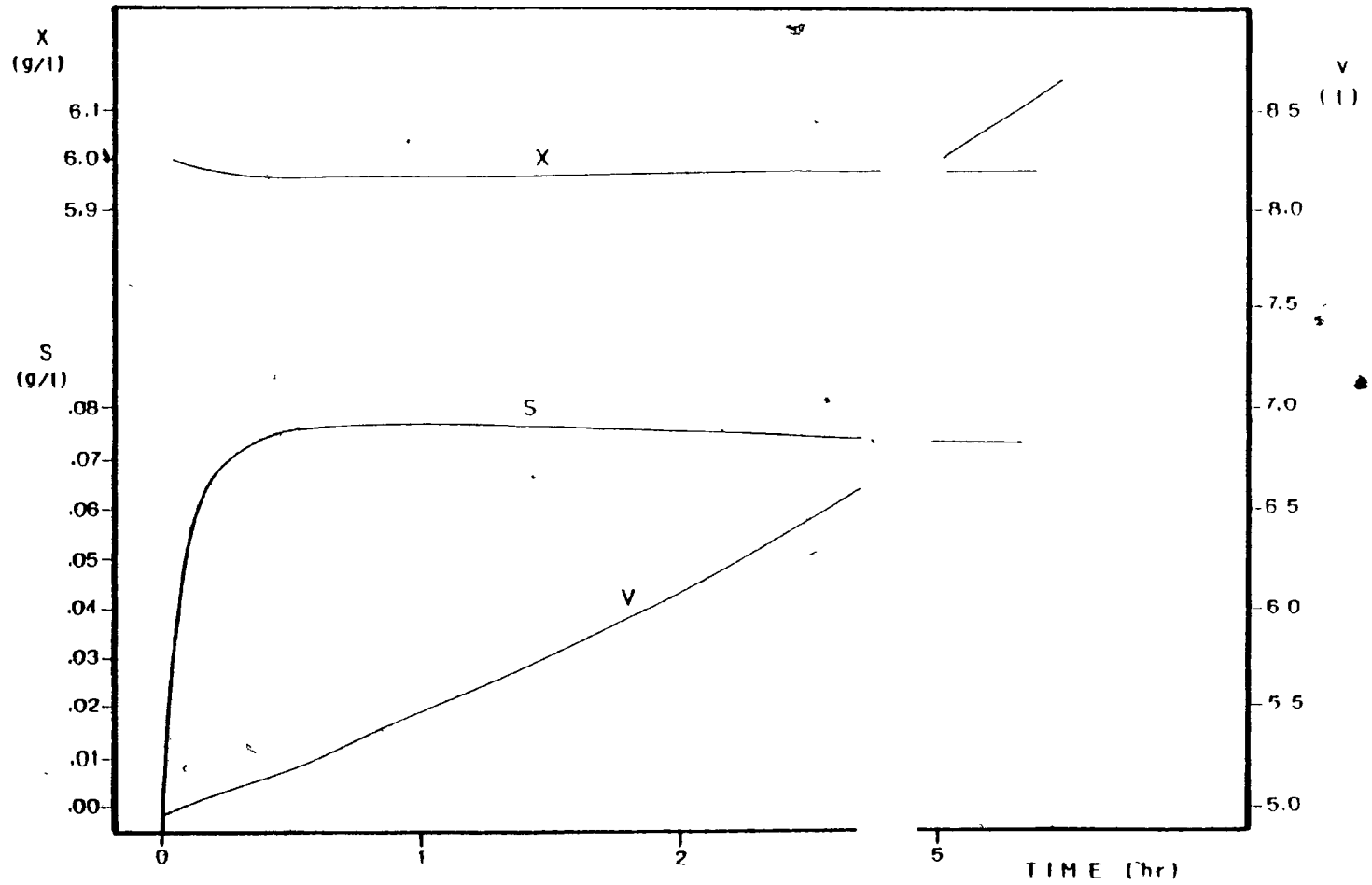

Fig. (2-1): Simulated transients of x,s,V versus time to applied constant inputs towards QSS (1) operating poing.

undergoes a slow but very small in magnitude transient. Practically, it can be said that QSS conditions are established rapidly. This method of establishing QSS is similar to that suggested by Dunn and Mor [10]. As will be shown, it does not provide a method for changing the QSS point or off-setting disturbances which will induce long slow transients in the uncontrolled system. Next, while D^1 is kept at .1 hr^{-1}, s1 is increased from 12.075 to 14.075 g/l. The system is expected to move to the QSS given second in table (2-II). Here, as shown in fig. (2-2), the total response takes over 30 hours to reach equilibrium. It is also seen that there is a strong interaction between x and s, although the change in the process conditions intended to change cell concentration only and leave substrate concentration constant. The latter rises rapidly to a peak and then drops towards its equilibrium value with the same slow rate as the cell concentration response.

In fig. (2-2) the volume increase is shown as well. Apparently such a large volume expansion cannot be handled in practice, and since the transients in fig. (2-2) more fairly represent what would occur in a laboratory, observation of the QSS is not feasible without a control system.

In addition to the numerical examples, information can be retrieved from the linear incremental model

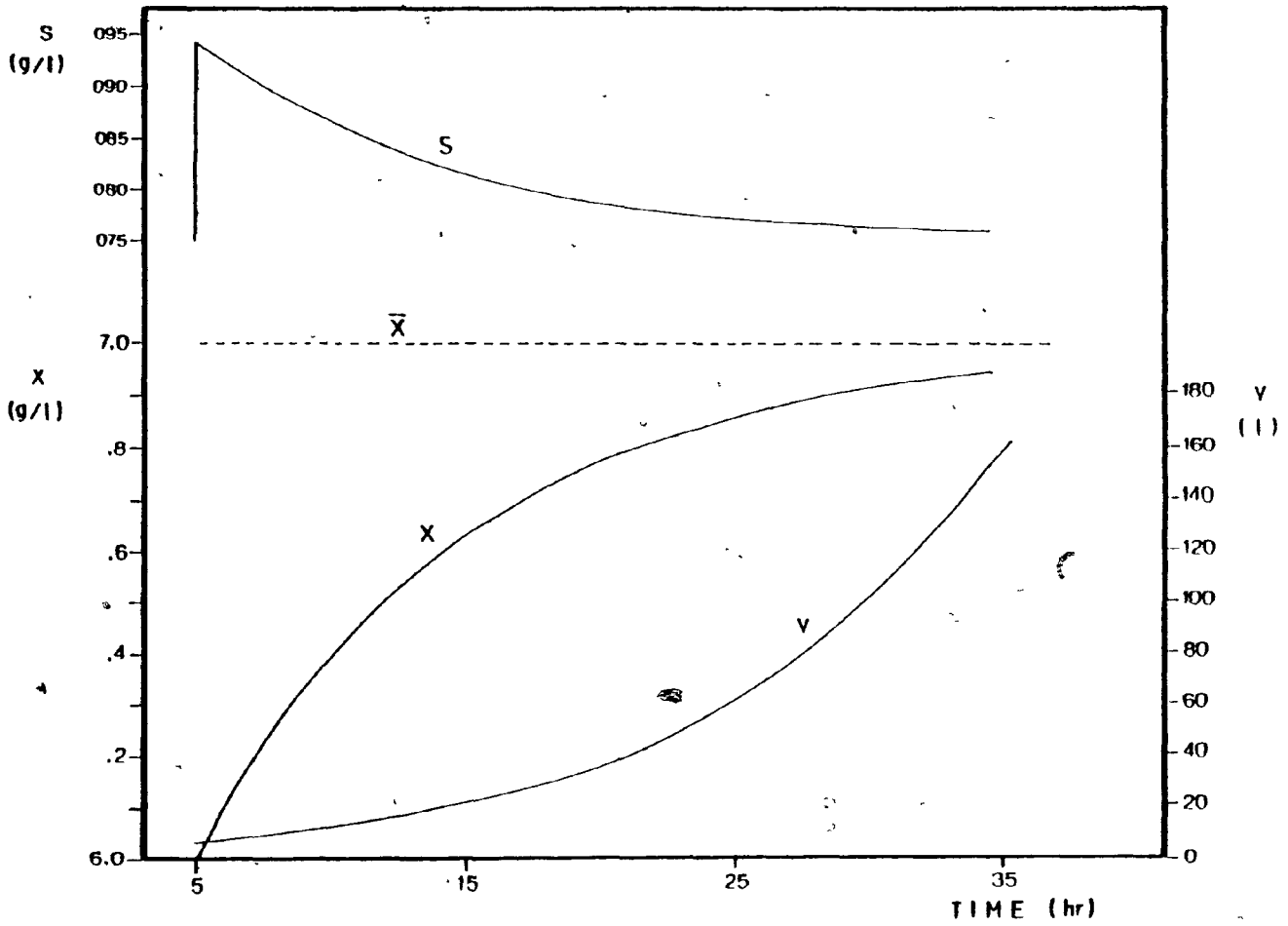

Fig. (2-2): Simulated transients of x,s,V versus time to applied constant inputs towards QSS (2) operating point.

linearizing about a QSS operating point [4].

Introducing reduced variables:

$$s^* = \frac{s - \bar{s}}{\bar{s}} \qquad x^* = \frac{x - \bar{x}}{\bar{x}}$$

$$s1^* = \frac{s1 - \overline{s1}}{\overline{s1}} \qquad D^* = \frac{D - \bar{D}}{\bar{D}}$$

and the parameters

$$a = \left(\frac{\partial \sigma}{\partial s}\right)_{QSS} \qquad b = \left(\frac{\partial \mu}{\partial s}\right)_{QSS}$$

the linear model is

$$\frac{dx^*}{dt} = b\bar{s}s^* - \bar{D}\,D^*$$

$$\frac{ds^*}{dt} = -(\bar{D} + a\bar{x})\,s^* - \frac{\bar{D}(\overline{s1} - \bar{s})}{\bar{s}}\,x^* + \frac{\bar{D}(\overline{s1} - s)}{\bar{s}}\,D^* + \frac{\bar{D}\,\overline{s1}}{\bar{s}}\,s1^*$$

Assuming constant yield, $\frac{b}{a} = \frac{\bar{\mu}}{\bar{\sigma}} = Y$, the above equations can be written in a matrix form as:

$$\begin{bmatrix} \frac{ds^*}{dt} \\ \frac{dx^*}{dt} \end{bmatrix} = \begin{bmatrix} -(\bar{D} + a\bar{x}) & -\frac{\overline{Dx}}{Y\bar{s}} \\ aY\bar{s} & 0 \end{bmatrix} \begin{bmatrix} s^* \\ x^* \end{bmatrix} + \begin{bmatrix} \frac{\overline{Dx}}{Y\bar{s}} & \frac{\bar{D}\,\overline{s1}}{\bar{s}} \\ -\bar{D} & 0 \end{bmatrix} \begin{bmatrix} D^* \\ s1^* \end{bmatrix} \qquad (2\text{-}16)$$

or more compactly as,

$$\frac{d\,\underset{\sim}{z}}{dt} = \underset{\sim}{A}\,\underset{\sim}{z} + \underset{\sim}{B}\,\underset{\sim}{u}$$

Information concerning the rate of approach to QSS can be found from the eigenvalues of matrix A.

$$\lambda_1 = -\bar{D}$$
$$\lambda_2 = -a\,\bar{x}$$

The approach to equilibrium is by way of decaying exponentials having time constants the negative reciprocals of the eigenvalues.

$$\tau_1 = \frac{1}{\bar{D}}$$
$$\tau_2 = \frac{1}{a\,\bar{x}}$$

For the numerical case simulated previously, $\tau_1 = 10$ hours and $\tau_2 = .08$ hours. These are in agreement with the simulations since three or four time constants are required to reach equilibrium.

Information concerning the sustained change in the state variables s and x to applied sustained changes in D and s1 can be obtained from the influence coefficient matrix $-\underset{\sim}{A}^{-1}\,\underset{\sim}{B}$, which yields:

$$\begin{bmatrix} s^* \\ x^* \end{bmatrix} = \begin{bmatrix} \frac{\bar{D}}{a\ Y\ \bar{s}} & 0 \\ \frac{\bar{D}}{a\ \bar{x}} & -\frac{Y s\bar{l}}{\bar{x}} \end{bmatrix} \begin{bmatrix} D^* \\ sl^* \end{bmatrix} \qquad (2\text{-}17)$$

The only non-zero off diagonal element is quite small as seen in the numerical case

$$\begin{bmatrix} s^* \\ x^* \end{bmatrix} = \begin{bmatrix} 1.50 & 0 \\ .008 & -1.005 \end{bmatrix} \begin{bmatrix} D^* \\ sl^* \end{bmatrix}$$

which means that the system may be considered to be decoupled in terms of sustained changes, suggesting that the control strategy should use D to control s and sl to control x.

Further information can be obtained from the transient response of the system. Given an initial state s* (o) and x* (o) and constant inputs D* and sl*, the transient response can be described as:

$$\underset{\sim}{z}\ (t) = \underset{\sim}{\phi}(t)\ \underset{\sim}{z}\ (o) + \underset{\sim}{\Delta}(t)\ \underset{\sim}{\mu}$$

which gives:

$$\begin{bmatrix} s^*\ (t) \\ x^*\ (t) \end{bmatrix} = \frac{1}{1 - \frac{\bar{D}}{a\bar{x}}} \begin{bmatrix} e^{-a\bar{x}t} - \frac{\bar{D}}{a\bar{x}}\ e^{-\bar{D}t} & \frac{\bar{D}}{aY\bar{s}}\ (e^{-a\bar{x}t} - e^{-\bar{D}t}) \\ \frac{Y\bar{s}}{\bar{x}}\ (e^{-\bar{D}t} - e^{-a\bar{x}t}) & e^{-\bar{D}t} - \frac{\bar{D}}{a\bar{x}}\ e^{-a\bar{x}t} \end{bmatrix} \begin{bmatrix} s^*\ (o) \\ x^*\ (o) \end{bmatrix} +$$

$$+\begin{bmatrix} \frac{\bar{D}}{a\bar{Y}\bar{s}}\left(1 - e^{-a\bar{x}t}\right) & \frac{\bar{D}}{a\bar{x}}\left(e^{-\bar{D}t} - e^{-a\bar{x}t}\right) \\ -\frac{\bar{D}}{a\bar{x}}\left(1 - e^{-a\bar{x}t}\right) & \frac{\bar{Y}\bar{s}1}{a}\left(1 - \frac{1}{1 - \frac{\bar{D}}{a\bar{x}}}e^{-\bar{D}t} + \frac{\frac{\bar{D}}{a\bar{x}}}{1 - \frac{\bar{D}}{a\bar{x}}}e^{-a\bar{x}t}\right) \end{bmatrix}\begin{bmatrix} D^* \\ s1^* \end{bmatrix}$$

(2-18)

Since the first column of the matrix Δ contains exponential terms involving only the larger eigenvalue, the process will respond rapidly to changes in dilution factor which produces large changes in s but only very small changes in x, as shown by the influence coefficient matrix. Therefore, fast non-interacting control of substrate concentration can be easily achieved using dilution factor as the manipulated variable.

Similarly, since the second column of the matrix Δ contained exponential terms involving the smaller eigenvalue, the response of x and s to changes in s1 is long. More specifically, it is anticipated that a change in s1 will produce a long transient in s, but since the steady state gain is zero, the final value of s will not be affected by a sustained change in s1, as already indicated by the influence coefficient matrix. On the contrary, the final value of x to changes in s1 is strongly affected but the transient response, being dominated by the small eigenvalue, will be slow as well.

Examining each element of the matrix ϕ, the nature of transients in the uncontrolled system due to initial displacements from equilibrium can be seen. Two things are to be seen here. First, the induced transient displacement in s by a displacement in x is of substantial magnitude and long response time (element ϕ_{12}, $\frac{\bar{D}}{aY\bar{s}} = 1.5$ for the numerical case), and second, the very small in magnitude displacement in x, induced by a displacement in s (element ϕ_{21}, $\frac{Y\bar{s}}{\bar{x}} = .0050$).

Summarizing, the prior study of QSS and the system analysis which followed have led to the following assessments:

a. Quasi-steady states exist over a wide range of substrate and cell concentrations. Each pair of D and s1 corresponds to a QSS operating point.

b. The rate of approach to QSS is slow, requiring such a large volume expansion as to preclude the possibility of attaining the state.

c. Cell concentration transients are fast unless they are induced by cell concentration transients.

d. If a control system is to be designed, D should be used to control s, and s1 to control x.

e. Fast noninteractive control over substrate concentration can be achieved using dilution factor as the manipulated variable.

f. In the design of the cell concentration controller the

strong interaction between s and sl must be taken into account.

2.2 THE CONTROL SYSTEM

As indicated from the previous analysis, dilution factor, D, is used to control substrate concentration, s, and substrate concentration in the feed, sl, to control cell concentration, x.

Substrate concentration in the feed is manipulated utilizing the error in cell concentration:

$$sl = k_c (x_D - x) + \overline{sl} \qquad (2\text{-}19)$$

which is a simple proportional controller. x_D is the desired cell concentration, k_c is the controller gain and $\overline{sl}$ is the level of sl when the error is zero, namely, the required feed substrate concentration at the QSS.

Dilution factor, the second manipulated variable, is manipulated to keep substrate concentration constant. Since substrate concentration transients are fast, adequate control can be achieved providing only the "steady state" value of D at the current cell concentration. More specifically, setting $\frac{ds}{dt} = 0$ equation (2-3) leads to:

$$D = \frac{\sigma x}{sl - S} \qquad (2\text{-}20)$$

The above equation is not a feasible control law for D because the specific uptake rate, σ, is in general an unknown function of s, besides the fact that substrate concentration measurement is required. Therefore, the previous equation is used to suggest the following approximate control law for D.

$$D = \frac{\hat{\sigma} x}{s1 - s_D} \qquad (2\text{-}21)$$

where $\hat{\sigma}$, is an estimate of σ at the desired QSS operating point and s_D is the desired rather than actual substrate concentration in the fermentor.

Since σ is an unknown function of s, the desired substrate concentration s_D, may not correspond exactly to the selected $\hat{\sigma}$. As a result, since $s1 >> s_D$ which means that $D \approx \frac{\hat{\sigma} x}{s1}$, substrate concentration will be controlled at the corresponding s_D implied by the estimated $\hat{\sigma}$. In other words, the actual set points are cell concentration and specific substrate uptake rates.

Equations (2-19) and (2-21) represent the proposed control law for setting s1 and D. However, the range of variation must meet the following physical constraints:

$$0 \leq s1 \leq s1_{max} \qquad (2\text{-}22)$$

$$0 \leq F \leq F_{max} \qquad (2\text{-}23)$$

Since volume is growing during the fermentation, there is a time varying constraint on D:

$$D \leq \frac{F_{max}}{V} \qquad (2\text{-}24)$$

Besides that, since D and sl are inversely related according to equation (2-21), the upper bound on D implies a lower bound on sl:

$$sl_{min} \leq sl \leq sl_{max} \qquad (2\text{-}25)$$

where $sl_{min} = s_D + \frac{\hat{\sigma} x}{D_{max}}$

which can be written as:

$$sl_{min} = s_D + \frac{\hat{\sigma} x V}{F_{max}} \qquad (2\text{-}26)$$

Like the upper bound on D the lower bound on sl is variable and must be computed as part of the control computation.

The controller gain, k_c, the only adjustable parameter, is to be selected by trial and error. For $k_c = 250$ satisfactory results were obtained.

At this point the control system is described sufficiently to permit simulation of its performance. The process parameters

shown in table (2-I) are used in the following simulations.

In fig. (2-3) the transient response of the system is shown for a set point change of 1 g/l in cell concentration. The controlled process equilibrates again at the new QSS point (the second in table (2-II)) in about 2 hours. As shown in the graph, there is practically no change in substrate concentration. Noninteraction is achieved.

In fig. (2- 4) proceeding from the same initial state (the QSS point given first in table 2-II), the specific substrate uptake rate, $\hat{\sigma}$, is changed from .200 to .225 hr^{-1}. The system equilibrates very fast (note the time scale) to the new QSS point at a higher substrate concentration, implied by the higher uptake rate.

To complete the description of the simulation runs, figures (2-5) and (2-6) show the behaviour of the manipulated variables, D and s1, for the cell and substrate concentration transients respectively.

In both runs the volume expansion was not large, making the QSS accessible in a laboratory apparatus.

Summarizing, the proposed control system has the following features:

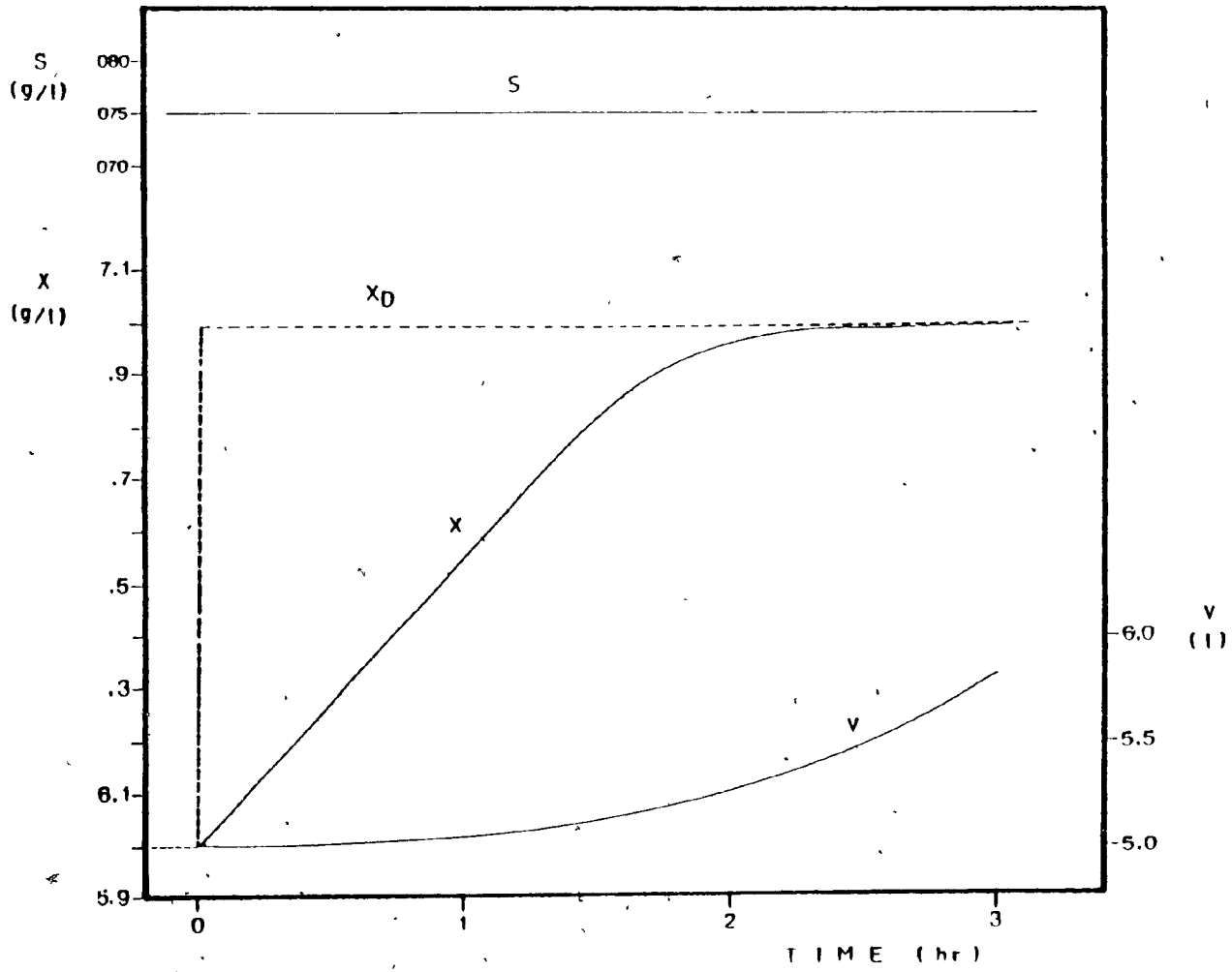

Fig. (2-3): Simulated closed loop response to step change in x_D.

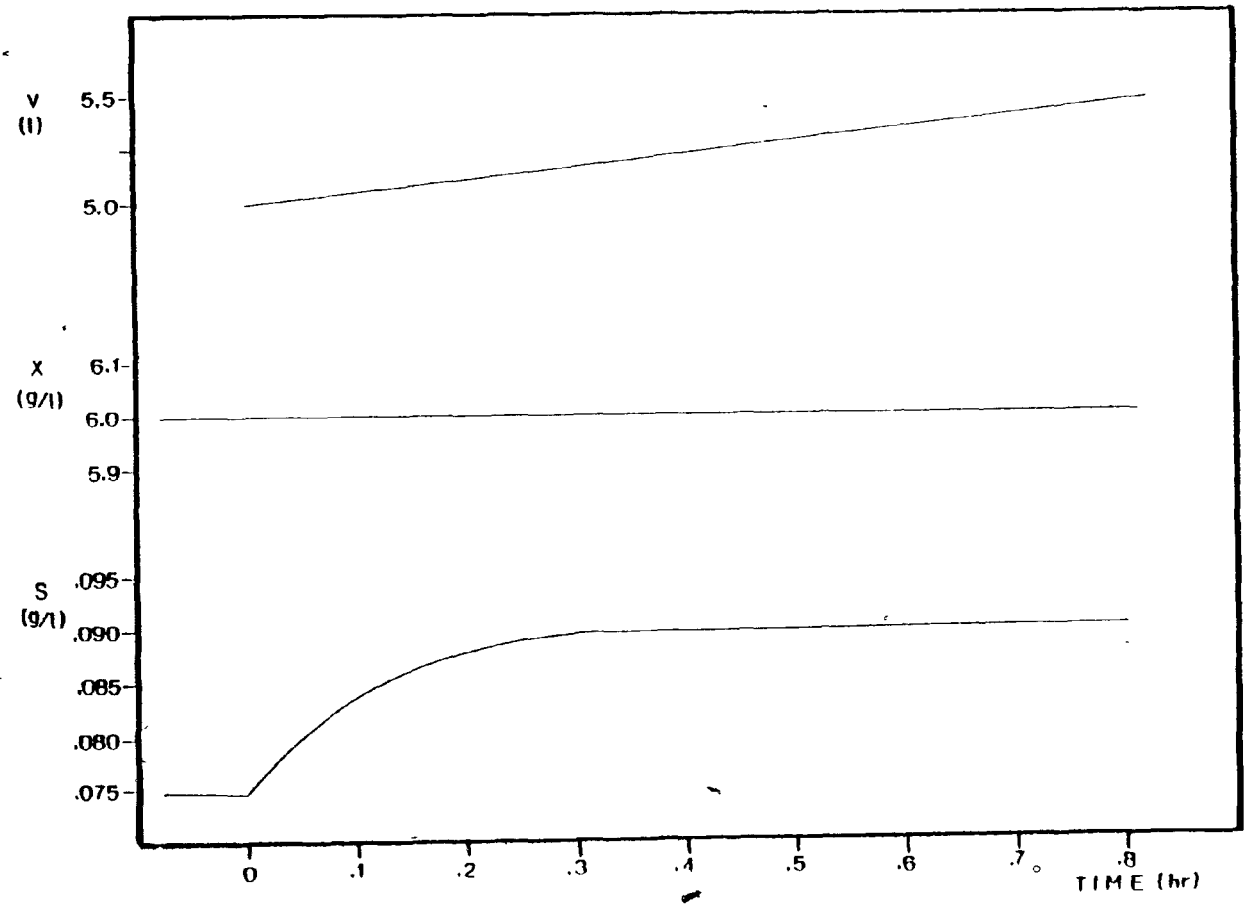

Fig. (2-4): Simulated closed loop response to step change in $\hat{\sigma}$.

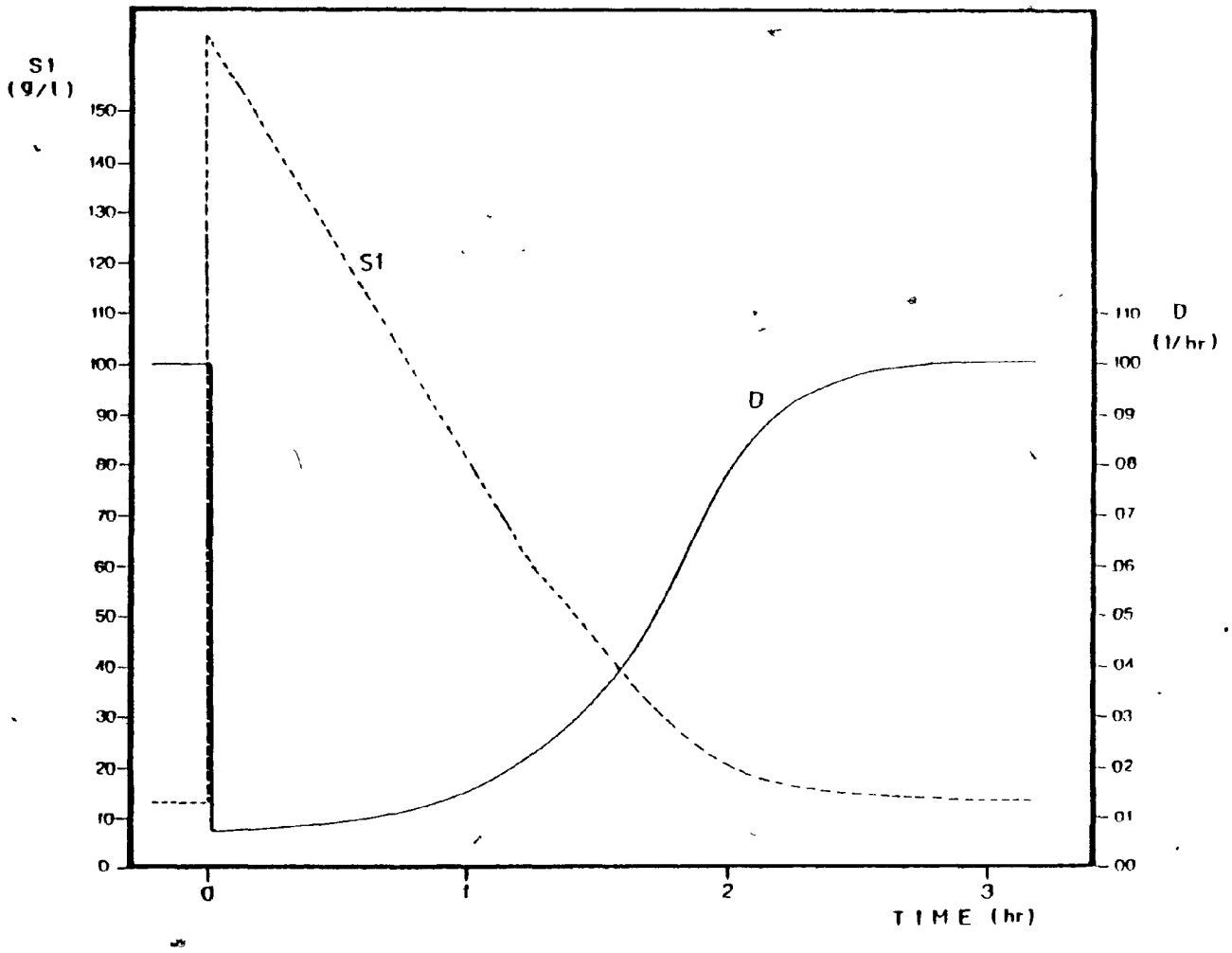

Fig. (2-5): Simulated behaviour of the manipulated variables for the step change in x_D.

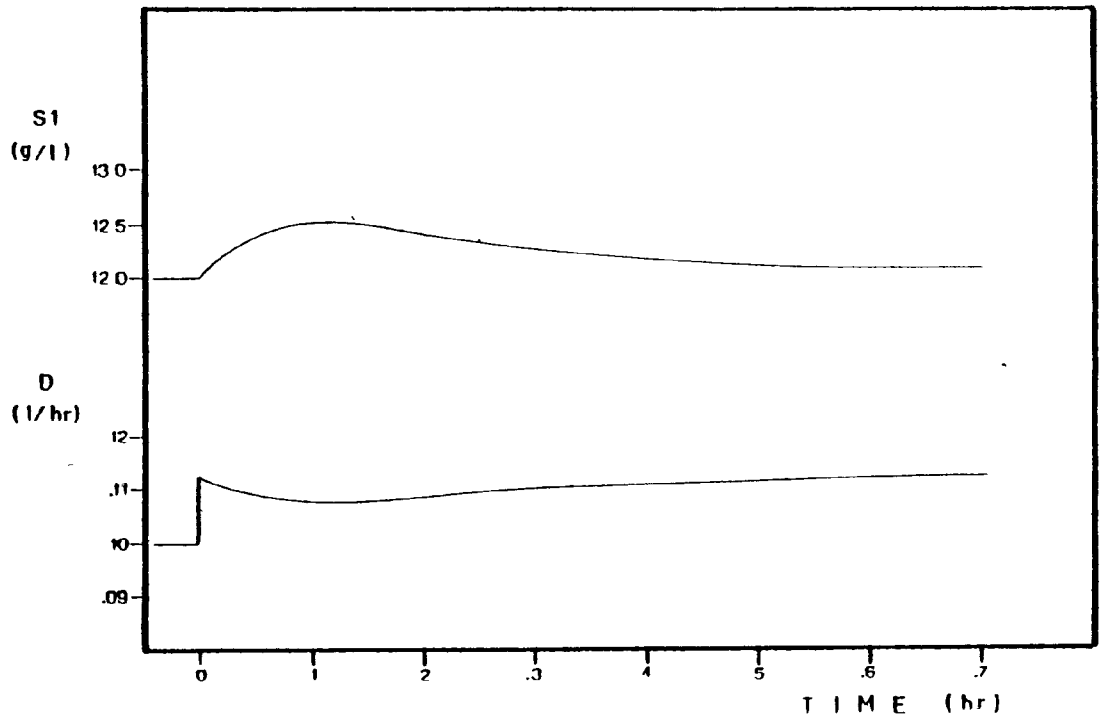

Fig. (2-6): Simulated behaviour of the manipulated variables for the step change in $\hat{d}$.

a. Speeds up the approach to QSS for all changes,

b. has the ability to force the system to any QSS point where both x and s are independently specified,

c. requires only one measured variable, the cell concentration, and

d. has a noninteractive character.

CHAPTER 3: IMPLEMENTATION

In this chapter the modifications of the control system required for implementation and the software description are considered only. Details concerning the experimental apparatus, growth conditions, medium composition and analytical techniques are given in Appendix A.

3.1 CONTROL SYSTEM MODIFICATIONS

The control system, as proposed by Boyle [4] [5], manipulates substrate concentration in the feed and dilution factor. Both manipulated variables are somewhat indirect in physical terms. The final control elements must produce a specified feed rate at a specified concentration. This can be done blending two streams, a very concentrated one, F_A, and a dilute one, F_W, which can be water for simplicity.

The two streams F_A and F_W are calculated from the overall and partial mass balances on the feed.

$$F_A + F_W = F$$

$$s_A F_A = s_1 F$$

where s_A is the substrate concentration of the concentrated stream.

The above equations give:

$$F_A = \frac{s_1}{s_A} F \qquad (3\text{-}1)$$

$$F_W = \frac{s_A - sl}{s_A} F \qquad (3\text{-}2)$$

Since there are two additional streams, a stream of acid and a stream of base, needed to control pH, the actual water stream, F_B, entering the fermentor should be the remainder of the previous calculated water stream, F_W, minus the sum of the two neutralizing streams.

$$F_B = F_W - F_N \qquad (3\text{-}3)$$

where: $F_N = F_{Acid} + F_{Base}$

The physical constraints should be re-examined as well. These are now:

$$0 \leq F_A \leq F_{AMAX} \qquad (3\text{-}4)$$

$$0 \leq F_B \leq F_{BMAX} \qquad (3\text{-}5)$$

Eliminating F from equations (2-21), (3-1) and (3-2):

$$F_A = \frac{\hat{\sigma} x V}{s_A} \frac{sl}{sl - s_D} \qquad (3\text{-}6)$$

$$F_W = \frac{\hat{\sigma} x V}{s_A} \frac{s_A - sl}{sl - s_D} \qquad (3\text{-}7)$$

The upper bounds on F_A and F_W imply lower bounds on sl. The two lower bounds are:

from eq. (3-6) $$sl_{MIN(a)} = \frac{s_D}{\frac{s_A F_{AMAX}}{\hat{\sigma} x V} - 1} + s_D \qquad (3\text{-}8)$$

and from eq. (3-7) $$sl_{MIN(b)} = \frac{s_A + s_D \dfrac{s_A F_{WMAX}}{\hat{\sigma} x V}}{\dfrac{s_A F_{WMAX}}{\hat{\sigma} x V} + 1} \qquad (3\text{-}9)$$

The last two equations are the time varying constraints which should be calculated as part ofthe control computation.

One should note that F_{WMAX} is a variable:

$$F_{WMAX} = F_{BMAX} + F_N \qquad (3\text{-}10)$$

The above equation implies that the upper bound on sl is no longer s_A, and this bound should be calculated as well

$$sl_{MAX} = s_A \frac{F_{AMAX}}{F_{AMAX} + F_N} \qquad (3\text{-}11)$$

otherwise if sl is set equal to s_A a negative diluting water flowrate will will be required.

Another major change in the control system, due to cell concentration measurement technique, is the introduced 20 minutes delay in the feedback path. As it will be explained later, a measurement of the cell concentration was available every 20 minutes with a 20 minutes delay. This way the controller was realized as a discrete controller with a 20 minutes sampling interval, as far as cell concentration is concerned. Less obvious from the mathematical development is the need to measure fermentor volume, which was calculated rather than measured by the computer every 6 seconds.

Obviously a smaller gain for the proportional controller (eq. (2-19)) had to be used. By trial and error a gain at 25 was found, giving satisfactory results.

To summarize, the actually implemented control equations are as follows:

$$sl = kc\,(x_D - x) + \overline{sl}$$

$$sl \leq sl_{MAX}$$

$$sl_{MAX} = s_A \frac{F_{AMAX}}{F_{AMAX} + F_N}$$

$$F_N = F_{ACID} + F_{BASE}$$

$$sl \geq MAX\,[sl_{MIN(a)},\ sl_{MIN(b)}]$$

$$sl_{MIN(a)} = \frac{s_D}{\frac{s_A F_{AMAX}}{\hat{\sigma} x V} - 1} + s_D$$

$$sl_{MIN(b)} = \frac{s_A + s_D \frac{s_A (F_{BMAX} + F_N)}{\hat{\sigma} x V}}{\frac{s_A (F_{BMAX} + F_N)}{\hat{\sigma} x V} + 1}$$

$$F_A = \frac{\hat{\sigma} x V}{s_A} \frac{sl}{sl - s_D}$$

$$F_B = \frac{\hat{\sigma} x V}{s_A} \frac{s_A - sl}{sl - s_D} - F_N$$

From the above it is seen that the overall character of the control system is much more than proportional feedback control.

More precisely, it has the following features:

(a) proportional feedback control

(b) calibrated decoupling

(c) nonlinear time varying constraints.

The decoupling equations and the time varying constraints necessitate the use of an on-line computer in the implementation.

3.2 SOFTWARE DESCRIPTION

3.2.1 PROCON SYSTEM

The minicomputer is driven by a software package known as PROCON [6] which is related to the commercially available package known as DATCON [9]. PROCON is a computerized data acquisition and PROcess CONtrol system for both supervisory and direct digital control. It allows itself to be adapted to specific control and data reduction tasks through conversational interactions with the process engineer, without reprogramming, while remaining on line.

Control is based on measured and computed variables with cascading of control loops. Six control algorithms are implemented:

1. Positioner
2. Proportional control
3. Integral plus proportional control (P + I)
4. Integral (with output limiting) plus proportional control (P + I + L)
5. Derivative, integral (with output limiting) plus proportional control (P + I + L + D)

6. A general computational algorithm.

PROCON provides an advanced control loop start up/shut down program which relieves the operator of much of the complexity of changing controllers from local to computer mode, or of converting from basic to more advanced computer control schemes. The process engineer may select from a range of options which can provide for control changes which do not disturb the dynamic state of the process (bumpless and rampless transfer).

In addition to the data acquisition and control mode, the PROCON system provides a conversational mode which handles operator communications, logging of data and full control over the system by the process engineer. The primary communications device is the teletype. The operator command mode permits the process to:

1. Display measured and computed values.
2. Access the measurement, setpoint and control status of control loops.
3. Modify the setpoint and status of control loops.
4. Request special logs.

The log service routine outputs logs either on demand or periodically. The logs are prepared from current data according to formats which have been selected by the process engineer.

The process engineer command mode permits him to set up the entire data acquisition and control process on line, in a conversational mode through the teletype keyboard printer, without reprogramming, without even stopping the data acquisition and control process.

3.2.2 LOOP STRUCTURE

An important aspect of the implementation is the performed functions of the minicomputer. In addition to the control equations, the problems of neutralization (pH control) and precise control of the feeding flowrates should be faced.

In the actual implementation there are two input signals, pH and cell concentration, and four output on-off signals which drive the four pumps. Fifty-eight PROCON loops were written, performing the following functions:

(i) computation of the control algorithm
(ii) computation of the current volume in the fermentor
(iii) flowrate control
(iv) pH control
(v) periodical or upon request logging of the current values of selected loops.

In Figure (3-1) a simplified loop structure diagram is shown which is divided into four major sections to facilitate the description.

FIG 3-1 SIMPLIFIED LOOP-STRUCTURE DIAGRAM

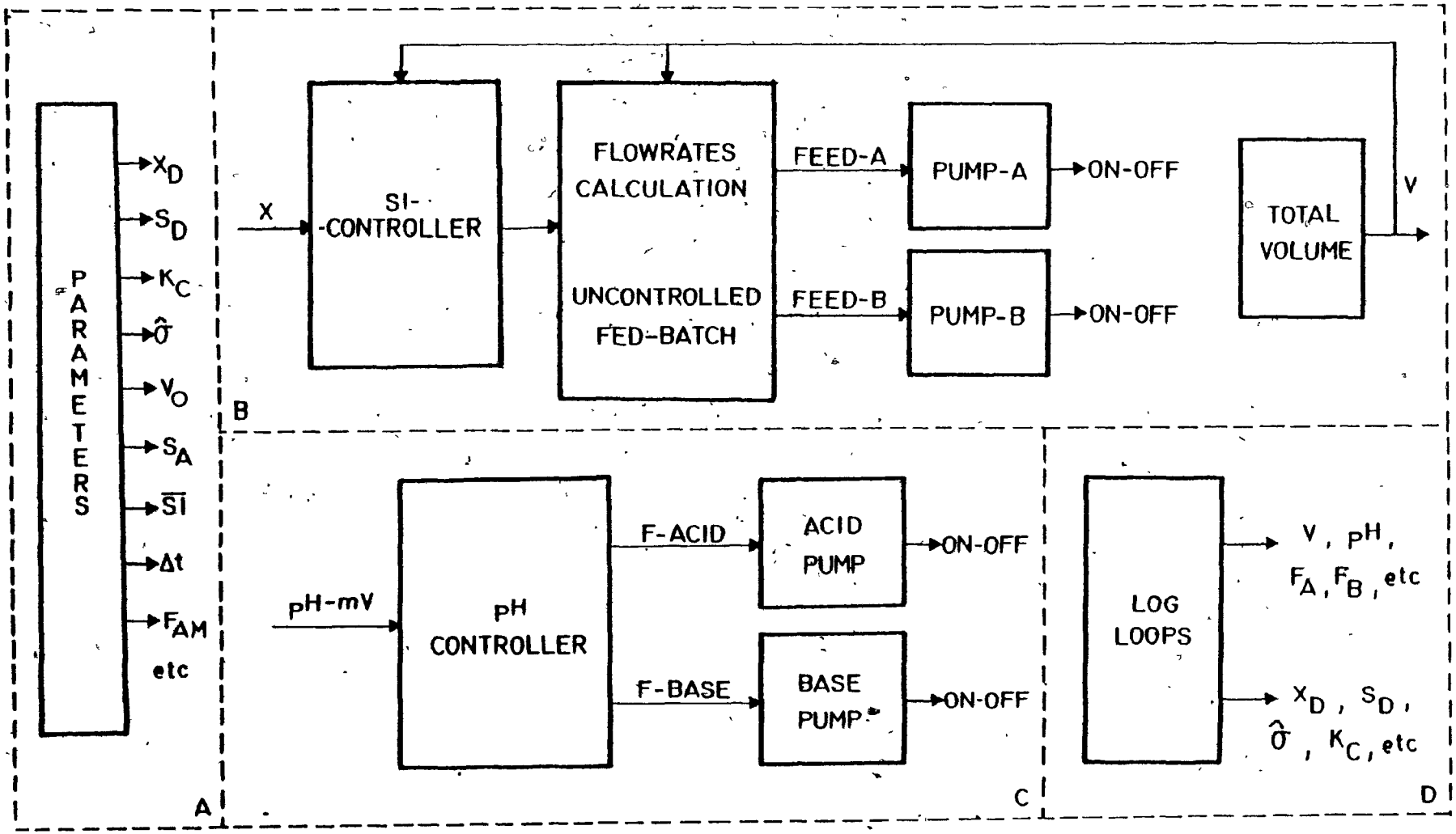

A-Parameters

Fourteen PROCON loops, most of them computational, are represented by the block "parameters". All required parameters such as k_c, $\hat{\sigma}$, Vo, $\overline{sl}$, s_D, x_D, etc. are entered into the minicomputer.

B-Process Controller

In this section the main process controller is presented. It is characterized by the input, cell concentration, an internal computation of the volume and the two output on-off signals which drive the two feeding pumps.

The block "sl-controller" represents eight PROCON loops which calculate the substrate concentration in the feed, sl, given the cell concentration which is entered into the minicomputer through the teletype and the current volume which is calculated internally. The calculated value of sl is further checked to see that it satisfies the time varying constraints (equations 3-8, 3-9 and 3-11) which are calculated as well.

The block "flowrates calculation--uncontrolled fed-batch" represents four PROCON loops which calculate the two feeding flowrates, given the output of the previous block, and the current volume. Besides this, there are two additional loops which calculate the two feeding flowrates for uncontrolled runs, providing an overall feedrate F such that $F = F_0 \exp(\alpha t)$, at any specified constant substrate concentration sl.

Each one of the blocks "pump-A" and "pump-B" represents three PROCON loops where the continuous feedrates F_A and F_B are converted to two on-off signals which drive the pumps. The flowrate control is accomplished as follows. The continuous feedrate (F_A or F_B) is treated as the set-point to a P + I controller, the output of which is the setpoint of a time positioner (on-off controller) whose measurement is continuously zero. The output of the latter is fed back as measurement to the P + I controller after it has been multiplied by the feedrate of the pump (F_{AMAX} or F_{BMAX}). The proportional gain and the reset constant were determined by trial and error from performed simulations of the flowrate controller, the performance of which was experimentally checked.

Finally, the block "volume" represents five PROCON loops which calculate the current total volume, given the initial volume and the on-off output signals which drive the pumps. Besides this calculation, the sampling volume, 25 ml, is subtracted from the total volume whenever a new cell concentration measurement is entered into the computer. At the end of each run the total volume calculated by the computer was found to be in agreement with the actual total volume in the fermentor.

C- pH Controller

The block "pH - controller" represents six PROCON loops where the input signal (pH as mV) is converted to pH units and filtered. A set of control (P + I) and computational loops

is further used to produce the appropriate acid and base flow-rates to control the pH.

The blocks "pump-AC" and "pump-BA" similarly produce on-off signals to drive the acid and base pumps, respectively.

D - Data Logs

In this section seven computational and log loops output at regular intervals or on operator request parameters and variables, such as V, pH feedrates, accumulative base and acid used, k_c, $\hat{\sigma}$, x_D, s_D, $\overline{sl}$, etc.

A detailed loop diagram is shown in Appendix C. Fifty-eight PROCON loops were required in total, making use of all the available computer memory, that is 12 K 8 bit words for the software package and 4^K for the loops. In Table (3-I) the numbers of all PROCON loops and the corresponding blocks are tabulated. Listing of all loops, a table where the task of each loop is explained, and a typical output are available in Appendix C as well.

TABLE 3-I

BLOCK	LOOP NUMBER
Parameters	1,2,3,5,6,7,8,9,21,22,23, 24,25,26
sl - Controller	20,27,28,29,30,31,32,33
Flowrates - Calculation Uncontrolled Fed-Batch	34,35,38,39,40,41
Pump-A	70,71,72
Pump-B	73,74,75
pH - Controller	15,16,17,50,51,52
Pump-AC	76,77,78
Pump-BA	79,80,81
Volume	10,11,18,19,83
Data Logs	53,54,82,90,91,92,99

CHAPTER 4: EXPERIMENTAL RESULTS AND DISCUSSION
EVALUATION OF THE CONTROL SYSTEM

A standard experimental evaluation of a control system involves investigation of open loop response to constant inputs, closed loop response to set point changes, closed loop response to disturbances and non linearities of the system. Taking the above as a guideline, ten experiments were designed and performed, a list of which is given in Appendix B. In the following discussion the runs are presented in an order designed to facilitate the evaluation.

4.1 CELL CONCENTRATION TRANSIENTS

4.1.1 OPEN LOOP RESPONSE

In run # 9 the open loop response of the process was tested. Starting with an initial cell concentration of 5.42 g/l and an initial volume of 5 l, the dilution factor, D, was set equal to .1 hr^{-1} and the substrate concentration in the feed, s1, to 14.07 g/l. Under these constant inputs the process was expected to move towards a QSS operating point in the vicinity of 7 g/l. As already discussed in section 2.1.2, cell concentration transient should be very slow, more than 30 hr and the total volume expansion required to reach QSS is much larger than that which a laboratory fermentor can handle. The experimental results together with the simulated transient predicted by the model are shown in Figure (4-1). Despite the scatter in the data, there is a definite underlining trend which shows that cell concentration is

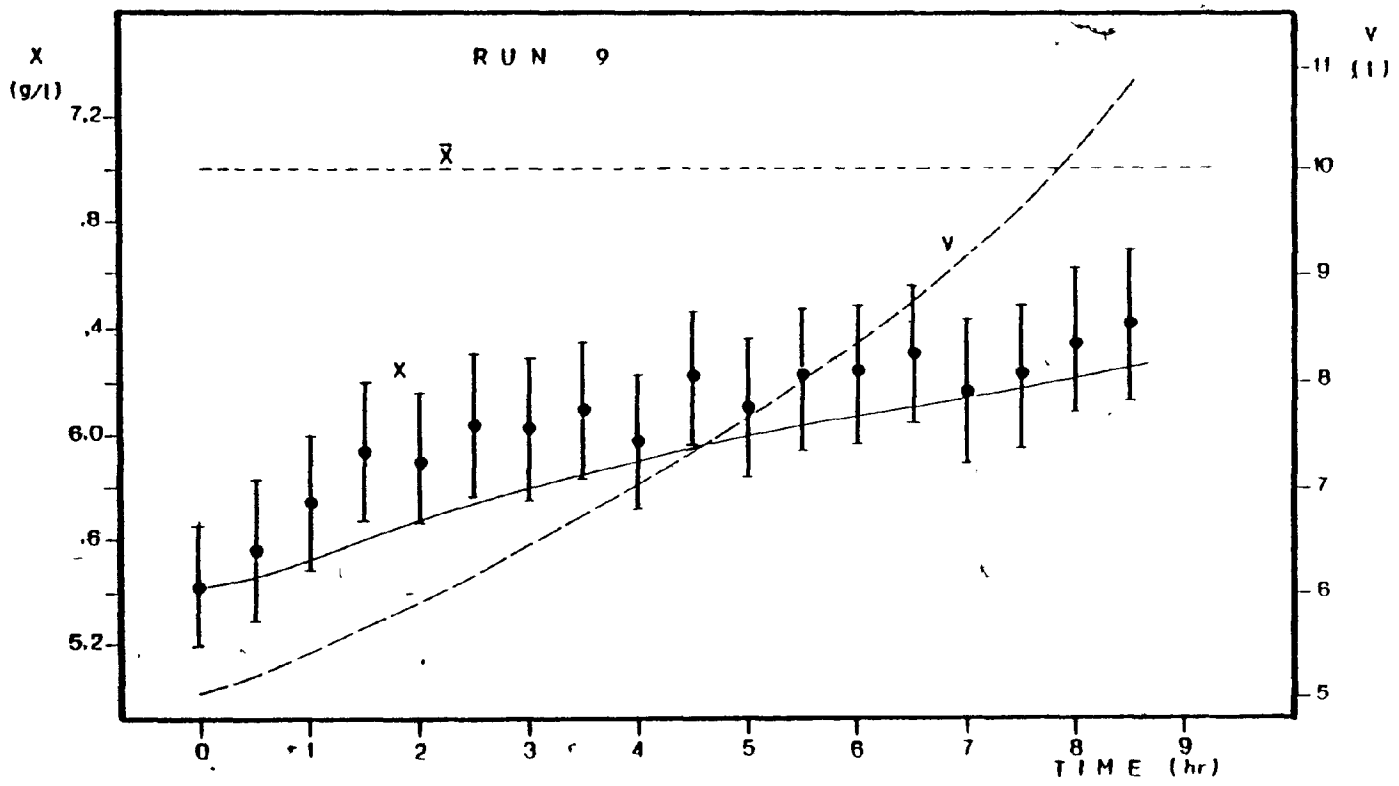

Fig. (4-1): Run # 9, x and V versus time (—— simulation, ● x-data, — — volume).

following the predicted pattern. As it was anticipated the volume reached 10 l, ready to overflow, while only 65% of the total change in cell concentration was completed in 8.5 hr as shown in Figure (4-1). It has been made clear now that observation of the QSS in a laboratory apparatus is not feasible without a control system.

The observed scatter in the data is primarily due to the experimental error in the cell concentration measurement. In Figure (4-1) the 95% confidence interval for each measurement is shown as well, based on error analysis which is available in Appendix A. It should be emphasized here that the feedback system is to rely on this noisy data.

4.1.2 CLOSED LOOP RESPONSE TO SET POINT CHANGES

In run # 3 the closed loop response of the system to set point changes (x_D) was tested. Starting at a QSS in the vicinity of 5 g/l (x_D = 5.36 g/l) at time zero a step change in the desired cell concentration was performed (x_D = 6 g/l). As shown in Figure (4-2) cell concentration moved up to 6 g/l in less than two hours. After the system was kept at the new QSS for two hours, two step changes at 1 g/l in x_D were performed at times 4 and 8 hours. Again, cell concentration moved up to 7 g/l and then to 8 g/l requiring less than two hours for each transient, Figure (4-2).

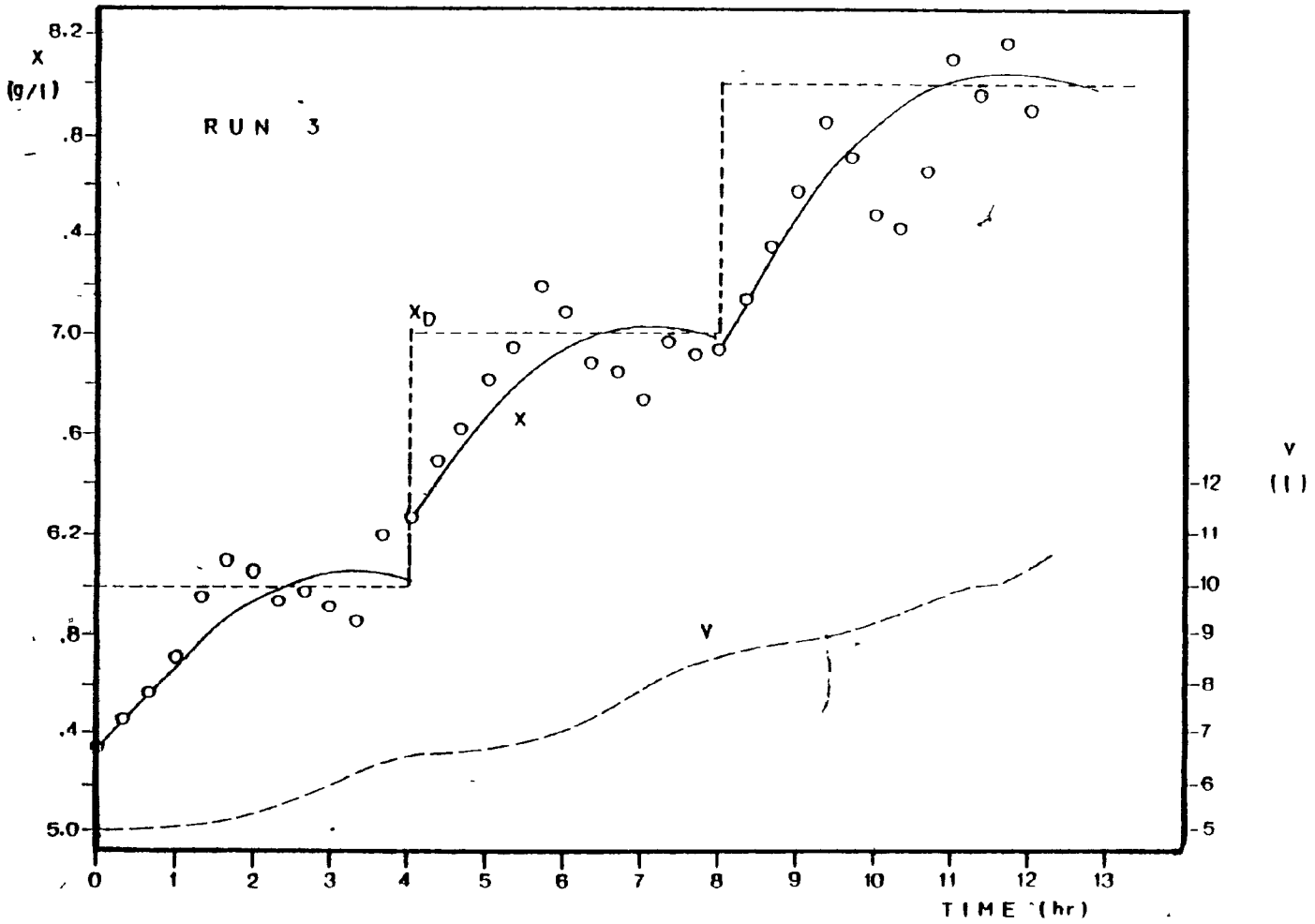

Fig. (4-2): Run # 3, x and V versus time (—— simulation, o x-data, — —volume).

In order to make a better comparison between the actual and the simulated response of the system, a simulation of the transient induced at a time 4 hours is shown in Fig. (4-3). Comparing cell concentration transients, as shown in Figures (2-3) and (4-3), it is seen that in the latter simulation some overshoot and oscillation phenomena are introduced. This is primarily due to the delay introduced by the cell concentration measurement technique in the feedback path. A higher control gain would result in a slightly faster response, however, oscillations would not dump out as fast. It should be emphasized that in the selection of the controller gain one should take into consideration the level of noise added to the cell concentration measurement. As explained in Appendix A, samples were taken every 20 minutes and the dry cell weight of the sample was measured after 40 minutes of drying time. In order to minimize the delay, a first measurement was taken after 20 minutes and was fed back into the computer. This first estimate was overestimated from 0 to 3% in addition to the experimental error of the gravimetric analysis which was found to be 2.2%. Therefore, as the control system was relying on this noisy data, the selection of the proportional gain should come as the result of a compromise among fast response, undesirable oscillatory behaviour at the QSS, and undesirable amplification of the measurement noise by the proportional gain. In Fig. (4-2), each transient was simulated separately using the actual cell concentration as x(o) at times 0, 4 and 8 hours.

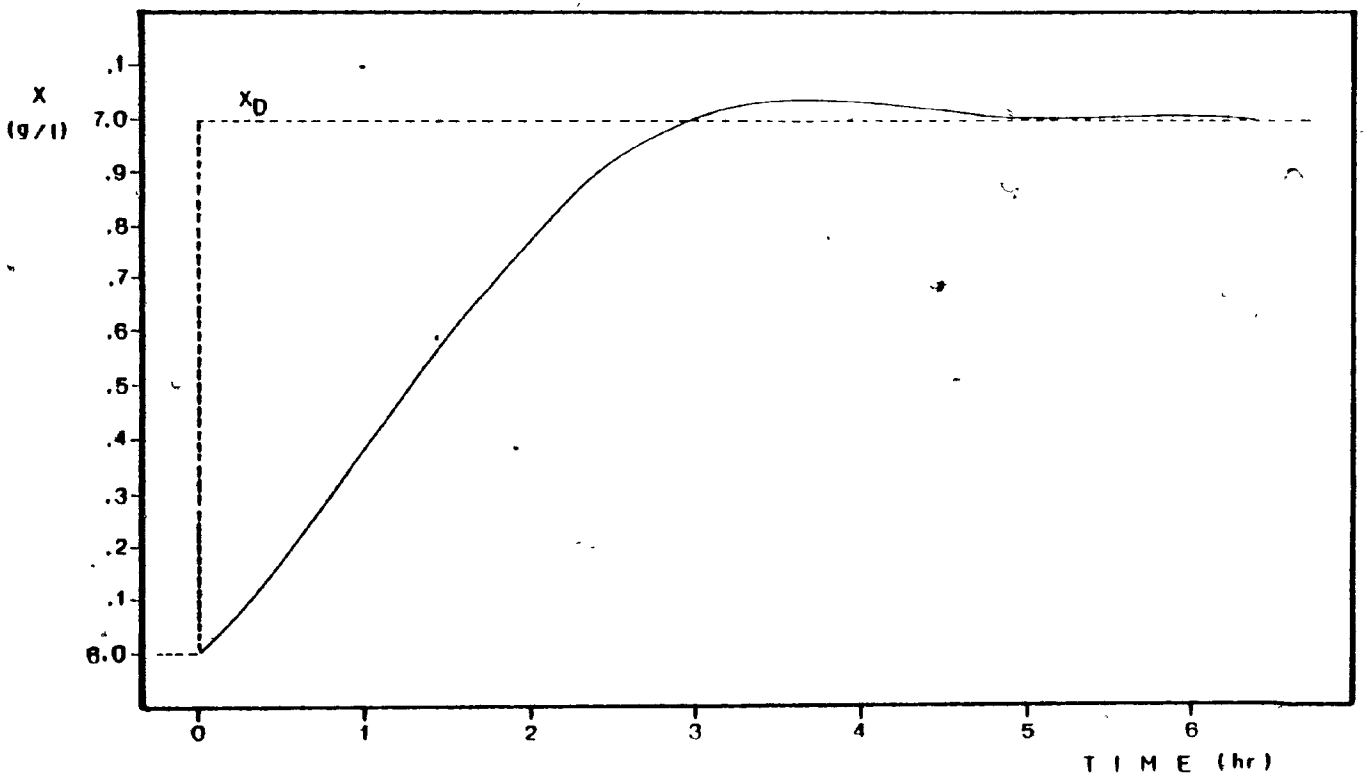

Fig. (4-3): Run # 3 simulated response of second step change in x_D.

In Fig. (4-4) the behaviour of the manipulated variables of the previous simulated transient at time 4 hours is shown. It is seen that after the performed step change in the set point, s1 jumps up abruptly and then decreases towards it steady-state level at the new QSS. The other manipulated variable, D, follows the reverse action, namely drops down close to zero increasing towards its previous steady state value as the system approaches QSS. Comparing Fig. (4-4) to Fig. (2-5), where a continuous cell concentration measurement is assumed, it is seen that in the implemented controller the manipulated variables change stepwise and the change in s1 is approximately three times smaller in the beginning of the transient, as a smaller controller gain was used. In Fig. (4-5) the actual behaviour of the manipulated variables is shown. As expected, D and s1 follow the same pattern shown in Fig. (4-4) but with a more oscillatory character due to the noise added to the cell concentration.

Finally, from the small volume expansion, shown in Fig. (4-2), it is seen that with the control system cell concentration transients were sped up so that observation of three different QSS operating points was possible in a single run.

Up to now only positive step changes in the desired cell concentration were considered. In runs # 7 and # 8-a, the response of the system to negative step changes in x_D was observed.

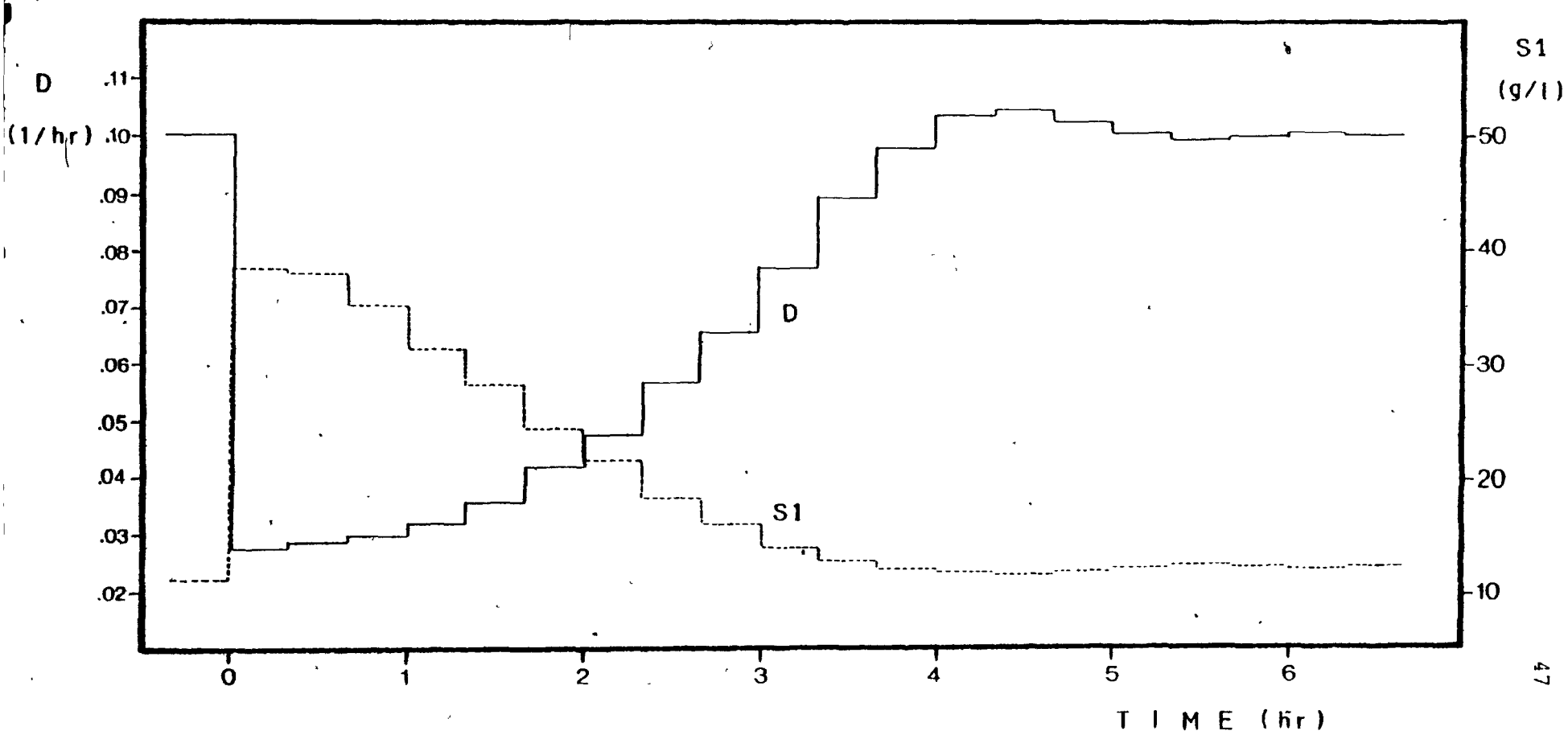

Fig. (4-4): Run # 3, simulated behaviour of the manipulated variables of the second step change in x_D.

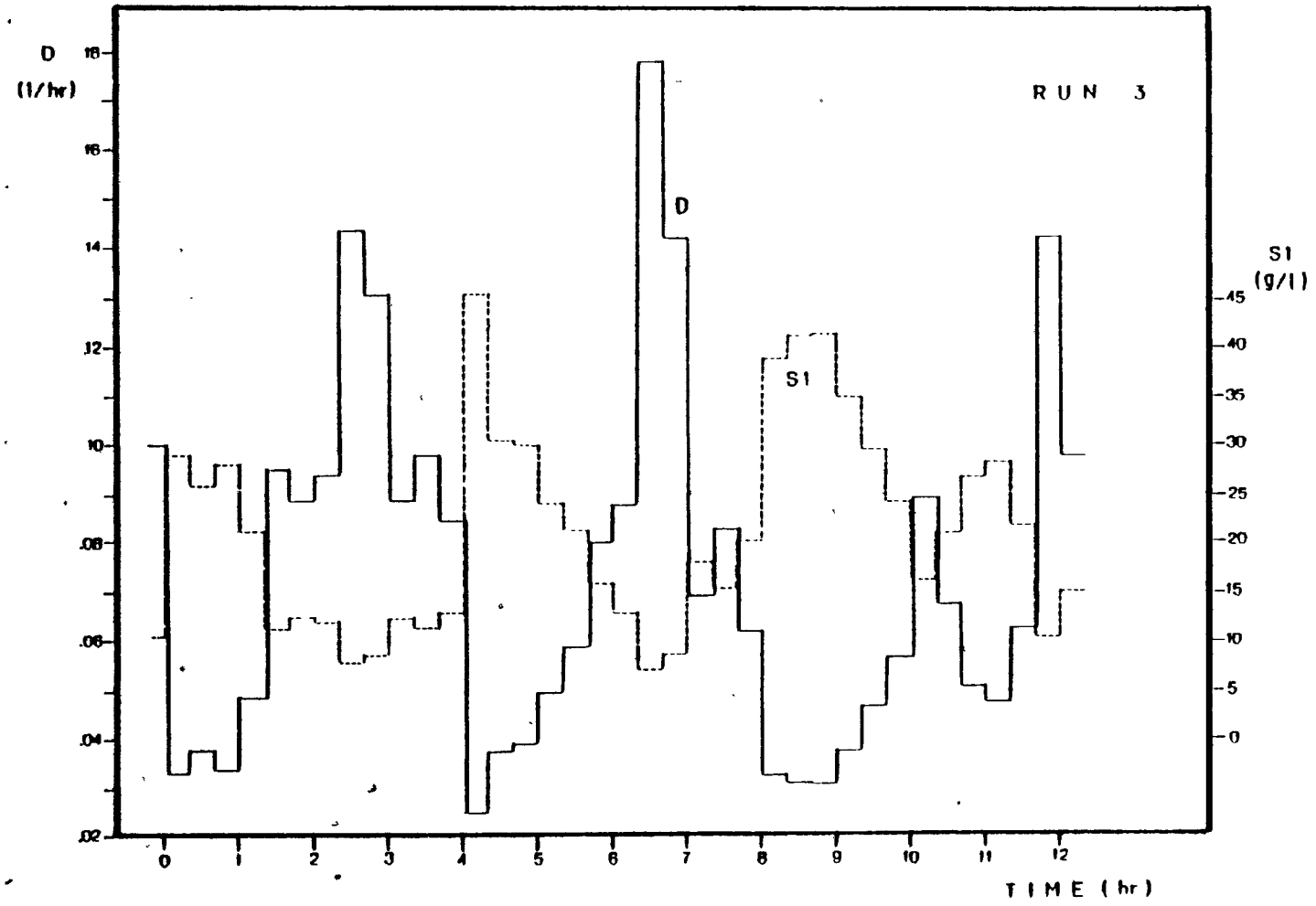

Fig. (4-5): Run # 3, behaviour of the manipulated variables.

In run # 8-a, as shown in Fig. (4-6), starting with 7.24 g/l cell concentration dropped to 6 g/l, the desired cell concentration, in approximately 1.5 hr. The manipulated variables, shown in Fig. (4-7), followed the reverse action followed in run # 3 where positive step changes in x_D were performed. The dilution factor jumped to a high value, decreasing to the nominal value, $\bar{D}$, as cell concentration was approaching x_D; while s1 moved down, increasing slowly to its nominal value, $\bar{s}1$, at the QSS. In this run the controller was saturated almost throughout the transient, i.e. the dilution factor was following the upper time varying constraint (eq. 2-24), forcing s1 to follow the lower time varying constraint (eq. 2-26). This is shown more clearly in Fig. (4-8), where the actual manipulated variables, F_A and F_B, are plotted versus time. The water feed flowrate, F_B, was kept at its maximum value, F_{BMAX}, while saturation occurred, forcing F_A to follow a particular trajectory implied by the time varying constraint (eq. 3-9).

The volume expansion, shown in Fig. (4-6), is larger than simple dilution, that is adding water until $x = x_D$, (Table 4-I) and this is because the control system dilutes in such a way that the cells are growing at a constant specific growth rate (i.e. s is kept constant). Since the controller was saturated almost through the whole transient, the total time t_f, required by the control system to move cell concentration down to the desired value, x_D, is highly dependent on the maximum flowrate of the diluting stream, F_{BMAX}. The higher F_{BMAX} is, the smaller t_f is.

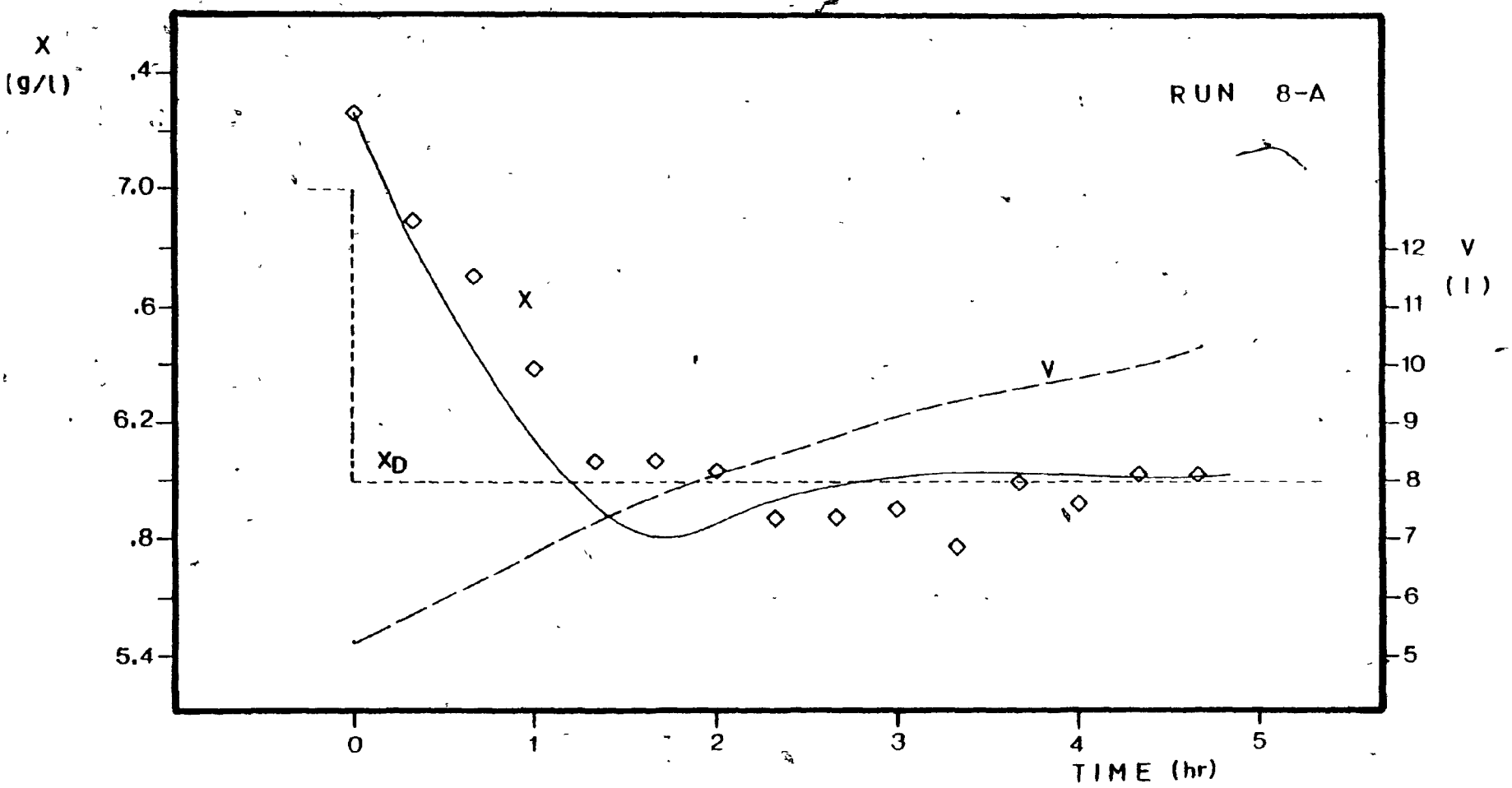

Fig. (4-6): Run # 8-a, x and V versus time (—— simulation, ◇ x-data, — — volume).

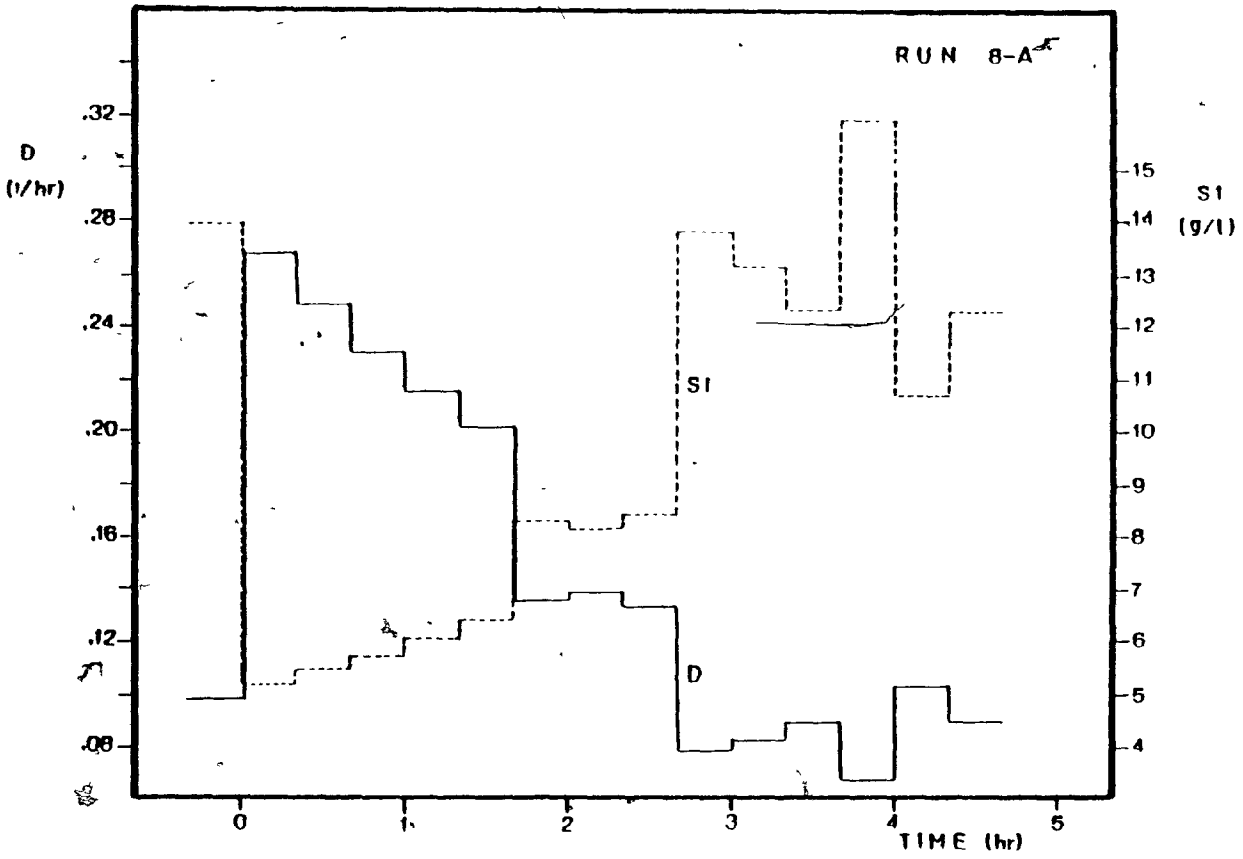

Fig. (4-7): Run # 8-a, behaviour of the manipulated variables.

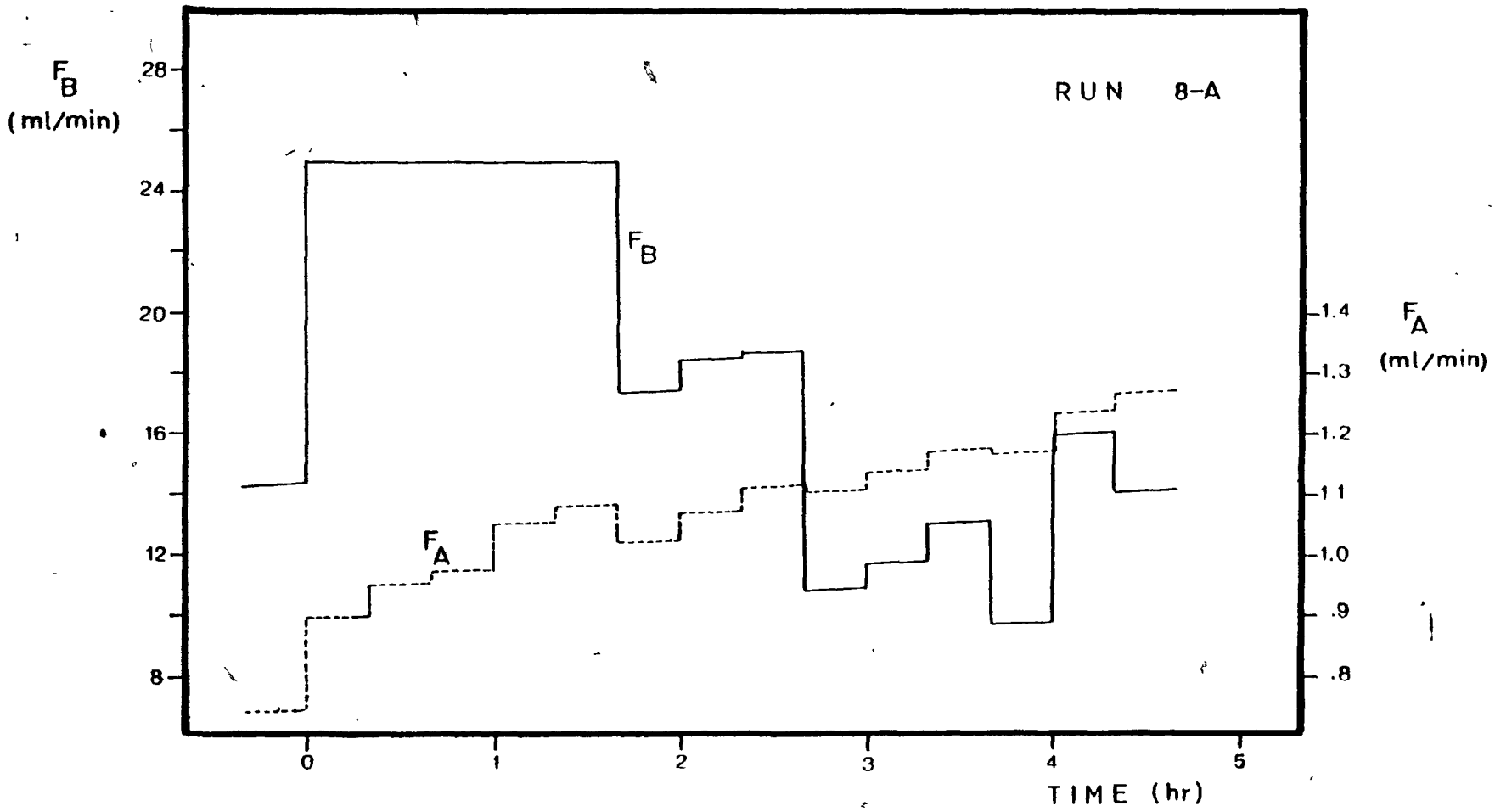

Fig. (4-8): Run # 8-a, F_A and F_B versus time.

A side effect of having a higher F_{BMAX} is that the total volume expansion will be less, but definitely higher than simple dilution. It reaches asymptotically the simple dilution volume expansion as the controller gain becomes higher, provided that the controller remains unsaturated.

TABLE 4-I

	V_o	V_f
simple dilution	5 l	6.05 l
control system	5 l	7.4 l

4.1.3 NON-INTERACTION

Non-interaction for the particular system used in this study means that when cell concentration is in a transient, substrate concentration remains constant and vice versa. As will be explained later, substrate concentration measurements are subject to very large experimental error due to the dynamic characteristics of the process. As the amount of substrate concentration data obtained in this work was not enough and not very reliable, non-interaction as well as substrate concentration transients are shown indirectly using cell concentration data only.

Since the specific growth rate, μ, is a function of substrate concentration, s, constant μ during cell concentration transients implies constant substrate concentration. By definition the specific growth rate is given by:

$$\mu = \frac{1}{X} \cdot \frac{dX}{dt} \qquad (4\text{-}1)$$

where X is the total biomass in the fermentor at time t. The above equation can be rewritten as:

$$\mu = \frac{d\ln X}{dt} \qquad (4\text{-}2)$$

Therefore, plotting ln X versus time, the specific growth rate is given by the slope of the regression line that fits the data.

As already discussed in chapter 2, in an uncontrolled run substrate concentration is changing drastically in the beginning and reaches close to equilibrium value, while cell concentration is still in the beginning of its transient. In the uncontrolled run # 9, as shown in Fig. (4-9), the slope is changing in the beginning, remaining practically constant after the first two hours. The interaction is clearly shown since the cell concentration transient induced a transient in substrate concentration, although the external conditions D and sl were set so as to change only the steady state value of the cell concentration.

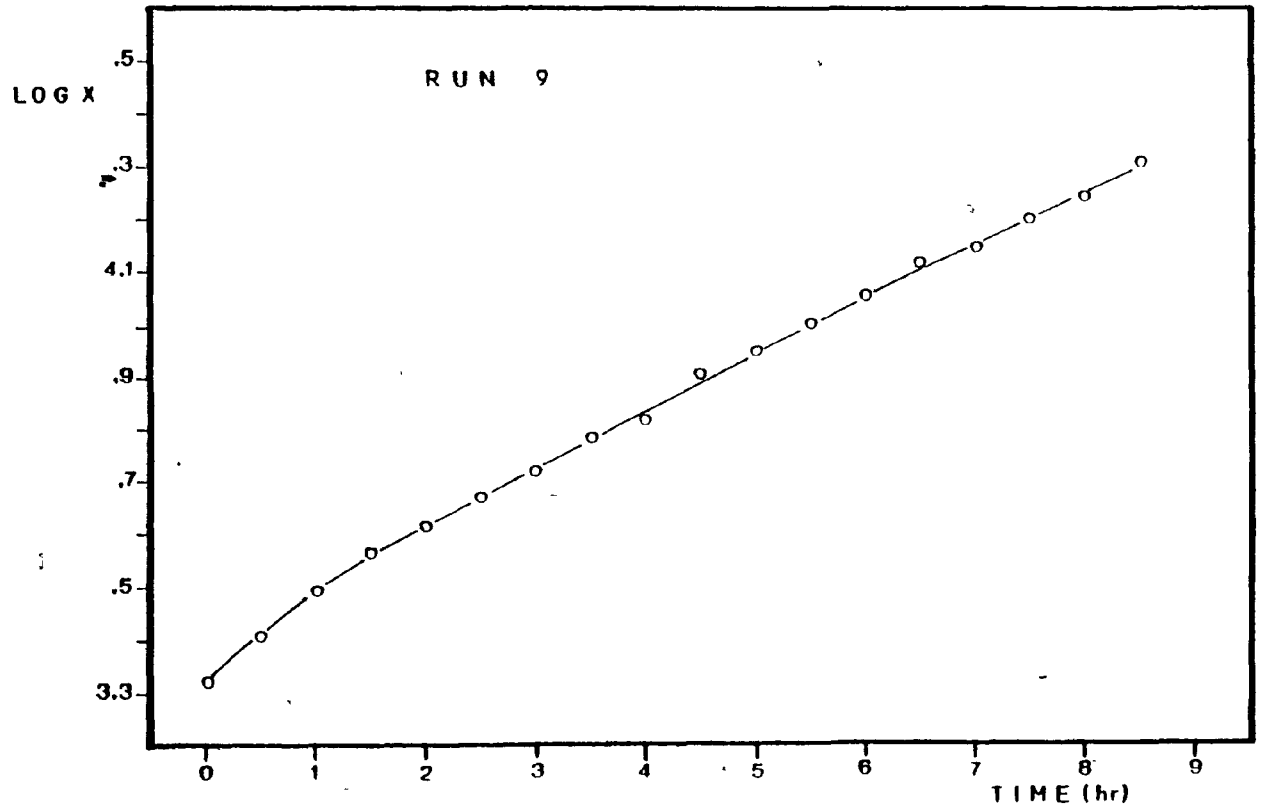

Fig. (4-9): Run # 9, ln X versus time.

In run # 3 cell concentration was forced to reach three different QSS points. It is shown in Fig.(4-10) that during cell concentration transients, the specific growth rate was kept constant (one should check the slope in the vicinity of times 0, 4 and 8 hours, the starting points of the three transients). Therefore, substrate concentration transients were not induced, providing sufficient proof that non-interaction was achieved with the implemented control system.

In Fig. (4-11), ln X versus time is plotted for run # 1 which is discussed in detail in section 4.1.5. In this run, a larger step change in the desired cell concentration (Δx = 2 g/l) was performed. Again it is seen that the specific growth rate was kept constant and therefore non-interaction was achieved.

Finally, in Fig. (4-12) the results from run # 8-a are shown where the controller was saturated almost throughout the transient. It is clear that the non-ineractive control properties were preserved even when the control outputs reached physical limits.

4.1.4 CLOSE LOOP RESPONSE TO DISTURBANCES

The control system implemented in this work was mainly designed to act as a regulator , in other words, to force the process to any desired QSS operating point. The fact that the control system involves a feedback controller makes possible

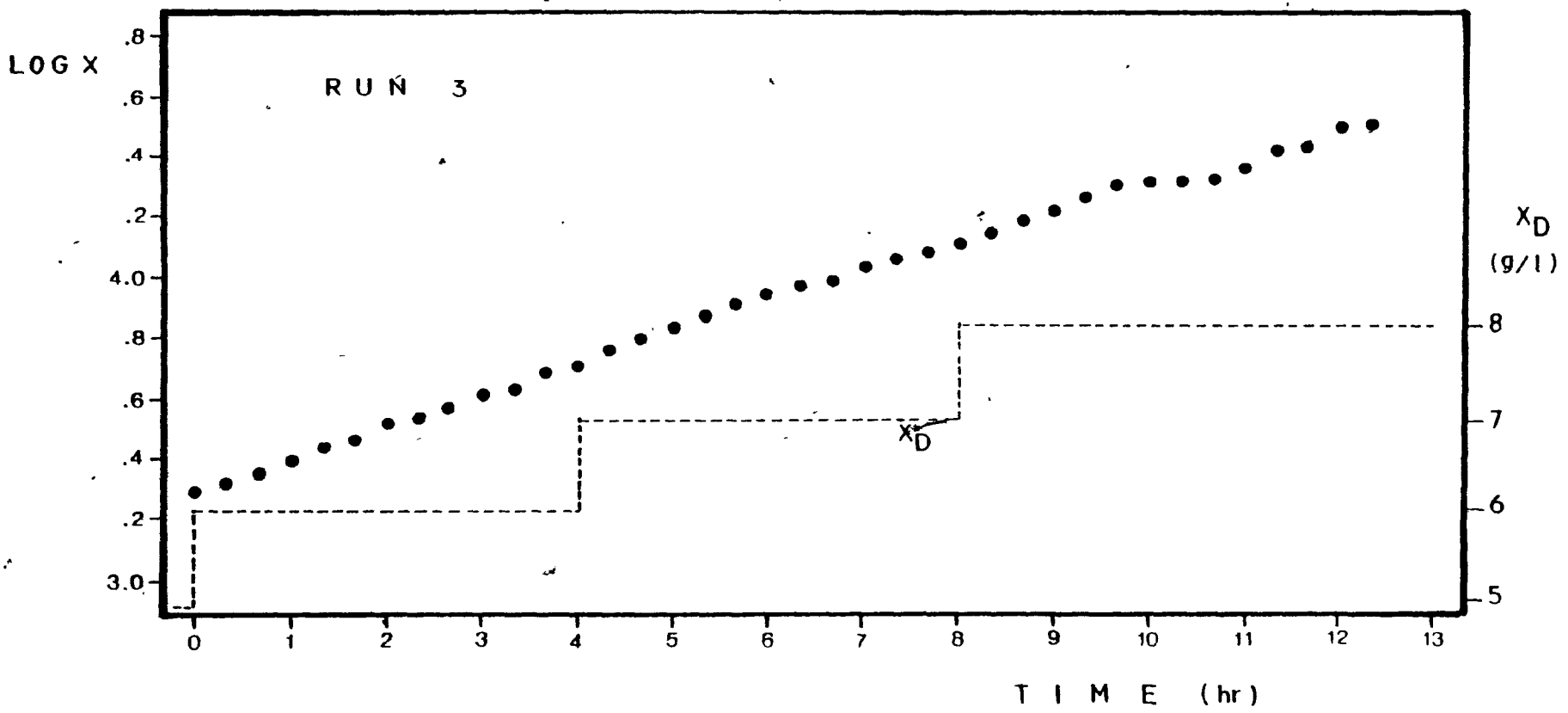

Fig. (4-10): Run # 3, ln X versus time.

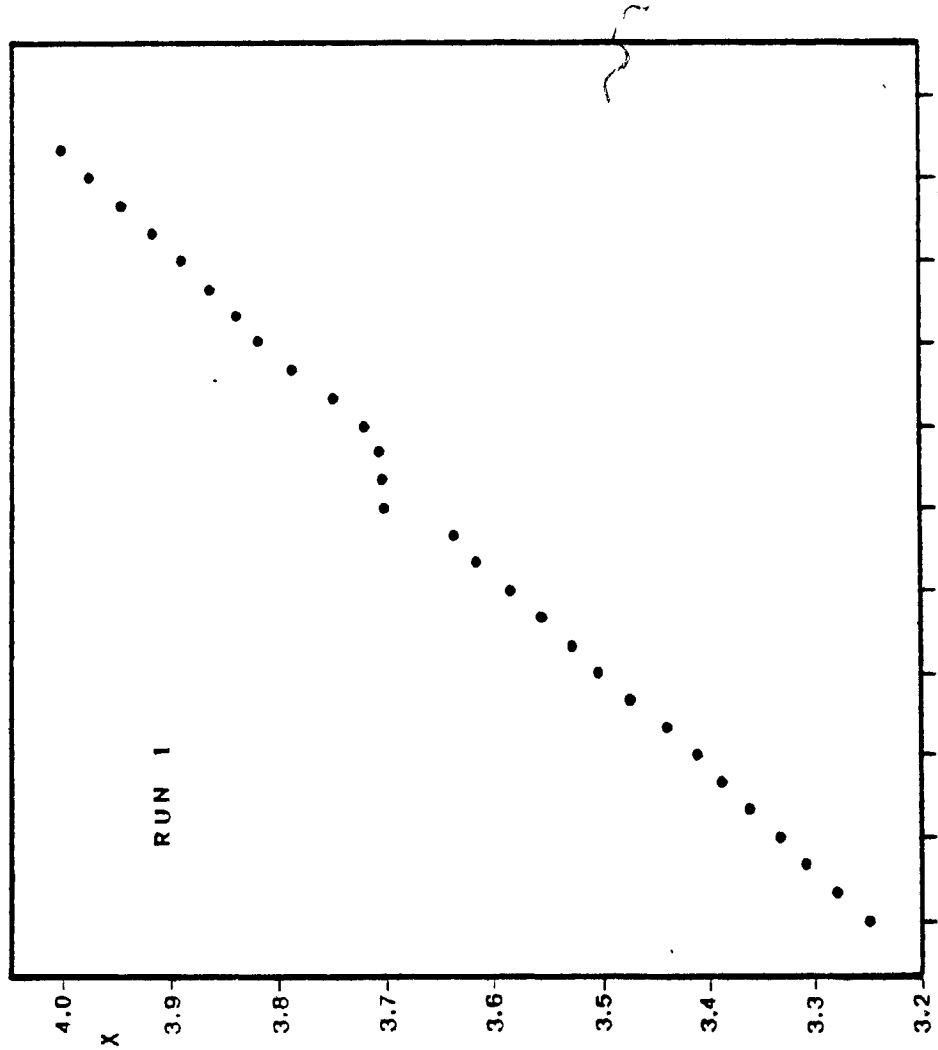

Fig. (4-11): Run # 1, ln X versus time.

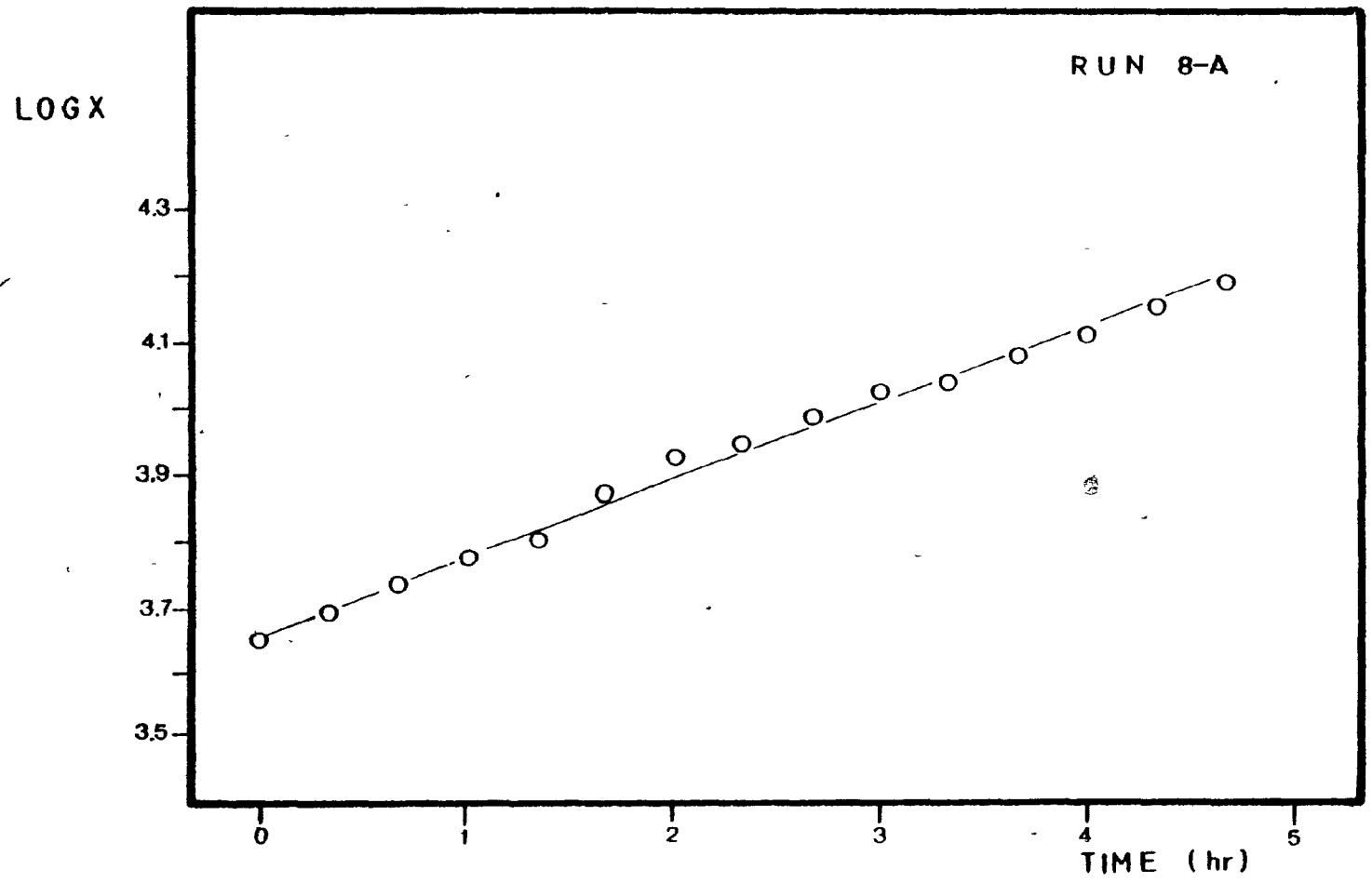

Fig. (4-12): Run # 8-a, ln. X versus time.

compensation of disturbances as well. Potential disturbances include such environmental factors as pH, temperature and dissolved oxygen level. Presumably there could also be strictly biological factors which might change and which would be unmeasurable: These correspond to the class of things called "noise" by control engineers. It should be noted here that feedforward control is not feasible, since the available models of the process do not include dependence on pH, temperature, dissolved oxygen, etc.

In this study, two particular cases were examined: (a) the response of the system to step changes in pH, and (b) the behaviour of the system under stochastic disturbance (noise).

(a) Response to step change in pH

In run # 8-b the system was kept in a QSS in the vicinity of 6 g/l and at time 40 minutes a step change in pH of 1.5 pH units was performed (from 5.1 to 3.6). In order to have an "ideal" step change in pH, a few ml of HCl 4N were dropped in the fermentor besides the performed step change in the set point of the pH controller. Cell concentration, as shown in Fig. (4-13), dropped down very fast to 5.50 g/l in less than 20 minutes, dropping further to 5.34 g/l in the next 20 minutes. Although there was a large change in cell concentration, the system recovered in less than 2 hr due to control action.

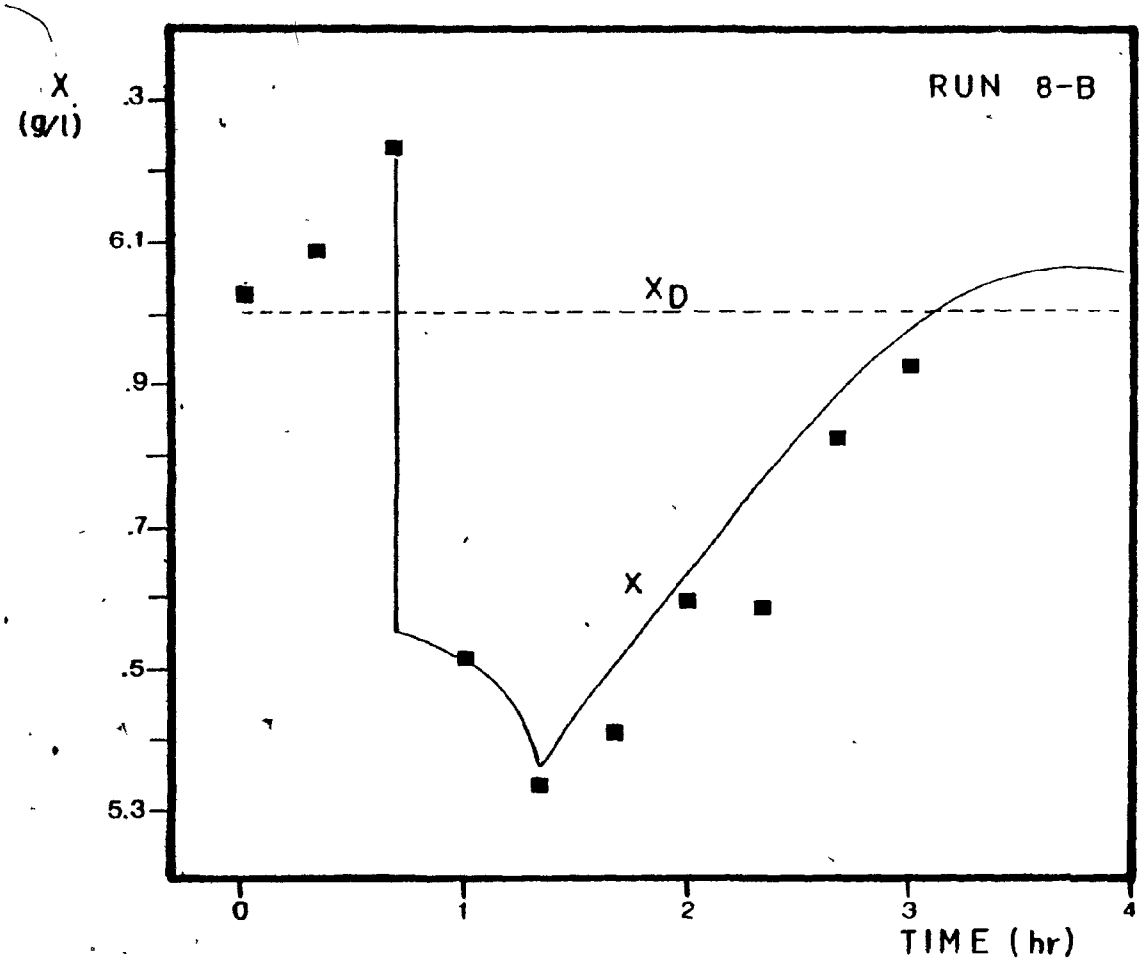

Fig. (4-13): Run # 8-b, x versus time
(—— simulation', ■ x-data).

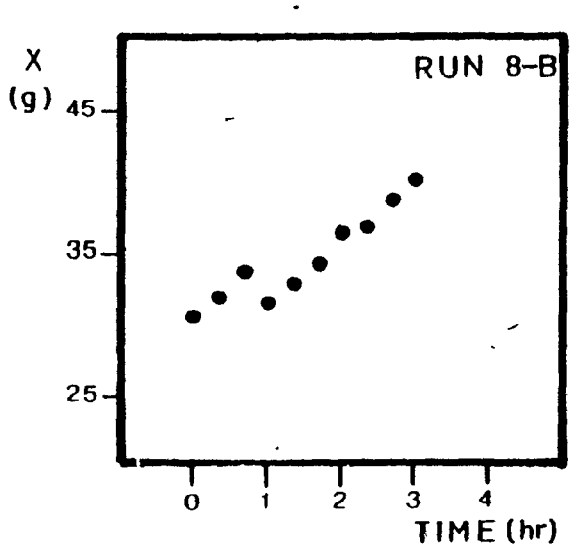

Fig. (4-14):
Run # 8-b, Total biomass versus time.

Apparently the step change in pH induced changes in the environmental conditions of the biological system. The effects of these changes are to be seen as induced changes in the overall yield, inhibition or even changes in the kinetic parameters. Despite all these possible changes the system recovered in terms of cell concentration, as anticipated since a feedback controller is used. More specifically, the abrupt drop in cell concentration following the acid addition suggests that a percentage of the biomass was killed and decomposed to such a degree that could not be identified by the cell concentration measurement technique used. This is clearly shown in Fig. (4-14) where the total biomass in the vessel is plotted versus time. A very simple model of the previous phenomenon can be based on death of a percentage of the cells present in the vessel, i.e. a displacement downward in x. The control response would be such as to restore equilibrium. This particular simulation is shown in Fig. (4-13). One should expect higher discrepancy between the simulated and the actual recovery, as the decomposed cells are nutrient source for the remaining biomass [11].

Finally, the fact that cells continued to grow at pH 3.6 is confirmed by other workers as well [12].

(b) System behaviour under stochastic disturbances

A control system in general is designed to give a satisfactory response to deterministic upsets, with the implicit assumption that if it can adequately respond to these, it will adequately respond to most stochastic disturbances encountered in practice.

Modern stochastic control theory suggests a completely different approach to controller design utilizing the properties of auto and partial correlation functions of the stochastic disturbances [3].

An optimal stochastic controller in general is designed in such a way that it minimizes the variance of the output. If such a controller is used, the auto and partial correlations of the output deviations (error) should be all zero after K lags (periods), where K is the periods of delay in the system.

Using the data from run # 2, the control system used in this study was tested by comparing its response to a minimum variance stochastic controller. In run # 2, from the very beginning, the system was kept in a QSS in the vicinity of 6 g/l to examine whether the controller would drift off the set-point over a period of time. As shown in Fig. (4-15), where x versus time is plotted, it did not. The output deviations from the desired value, x_D, in this run were obviously due to stochastic disturbances. The observed scatter in the data raises the plausible question whether the scatter is due to the experimental error in the measured variable exclusively, or not. The fact that the standard deviation of the output is 0.146, that is 2.7%, slightly higher than the standard error of measurement, which is 2.2%, suggests that the implemented controller was able to compensate stochastic disturbances very well.

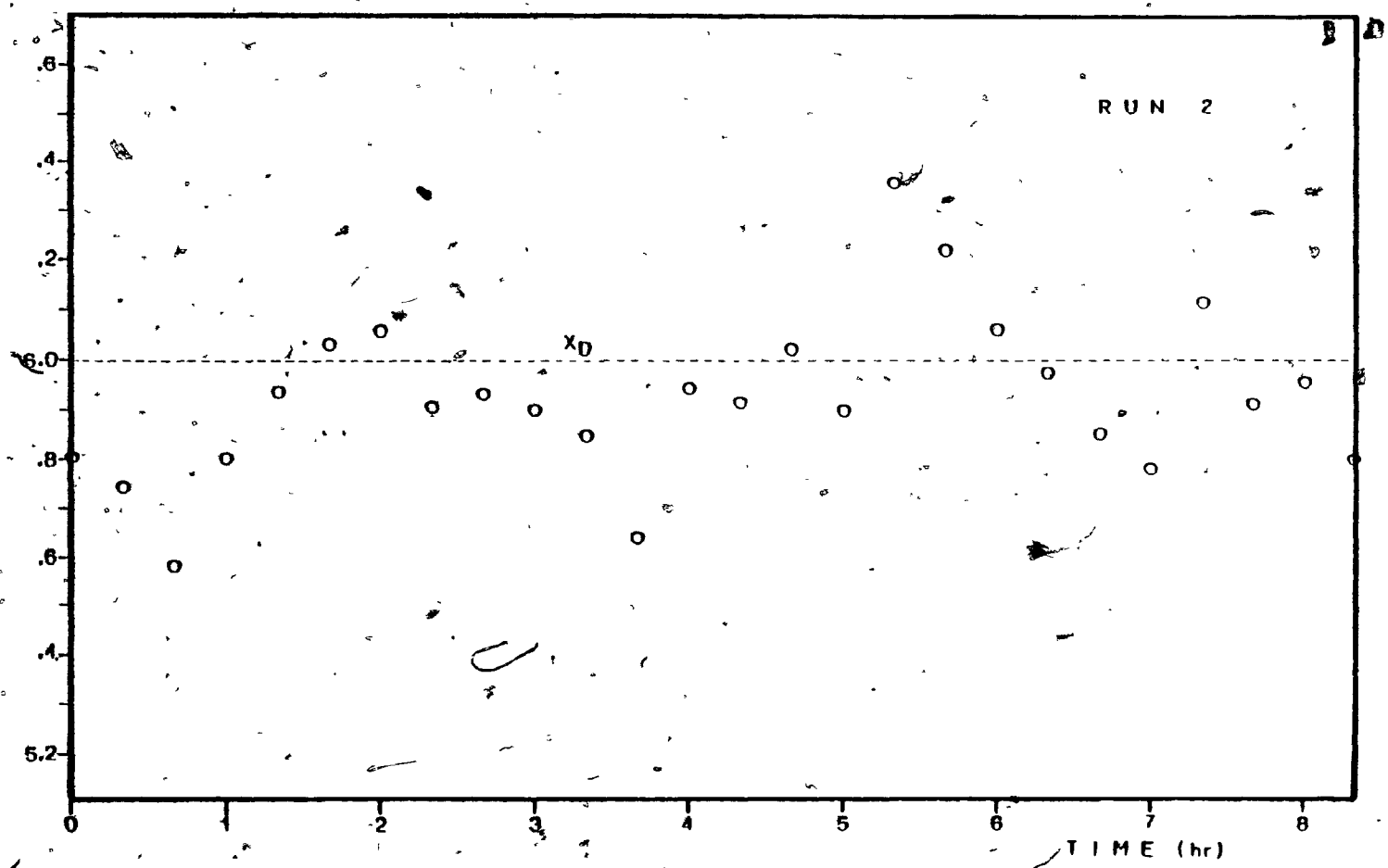

Fig. (4-15): Run # 2, x versus time.

The above conclusion is supported more rigorously as follows: Noting that $sl = k_c (x_D - x) + \overline{sl}$, the error can be calculated from :

$$\text{ERROR} = \frac{sl - \overline{sl}}{k_c} \qquad (4\text{-}3)$$

having in mind that saturation did not occur in this run. Thus, given the error series the auto and partial correlations were calculated and plotted, as shown in Fig. (4-16). The fact that the correlations are nonzero only at lag K = 1, suggests that the controller behaves like a minimum variance stochastic controller, taking also into consideration that one period delay was introduced to the system by the cell concentration measurement technique. Furthermore, the fact that the standard deviation of the output series is only slightly higher than the standard error of measurement supports the above, having in mind that the standard deviation of the output is equal to the standard error of measurement only in the case where all correlations at lags K > 0 are zero. However, there are some doubts, since the amount of data was not sufficiently large, although chi-square statistics were satisfactory.

From the above analysis it follows that it may not be possible to improve the controller performance by minimum variance control techniques.

In Appendix D, listing of the main program and the output are available. The subroutines which calculate the auto and partial correlationswith the relevant theory can be found in [3].

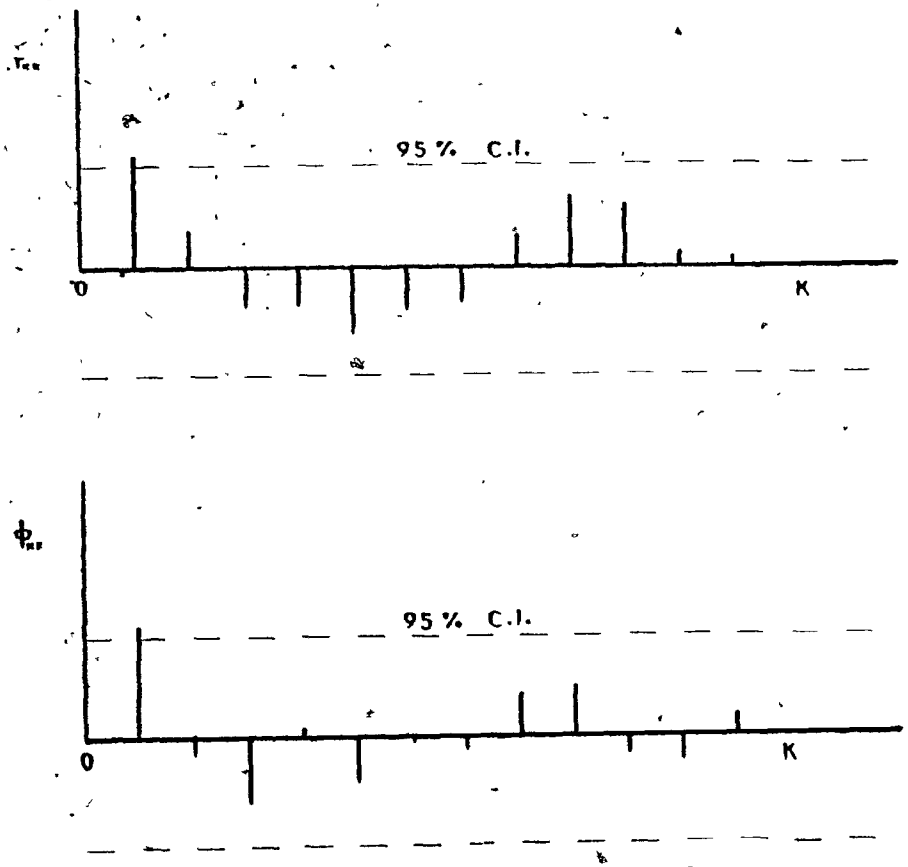

Fig. (4-16): Run # 2, auto and partial correlations of the data.

4.1.5 NON-LINEARITIES OF THE SYSTEM

An idea of how nonlinear a system is can be obtained from a fractional completion versus time plot, where step changes of different magnitude are applied. The closer to linear behaviour a system is, the more the fractional completion curves tend to coincide.

In run # 1 the system was in a QSS in the vicinity of 5 g/l and at time zero, a step change in the desired cell concentration of 2 g/l (x_D = 7 g/l) was performed. In Fig. (4-17) the transient response of the system is shown. Cell concentration moved up to 7 g/l in approximately 5 hr, which is approximately double the time required by the system to move up by 1 g/l. In Fig. (4-18) the fractional completion curves for run # 1 (Δx_D = 2 g/l), run # 3 (Δx_D = 1 g/l) and run # 6 (Δx_D = .40 g/l) are shown. It is seen that all three curves are quite apart indicating that the system is highly nonlinear. The fact that during all three transients no saturation in the controller occurred suggests that the nonlinear behaviour is due to the nature of the process exclusively.

This can also be seen analytically:
Since the specific growth rate, μ, is constant throughout the transient because of the non-interactive properties of the control system, substituting D (equation 2-21) and s1 (equation 2-19), into $\frac{dx}{dt} = (\mu - D)x$, it yields after integration to:

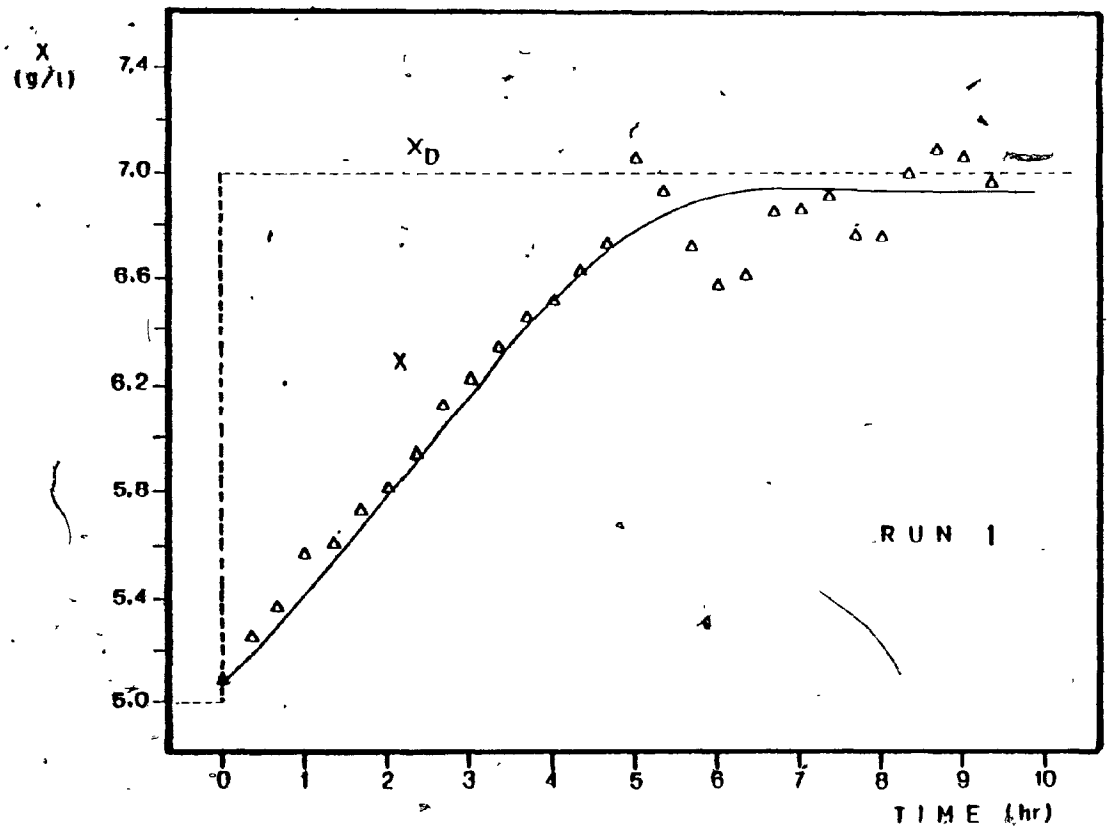

Fig. (4-17): Run # 1, x versus time (—— simulation, Δ x-data).

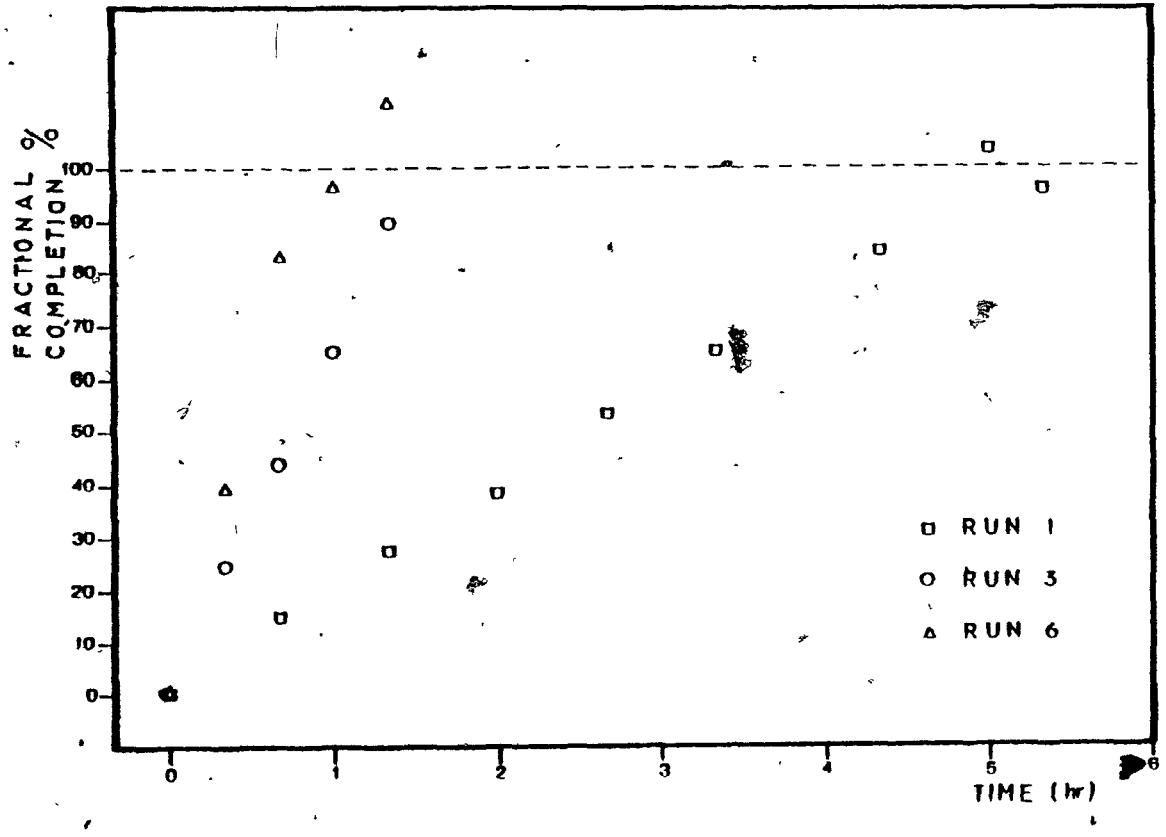

Fig. (4-18): Fractional completion curves for runs # 1, # 3 and # 6.

$$\frac{x}{x_D}\left(\frac{x_D - x_0}{x_0 - x}\right)^{\frac{1}{1+kY}} = e^{\mu(t - t_0)} \qquad (4\text{-}4)$$

Letting t_f be the time required to move x from x_0 to $x_f = .978\ x_D$ (a standard error of measurement away from the target), the following results, as shown in Table 4-II, are obtained for different starting points. Thus the non-linear nature of the process becomes apparent.

TABLE 4-II

$x_D - x_0$ (g/l)	t_f ** (hr)
.5	1.3
1.0	2.6
1.5	3.8
2.0	5.0

** calculated at the nominal conditions:

$x_D = 7$; $Y = 50\%$; $k = .30$; $k_2 = .15$; $D \simeq \mu = .100$

4.2 SUBSTRATE CONCENTRATION TRANSIENTS

The biological process examined in this work is modelled as a two input two output system. This being the case, the closed loop response of the system to both set point changes x_D and s_D (or better $\hat{\sigma}$) should be investigated. Step changes in the desired cell concentration, x_D, have already been considered in the previous sections. Therefore, step changes in $\hat{\sigma}$ are left to be examined.

According to the analysis presented in Chapter 2, step changes in $\hat{\sigma}$ should cause very fast substrate concentration transients while cell concentration is kept constant at the desired cell concentration. Since the specific growth rate μ is a function of substrate concentration, the changing levels in s should force the specific growth rate, μ, to move up or down to different levels. This can be seen as changes in the slope on plots of ln X versus time.

In run # 5, shown in Fig. (4-19), starting with an initial cell concentration of 5.7 g/l the system was forced to move to a QSS in the vicinity of 6 g/l. The system reached QSS in one hour and it was kept there for two additional hours. At time 3.33 hr a step change in $\hat{\sigma}$ from .190 hr^{-1} to .130 hr^{-1} was performed. As shown in Fig. (4-20), the step in $\hat{\sigma}$ forced substrate concentration to a lower level, corresponding to a smaller value in specific growth rate. At time 4.66 hr and thereafter step changes in $\hat{\sigma}$ were performed every hour. The resulting changes in the specific growth rate are shown in Fig. (4-20).

The actual uptake rate, σ, during the above step changes can be estimated as μ/Y. The overall yield, Y, can be obtained as the slope of the regression line on a plot of total biomass versus total glucose fed (Fig. 4-21)). Comparing σ and $\hat{\sigma}$, shown in Table (4-III), it is seen that they are in agreement. However, the low yields and specific growth rates that occurred at $\hat{\sigma}$ = .130 cannot be explained. Contrary to this occurrence,

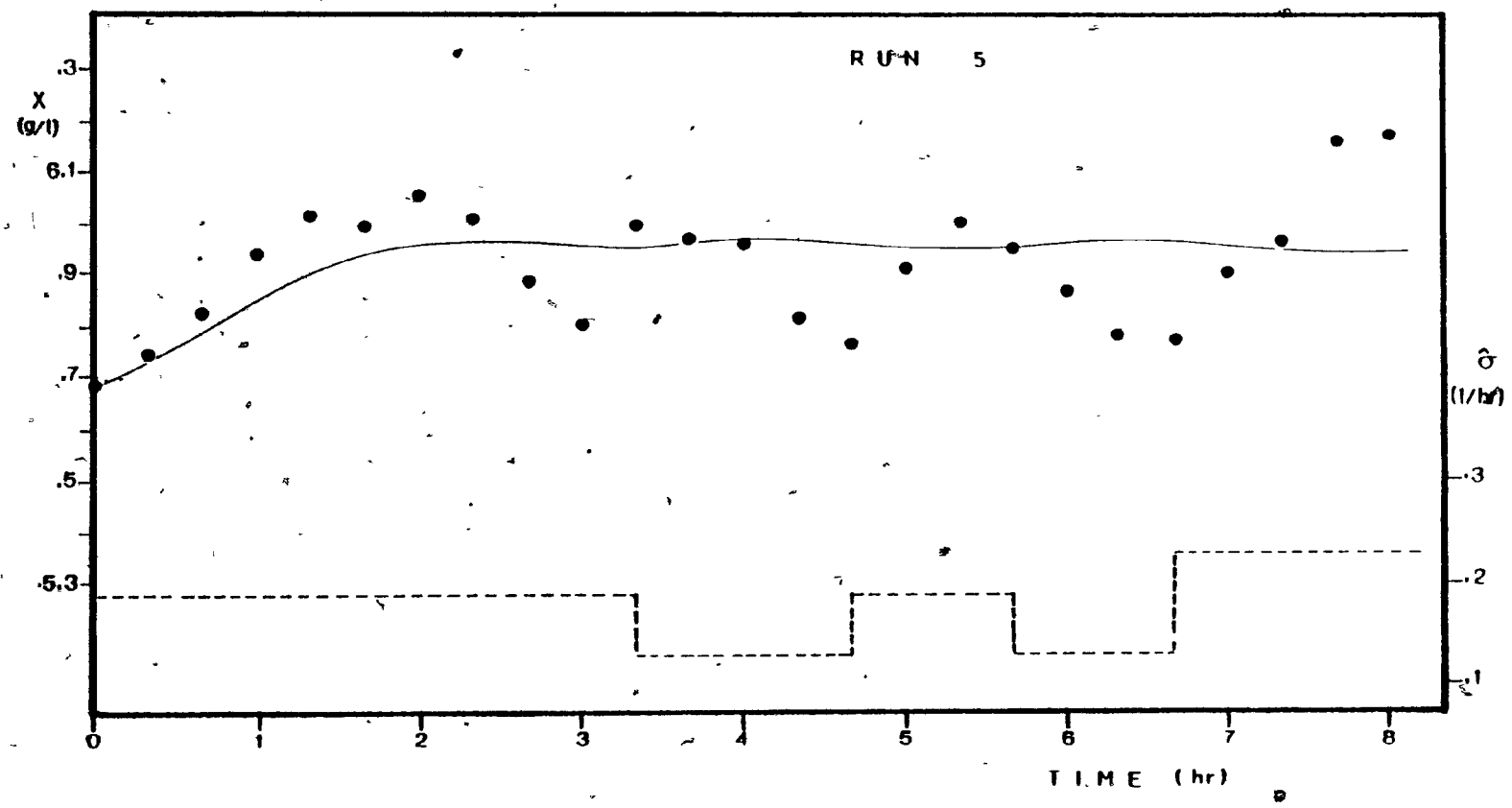

Fig. (4-19): Run # 5, x versus time (—— simulation, • x-data).

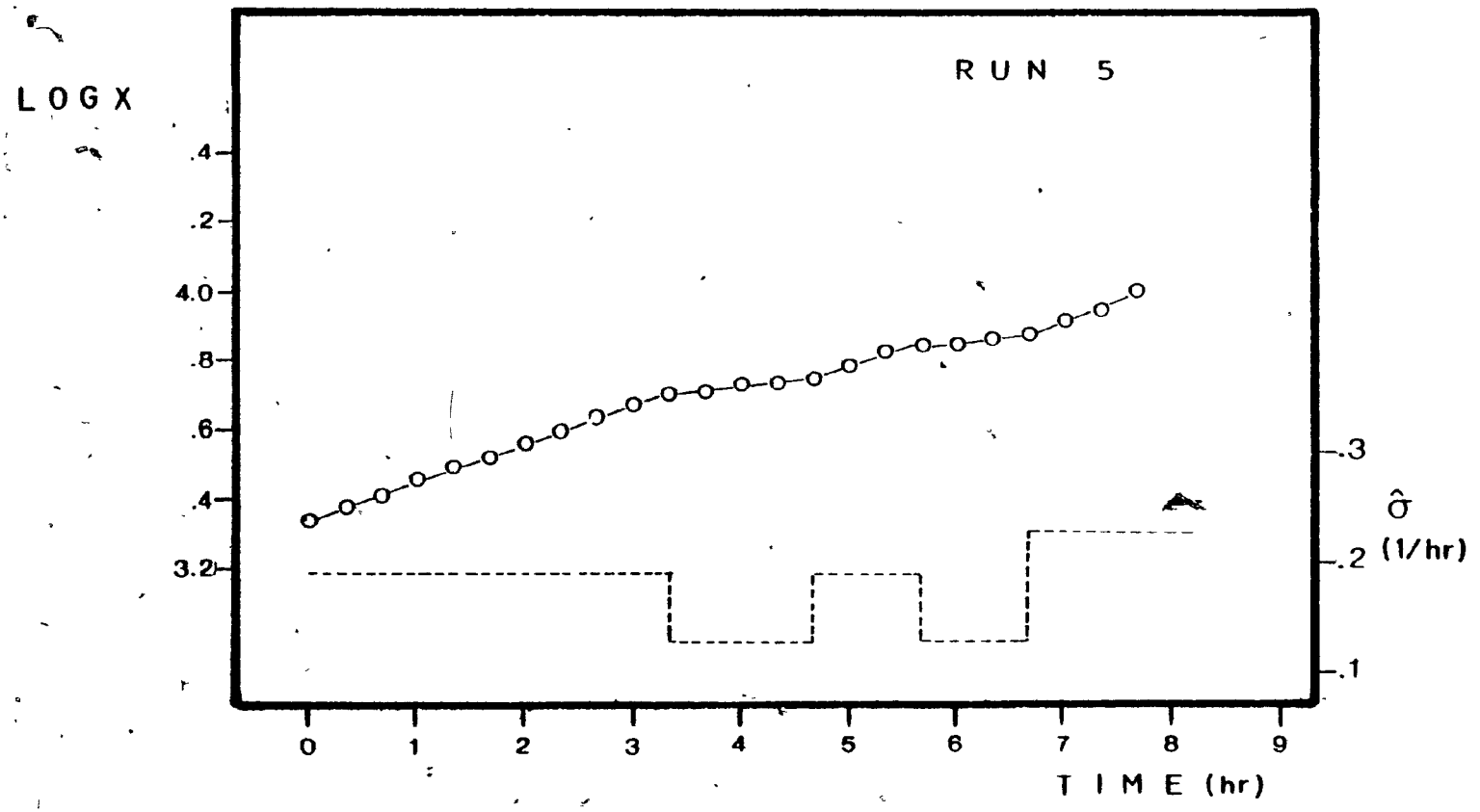

Fig. (4-20): Run # 5, ln X and $\hat{\sigma}$ versus time.

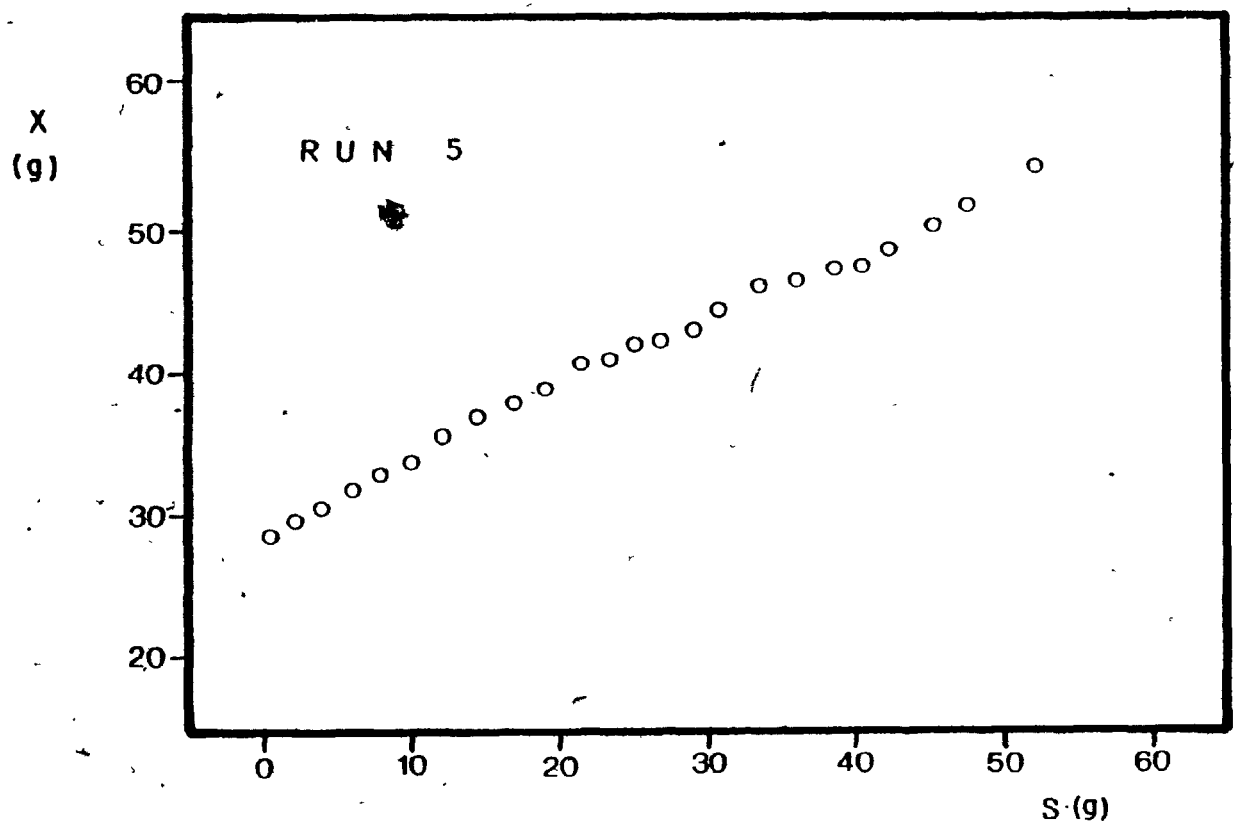

Fig. (4-21): Run # 5, total biomass X, versus total glucose fed, S.

one should expect higher yields at lower specific growth rates where the glucose effect is diminished.

The results from the previous experiment have shown that the control system was able to force substrate concentration to reach different levels. However, whether noninteraction was achieved during these transients, i.e., whether cell concentration was kept constant while substrate concentration was changing, should be examined.

As already discussed in Chapter 2, without the control system substrate concentration transients will induce very long but small in magnitude cell concentration transients. Therefore, since the experimental error in cell concentration measurement is of the same order, large step changes in $\hat{\sigma}$ should be performed if interaction is to be seen.

In run # 4-b, shown in Fig. (4-22), starting at a QSS in the vicinity of 6 g/l at time 40 minutes, a large step change in $\hat{\sigma}$ was performed (from .185 hr^{-1} to .370 hr^{-1}, i.e. a 100% step in $\hat{\sigma}$). Cell concentration was definitely affected. However, from Fig. (4-23) it is seen that the specific growth rate after the step in $\hat{\sigma}$ was practically zero for approximately one hour. This means that during that hour the microorganisms stopped growing, i.e., the overall yield was approximately zero (Fig. (4-24)). At time 1.66 hr the cells started growing again at a higher specific growth rate, implied by the higher $\hat{\sigma}$. Comparing

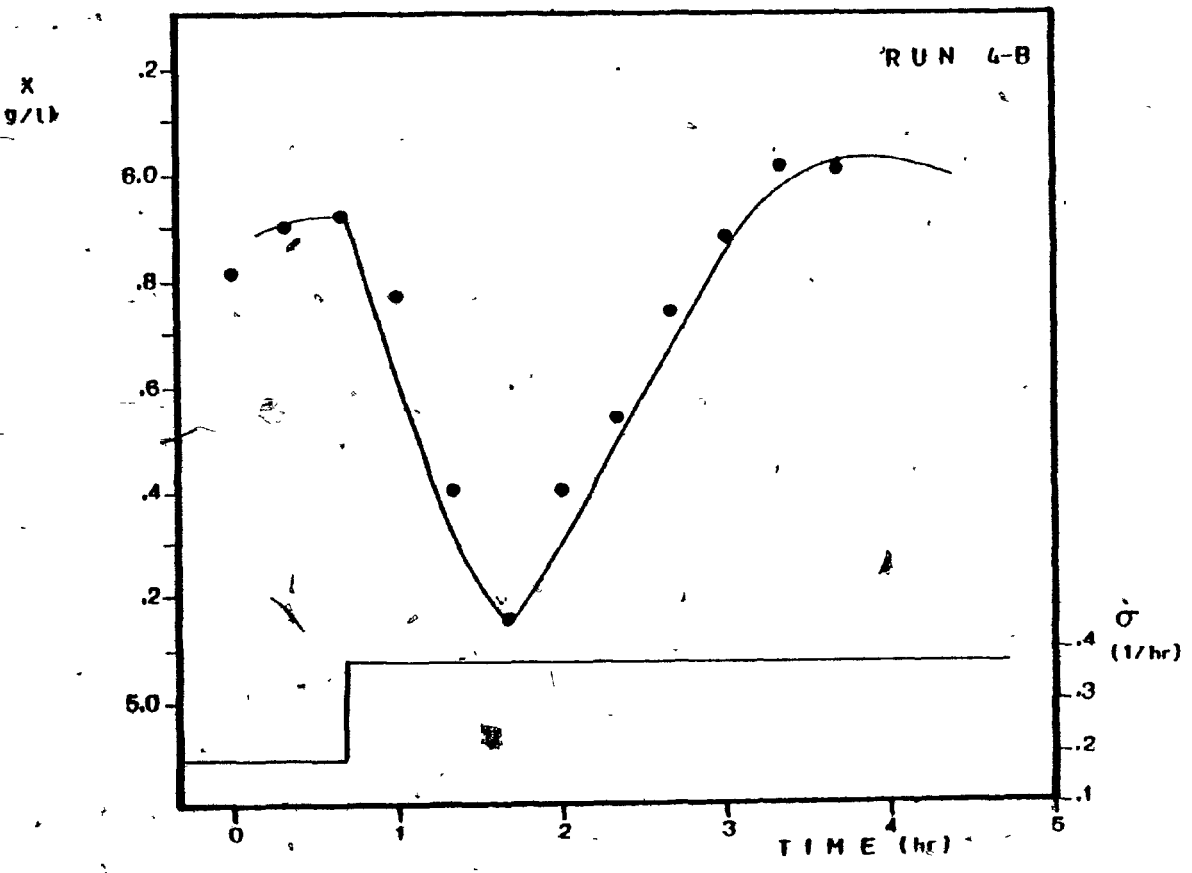

Fig. (4-22): Run # 4-b, x versus time (—— simulation, ● x-data).

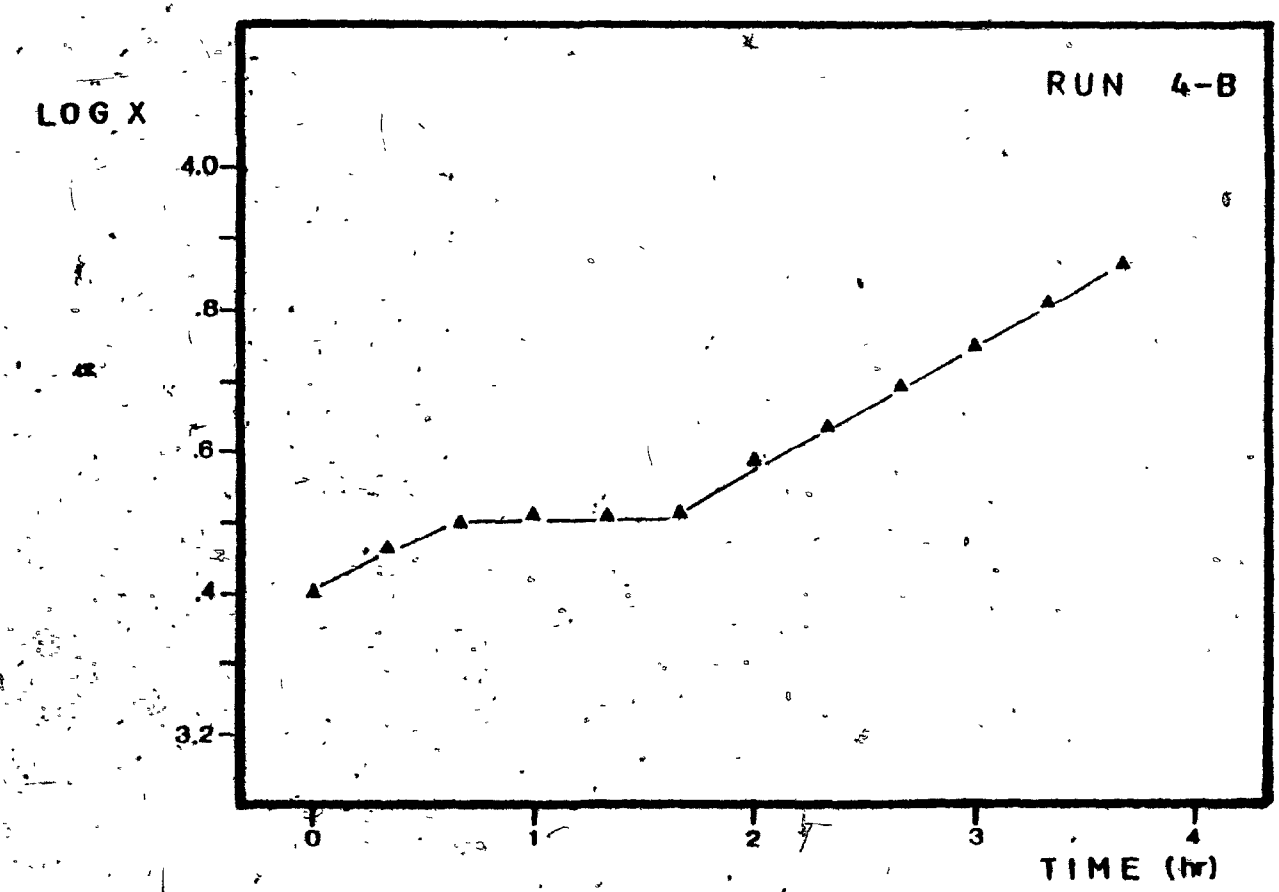

Fig. (4-23): Run # 4-b, ln X versus time.

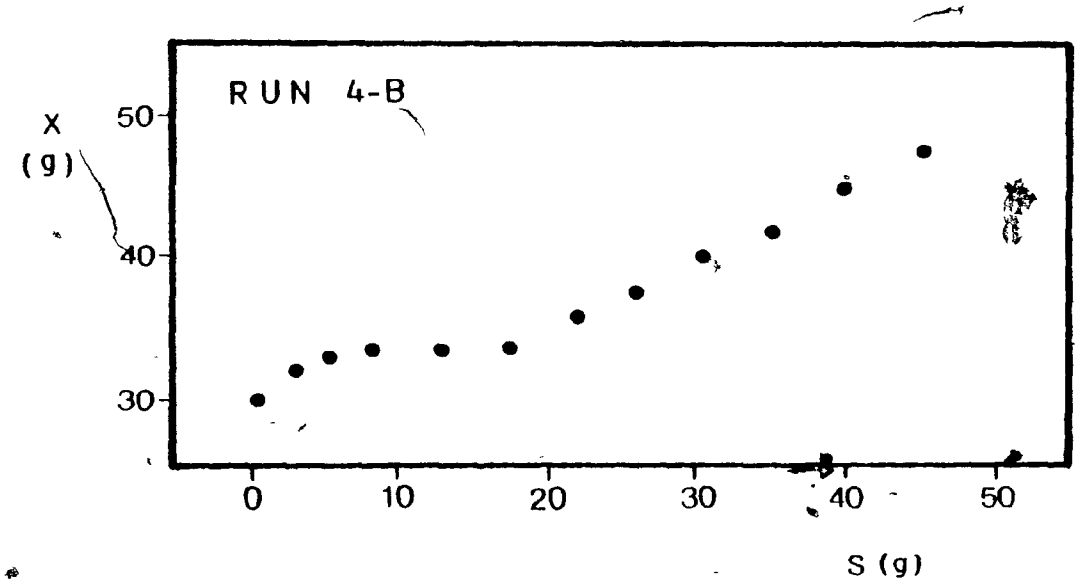

Fig. (4-24): Run # 4-b, total biomass, X, versus total glucose fed, S.

TABLE (4-III) **

μ	Y'	σ	$\hat{\sigma}$
.110	.57	.193	.190
.030	.23	.130	.130
.112	.61	.183	.190
.032	.26	.123	.130
.132	.58	.227	.288

TABLE (4-IV) **

μ	Y	σ	$\hat{\sigma}$
.127	.63	.202	.185
.179	.49	.365	.370

** All parameters excluding Y in hr^{-1}.

σ and $\hat{\sigma}$, shown in Table (4-IV), it is seen that the actual uptake rate before the step is overestimated while it is in satisfactory agreement following the step.

Summarizing, the large step change in $\hat{\sigma}$ produced changes in the overall yield which may be considered an imposed disturbance on the controlled system. Therefore, the response of the system may be considered as the response to a simultaneous step change in $\hat{\sigma}$ and an imposed disturbance. This particular response is simulated and shown in Fig. (4-22).

The previous effect of sudden changes in substrate concentration on cell growth has been confirmed in similar biological systems. It is found experimentally that shift experiments from one steady state to another in chemostat cultures cannot be described by the Monod equation. An empirical delay relation has been proposed to describe the response of cell growth to rapid changes [10]. Inhibition in cell growth may in addition occur as a result of cell age distribution and rapid changes in pH, temperature or dissolved oxygen [10].

4.3 PARAMETER ESTIMATION

As already shown, the specific growth rate is given by the slope of the regression line that fits the data on plots of ln X versus time. Similarly, the overall yield, Y, is estimated as the slope on plots of total biomass, X, versus total glucose fed, S.

Given the estimates of μ and Y, the actual specific uptake rate, σ, is calculated as μ/Y. This σ is to be compared with $\hat{\sigma}$, the desired uptake rate. In Table (4-V) μ, Y, σ, $\hat{\sigma}$ and $\hat{Y}$ are tabulated for all runs where $\hat{\sigma}$ was kept constant. $\hat{Y}$ is the assumed overall yield needed for the estimation of $\overline{sl}$, the substrate concentration in the feed at the QSS. The plots used for the estimation of μ and Y are available in Appendix E.

It is seen from Table (4-V) that σ and $\hat{\sigma}$ match satisfactorily, having in mind that a small difference between σ and $\hat{\sigma}$ should occur as in the estimation of $\overline{sl}$ the assumed overall yield, $\hat{Y}$, is different from the actual yield, Y. This is due to the fact that substrate control is not based on a direct measurement of substrate concentration and therefore errors in the process model will translate into response errors in the controlled system.

Parameter estimation of runs # 4-b and # 5, where step changes in $\hat{\sigma}$ were performed, has been considered in previous sections. The remaining run # 6, discussed in detail in the following section, is considered here.

The values of μ , Y and σ estimated after each step change in the desired uptake rate, together with $\hat{\sigma}$ and $\hat{Y}$ are tabulated in Table (4-VI). The overall yield, Y, in this run was practically constant at both high and low specific uptake rates, while in run # 5, which was similar to run # 6, very low yields occurred at low specific uptake rates. It is also seen that σ and $\hat{\sigma}$ match satisfactorily in this run as well.

TABLE (4-V) **

Run #	μ	Y	σ	$\hat{\sigma}$	$\hat{Y}$
1	.0835±.001	.56±.005	.149±.002	.156	.63
2	.1036±.002	.61±.012	.170±.005	.176	.565
3	.1008±.001	.56±.008	.180±.003	.185	.54
7	.0953±.005	.49±.023	.194±.014	.185	.54
8-a	.1085±.004	.57±.018	.190±.009	.185	.55

TABLE (4-VI) **

μ	Y	σ	$\hat{\sigma}$	$\hat{Y}$
.107±.002	.55±.010	.194±.005	.190	
.071±.008	.55±.010	.129±.008	.130	
.101±.004	.55±.010	.184±.006	.190	.54
.073±.007	.55±.010	.133±.008	.130	
.154±.004	.69±.008	.223±.005	.228	

** All parameters excluding Y in hr^{-1}

4.4 SUBSTRATE CONCENTRATION DATA

As already mentioned, difficulties were encountered in obtaining reliable substrate concentration measurements. A detail description of the problem is presented in this section.

The colormetric analysis used to measure substrate concentration, as explained in Appendix A, requires biomass free solution. Therefore all samples taken from the fermentor should be filtered. The total time required to remove the cells from the moment the sample is taken is approximately 50 to 60 seconds. During this time the cells are growing on glucose, dropping significantly the level of glucose concentration in the sample.

A quantitative expression of the introduced error versus filtering time is obtained, integrating simultaneously the governing equations:

$$\frac{dx}{dt} = \mu x \qquad (4\text{-}5)$$

$$\frac{ds}{dt} = -\sigma x \qquad (4\text{-}6)$$

In Table (4-VII), the results from the above integration are shown at the nominal condition: $x = 7$ g/l, $s = .080$ g/l, $Y = .50$, $k_1 = .30\ hr^{-1}$ and $k_2 = .15$ g/l. It is seen that after 60 seconds substrate concentration is underestimated by 35%. As cell concentration remains practically constant, numerical integration can be avoided by elimination of equation (4-5).

Integrating equation (4-6) backwards from s to s_m, the measured substrate concentration, after overall filtering time, Δt, it yields:

$$\int_{s_m}^{s} \frac{k_2 + s}{k_1 s}\, ds = \int_{\Delta t}^{0} -\frac{x}{Y}\, dt$$

$$\frac{k_2}{k_1} \ln \frac{s}{s_m} + \frac{s - s_m}{k_1} = \frac{x}{Y} \Delta t$$

$$\frac{k_2}{k_1} \ln\left(\frac{s - s_m}{s_m} + 1\right) + \frac{s - s_m}{k_1} = \frac{x}{Y} \Delta t$$

since $\left|\frac{s - s_m}{s_m}\right| \ll 1$, when Δt is small, it follows that

$\ln\left(\frac{s - s_m}{s_m} + 1\right) \simeq \frac{s - s_m}{s_m}$. Substituting, the following simple correction formula is obtained:

$$s = s_m + \frac{x \Delta t}{Y} \frac{k_1 s_m}{k_2 + s_m} \qquad (4\text{-}7)$$

In Table (4-VII) the predicted error from the above formula versus time is shown as well.

The above considerations were experimentally verified. In run # 6, shown in Fig. (4-25), the system was forced to a QSS in the vicinity of 5.5 g/l and thereafter step changes in $\hat{\sigma}$ were performed every 1.33 hours. In Fig. (4-26) the glucose

TABLE (4-VII)

Δt (sec)	Error in s (mg/l)	Predicted error in s from equation (4-7) (mg/l)
0	0	0
5	2.6	2.6
10	5.1	5.0
15	7.6	7.3
20	10.0	9.6
25	12.4	11.7
30	14.8	13.8
35	17.1	15.8
40	19.3	18.0
45	21.5	19.6
50	23.6	21.1
55	25.7	22.7
60	27.7	24.1

concentration measurements are shown which were obtained with an average filtering time of 60 seconds. As anticipated, most of the measurements are underestimated assuming that the performed simulation, with the nominal parameter values (k_1 = .30 and k_2 = .15), represents closely the true levels of substrate concentration. In the same figure the corrected concentration measurements are shown as well, which match the predicted levels within two times the standard error of measurement [13].

The existing discrepancies at times 5.66 and 6.00 hours may be explained by the way in which the implemented control system functions. Whenever inhibition in cell growth occurs substrate should accumulate in the vessel rather than stay at a constant concentration since the control system, ignoring inhibition, keeps on feeding substrate into the fermentor. Therefore, the observed discrepancies may be considered a result of occurred inhibition, probably due to cell age distribution. It appears that substrate concentration might be in a transient, dropping towards the level measured at times 3.00 and 3.33 hours.

In Fig. (4-27) and (4-28) glucose concentration measurements are shown from runs # 8-a and # 9 respectively, where the overall filtering time was reduced to less than 5 seconds. It is seen that measured and predicted concentration levels match satisfactorily.

From the previous analysis and the fact that the amount of reliable substrate concentration data is limited, it is seen why

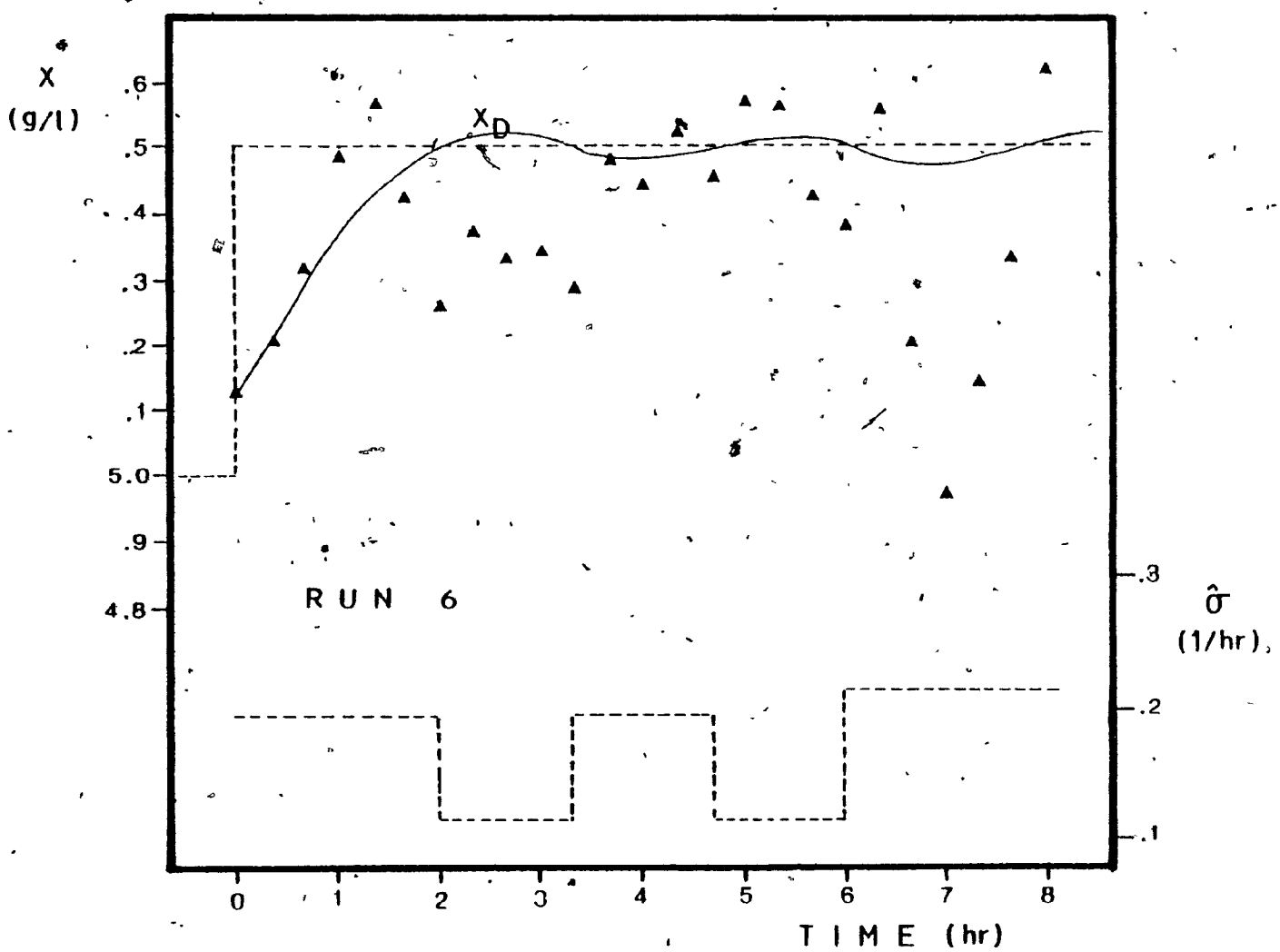

Fig. (4-25): Run # 6, x versus time (—— simulation, ▲ x-data).

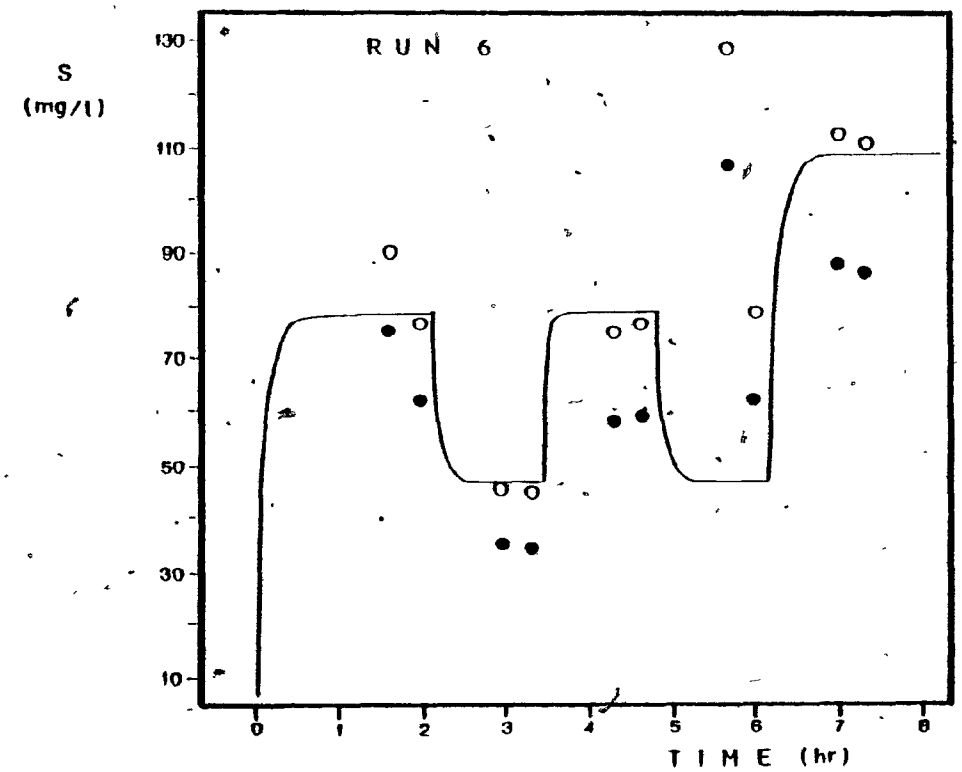

Fig. (4-26): Run # 6, substrate concentration versus time (—— simulation, ● measured S-data, O corrected measurements).

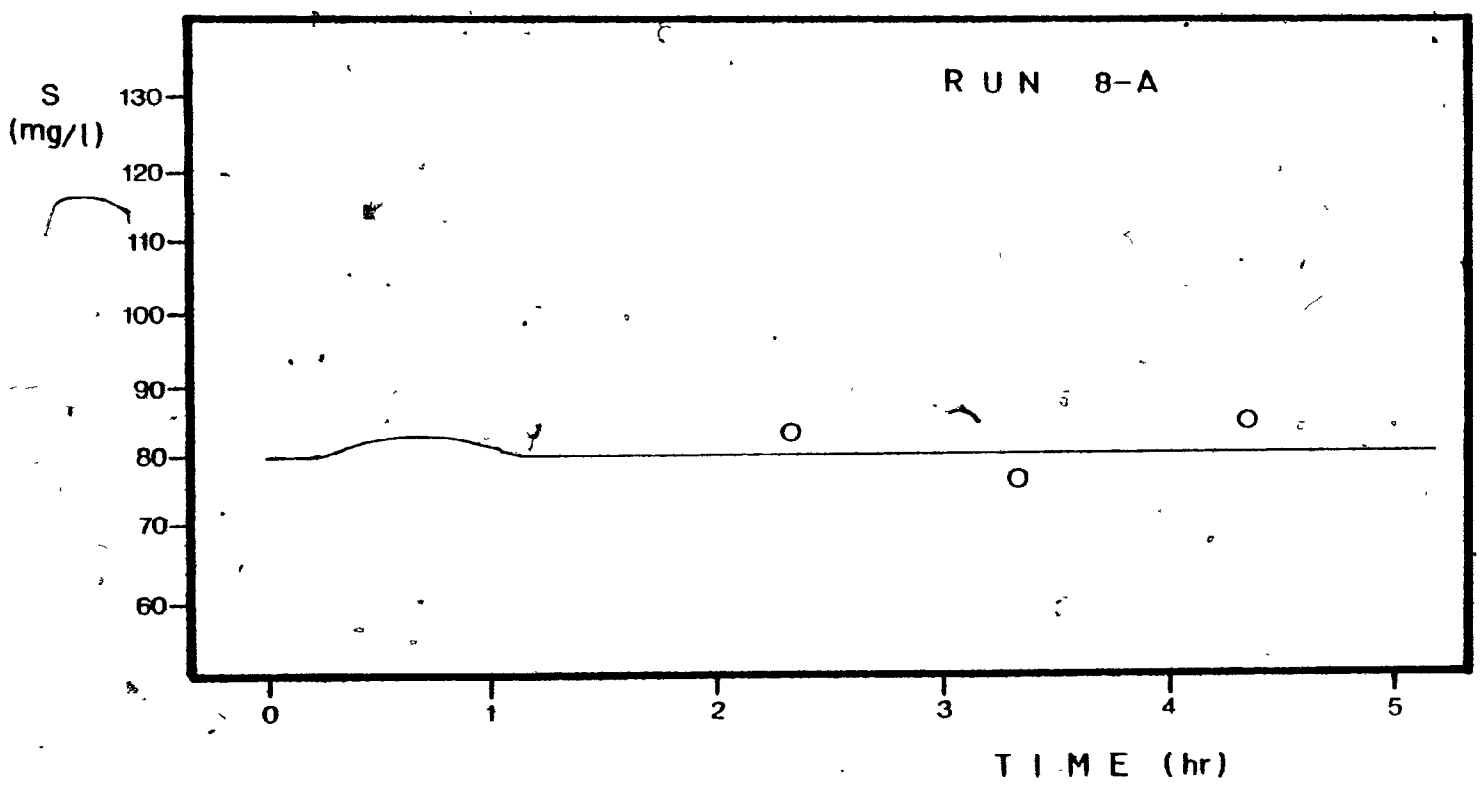

Fig. (4-27): Run # 8-2, substrate concentration versus time (—— simulation, O s-data).

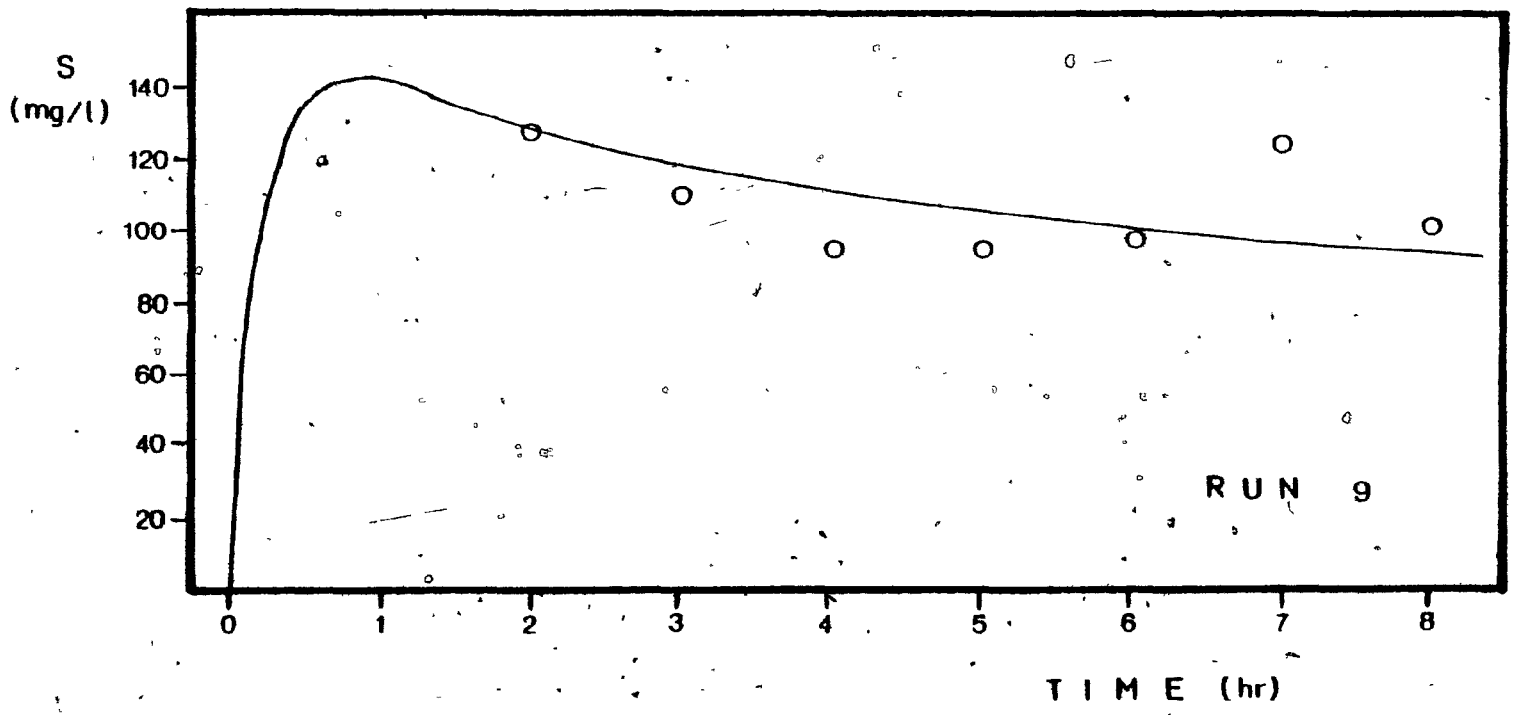

Fig. (4-28): Run # 9, substrate concentration versus time (—— simulation, O s-data).

non-interaction and substrate concentration transients were shown indirectly by use of cell concentration data only.

Furthermore, the kinetic parameters k_1 and k_2 in Monod equation could not be reliably estimated. A large amount of data is required because the structure of the Monod equation is such that small errors in s will translate into large errors in the estimates of k_1 and k_2. This is illustrated with a particular example shown in Table (4-VIII).

TABLE V-III

μ	s	k_1	k_2
(.106, .144)	(.086, .150)	.278	.139
(.106, .144)	(.090, .150)	.312	.175

An error of 4% in s produces errors of 12% and 25% in the estimates of k_1 and k_2 respectively.

In conclusion, further work is needed in this area to directly evaluate the substrate response of the control system.

CHAPTER 5: CONCLUSIONS AND RECOMMENDATIONS

5.1 CONCLUSIONS

(a) Cell concentration

- The implemented control system was able to reduce cell concentration transient response from approximately 25 hours to 2.5 hours, that is by a factor of 10. In addition, the required volume expansion is very small, making possible the observation of different QSS's in a single run.
- Due to the non-interactive control properties of the control system cell concentration transients did not induce transients in substrate concentration even when the control outputs reached physical limits.
- The control system was able to compensate for different kinds of disturbances which would drive cell concentration away from the desired value.
- The highly nonlinear nature of the process was experimentally confirmed. More specifically, the total time required for the completion of a transient was found to be proportional to the magnitude of the step in x_D performed.

(b) Substrate concentration

- The control system was able to move substrate concentration to different levels, forcing the cells to grow at specified constant growth rates.
- There are indications that non-interaction was preserved when small steps in substrate uptake rate were performed,

however, for large steps interaction did occur. An empirical delay relation may be used to describe the response of cell growth to rapid changes in substrate concentration.

(c) Yield

- Overall yields of 50 to 60% were obtained in all runs, even at high substrate uptake rates or lower pH.

5.2 RECOMMENDATIONS FOR FURTHER WORK

(a) Control system

- To improve the efficiency of the control system a continuous cell concentration measurement technique should be used. This way output oscillations about the desired value will be eliminated since the continuous version of the controller may be used without any delay in the feedback path, besides the noise reduction which will result in a tighter control. The use of spectrophotometer or turbidmeter with the possibility of on line calibration may be considered.
- Having established a reliable substrate concentration measurement, it is recommended that the substrate response of the control system be examined in detail.

(b) Biological system

- Since the economics of yeast production depend heavily upon the overall yield coefficient, it is of primary importance to the industry to examine how the overall yield depends on

substrate concentration, D.O., temperature and pH. This can be done performing a set of experiments where the response of the system is observed to step changes in each one at the above parameters while all the rest are kept constant.

- Further, collecting sufficient substrate concentration data, the kinetic parameters k_1 and k_2 can be estimated very reliably since the control system can hold the specific growth rate, μ, constant at any desired level.
- Finally, the indication of lag phase in the growth rate may be investigated performing large steps in the substrate uptake rate, $\hat{\sigma}$.

CHAPTER 6: BIBLIOGRAPHY

1. AIBA, S., et al., "Fed-batch culture of Saccharomyces cerevisiae: A perspective of computer control to enhance the productivity in bakers' yeast cultivation", Biotech. and Bioeng., 18, 1001-1016 (1976).

2. BIJKERK, A.H.E. and R.J. HALL, "A mechanistic model of the aerobic growth of Saccharomyces cerevisiae", Biotech, and Bioeng. 19 , 267-296 (1977).

3. BOX, G.E.P. and G.M. JERKINS, "Time series analysis: Forecasting and control", Holden Day Inc., San Francisco, (1976).

4. BOYLE, T.J., "Control of the quasi-steady state in fed-batch fermentation", 2nd International conference on computer applications in fermentation technology, University of Pennsylvania, Philadelphia, PA, (August 1978).

5. BOYLE, T.J., "A control system for fed-batch fermentation", Proceedings of the Joint Automatic Control Conference, ISA, Pittsburgh, PA (1978).

6. BOYLE, T.J., H. FRANKLIN and G. COLLINS, "A low cost minicomputer control system", AIChE 74th National meeting, Houston, Texas (1974).

7. BOYLE, T.J., H. FRANKLIN and G.C. BOGIE, "Computer control of small processes", Proceeding of the Symposium on Computers, Electronics and Control, ACTA Press, Calgary (1976).

8. COONEY, C.L., et al., "Computer aided material balancing for prediction of fermentation parameters", Biotech. and Bioeng., 19 , 55-67 (1977).

9. DATCON SYSTEM software package, Computer Inquiry Systems, Inc., Fort Lee, N. Jersey (1977).

10. DUNN, I.J. and J.R. MOR, "Variable volume continuous cultivation", Biotech. and Bioeng., 17, 1805-1822, (1975).

11. EDWARDS, V.H., et al., "Extended culture: The growth of Candida Utilis at controlled acetate concentrations", Biotech. and Bioeng., 12, 975-999 (1970).

12. EROSHIN, V.K., et al., "Influence of pH and temperature on the substrate yield coefficient of yeast growth in a chemostat", Biotech. and Bioeng., 18, 289-295 (1976).

13. GLUCOSE, H K , enzymatic quantitation of glucose by hexokinase, Fisher diagnostics, part No. 18321.

14. LIM, H.C., et al., "An analysis of extended and exponentially fed-batch cultures", Biotech. and Bioeng., 19, 425-433, (1977).

15. PERINGER, P., et al., "Mathematical model of the kinetics of growth of Saccharomyces cerevisiae", Biotech. and Bioeng., Symp. No. 4, 27-42 (1973).

16. PERINGER, P., et al., "A generalized mathematical model for the growth kinetics os Saccharomyces cervisiae with experimental determination of parameters", Biotech. and Bioeng., 16, 431-454 (1974).

17. PIRT, S.J., "The theory of the fed-batch culture with reference to the penicillin fermentation", J. Appl. Chem. Biotechnol., 24 , 415-424 (1974).

18. REED, G. and H.J. PEPPLER, "Yeast Technology", Avi publishing company, Inc., (1973).

19. SUOMALAINEN, H., "Changes in the cell constitution of bakers' yeast in changing growth conditions", Pure Appl. Chem., 7, 639-651 (1963).

20. WANG, H.Y., et al., "Computer-aided bakers' yeast fermentations", Biotech. and Bioeng., 19, 69-86 (1977).

21. WHITE, J., "Yeast Technology", Chapman and Hall, Inc., London (1954).

22. YOSHIDA, F., et al., "Fed-batch hydrocarbon fermentation with colloidal emulsion feed", Biotech. and Bioeng., 15, 257-270 (1973).

APPENDIX A: FURTHER ASPECTS OF IMPLEMENTATION

A-1 EXPERIMENTAL APPARATUS

A.1.1 THE FERMENTOR

A New Brunswick Scientific Company (New Brunswick, N.J.), laboratory fermentor with a 14 liter total capacity Pyrex glass vessel was used throughout this study, Fig. (A-1). The vessel has an internal diameter of 21 cm and stands 45.7 cm high.

The medium in the fermentor was agitated by two, four bladed turbine impellers, each 12 cm in diameter. The impellers were driven by a 1/3 HP Ball Bearing motor capable of speeds between 100 and 950 rpm.

There are four hollow baffles to break up the flow pattern of the broth. Each is 0.5 cm thick and 2.3 cm wide.

The temperature in the fermentor was controlled by circulating alternately either hot or cold water through two of the hollow baffles. A thermistor was used to sense the temperature in the vessel. When cooling was needed, cold tap water was allowed to flow through the baffles. The heating portion of the cycle involved shutting off the inlet tap water and then allowing the water to circulate internally through a heater. Temperature variations in the fermentor when controlled were within 1.3°C.

The third baffle acted as piping for air to the simple orifice sparger (2.5 mm) which was located directly beneath the impeller

FIGURE A-1

SYMBOLS

DO	Dissolved oxygen sensor
FI	Flow indicator
HCV	Hand control valve
MPC	Metering pump control
pH	pH Sensor
PI	Pressure indicator
SC	Speed control
TI	Temperature indicator
TC	Temperature controller
XM	Cell concentration measurement
↑	Signal to computer
↓	Signal from computer

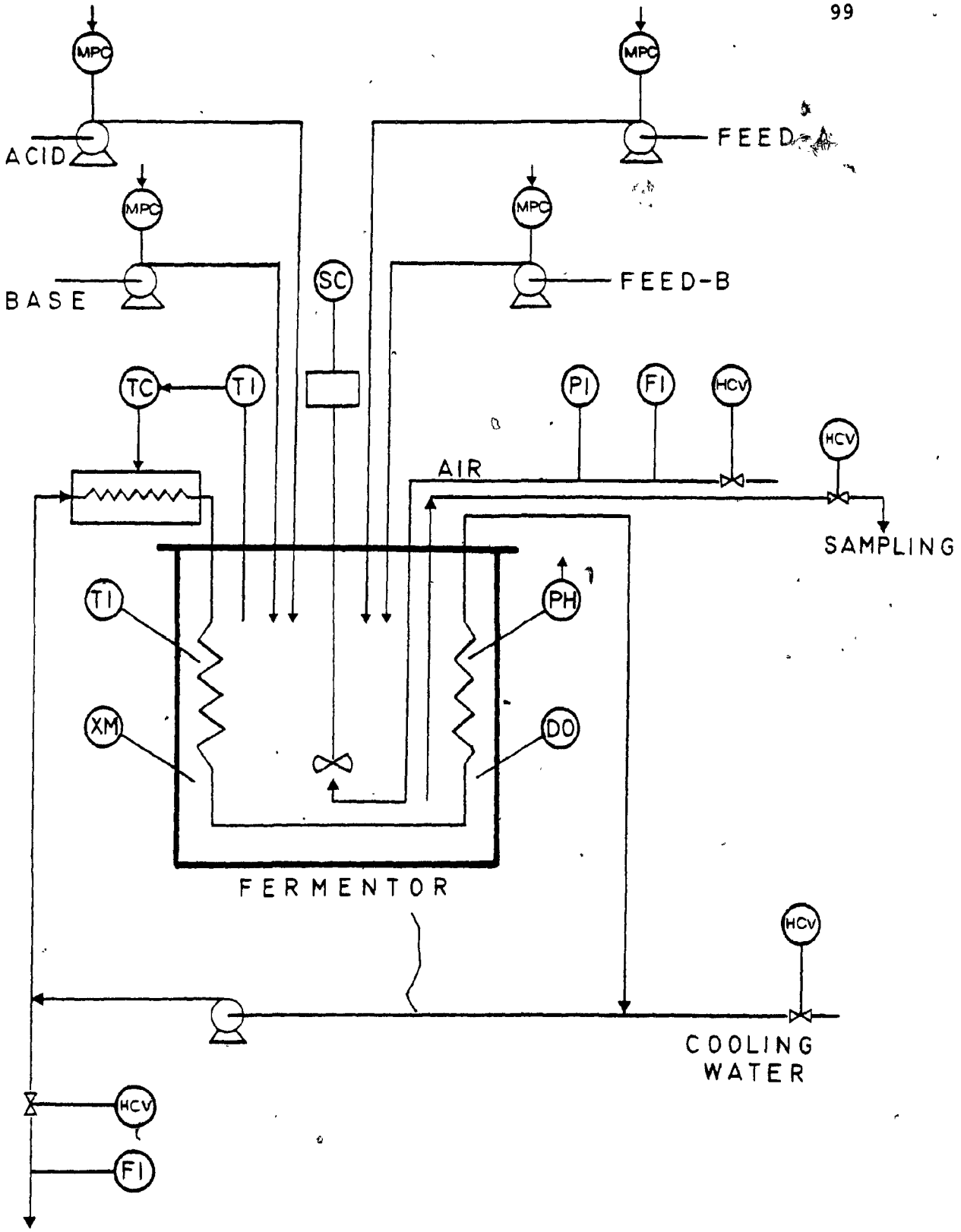
MPC
ACID
MPC
FEED-A
MPC
BASE
SC
MPC
FEED-B
TC
TI
PI
FI
HCV
HCV
AIR
SAMPLING
TI
PH
XM
DO
FERMENTOR
HCV
COOLING
WATER
HCV
FI

FIG A-1

shaft. The air flow was monitored either by a calibrated flow-meter with a range of 0 to 16 l/min for air at 23°C and atmospheric pressure, or by a pressure gauge. A glasswool filter was inserted in the air line to sterilize the entering air.

Effluent gas is passed through a small, water-cooled condenser, to minimize liquid loss and evaporation of the culture medium. Since liquid loss was still high, at air flow about 16 l/min, agitation 500 rpm and liquid volume in the vessel higher than 7 l, the device shown in Fig. (A-2) was connected to the output of the condenser, utilizing a very low speed peristaltic pump, which pumped back the removed droplets to the fermentor.

A.1.2 DISSOLVED OXYGEN ANALYZER

A Dissolved Oxygen Analyzer, model DO-40, manufactured by the New Brunswick Sc. Co., N.J. was used. The model DO-40 incorporates a direct-reading dissolved oxygen indicator to provide a continuous concentration measurement in solution of oxygen partial pressure in percent of oxygen. Probe standardization and zero adjustment is achieved by potentiomentric calibration.

A.1.3. pH METER

Orion's 407A Specific Ion Meter combined with an Ingold combination electrode (Instrumentation Laboratories, Lexington, Mass.) was used to provide a continuous measurement of pH.

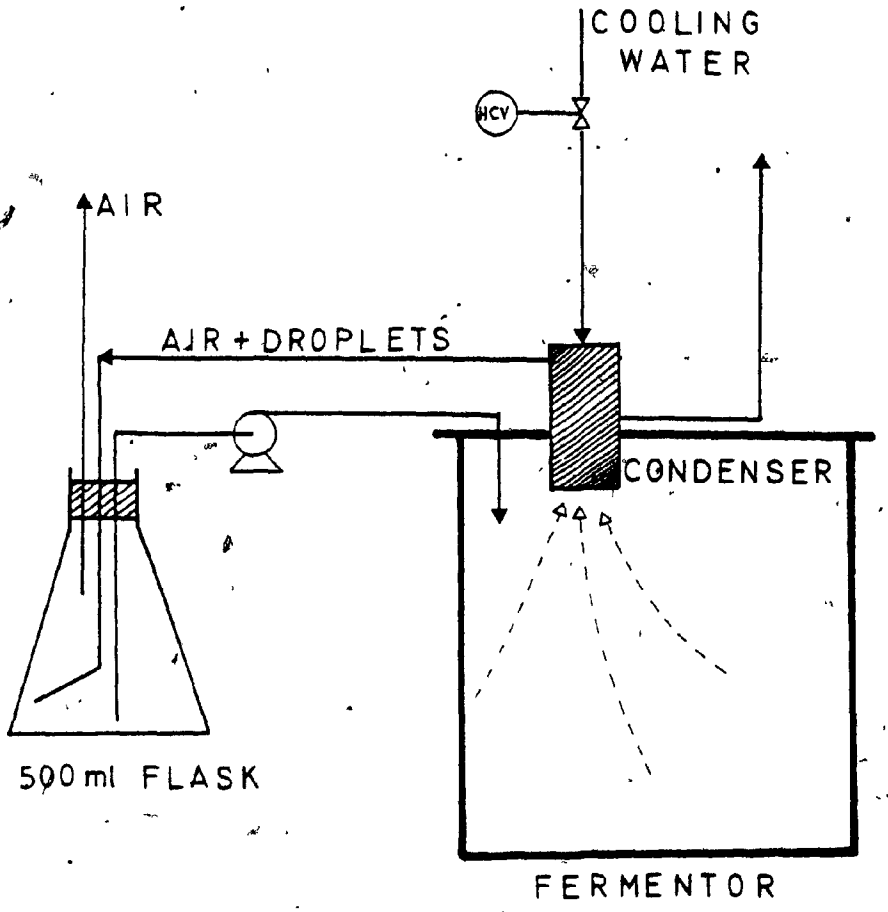

Fig. (A-2):

Schematic diagram of the device used to pump back the removed droplets to the fermentor.

A.1.4 SPECTROPHOTOMETER

A Bausch and Lomb Spectronic 70 spectrophotometer (Rochester, N.Y.) with a 325-925 n m wave length range was used for the glucose concentration measurement.

A.1.5 MINICOMPUTER.

The Interdata 7/16 minicomputer with 16,000 8 bit bytes of core memory, clock, serial communications adapters, teletype and data acquisition interface based on serial communications, was used in this work.

A.2 MATERIAL

A.2.1 ORGANISM

A commercial strain of Saccharomyces cerevisiae (baker's yeast) was used in this study. Compressed yeast from Lallemand Corporation was used for innocculation.

A.2.2 GROWTH CONDITION AND MEDIUM COMPOSITION

The growth medium contained per 20 g glucose: 2.15 g $(NH_2)_2CO$; 1.60 g KH_2PO_4; 1g $(NH_4)_2SO_4$; 1.2 g $MgSO_4.7H_2O$; 0.2 g $CaCl_2$; 10 ml of mineral solution and 10 ml of vitamin solution.

The stock vitamim solution contained, per liter: 5 g adenine; 2 g DL-methionine; 2 g m-inositol; 0.8 g thiamine HCl; 0.4 g Ca-pantothenate; 0.2 g pyridoxine; 0.2 g linstidine and 0.002 g biotin.

The stock mineral solution contained per liter: 0.08 g $MnSO_4.H_2O$; 0.2 g $FeSO_4.7H_2O$; 0.4 g $Na_2MoO_4.H_2O$; 4 mg $ZnSO_4.7H_2O$; 2 mg $CuSO_4.5H_2O$ and 2 mg $CoSO_4$.

The concentrated solution contained 150 g glucose per liter plus the equivalent quantities of the inorganic media except the minerals. The equivalent quantities of minerals and vitamins were added to the initial 5 l volume in the fermentor.

The fermentor with the initial 5 liters broth (water plus minerals) was sterilized by heating with steam at 120°C and 15 psia for 20 minutes. After the fermentor had cooled, filter-sterilized vitamin solution was added under aseptic conditions.

The media in the concentrated feed solutions were sterilized separately and mixed when cool. Sufficient amount of tap water was sterilized in a 4-liter bottle, to be used as the diluting stream.

The rotation speed of the impeller and the temperature of cultivation were kept at 500 rpm and 30°C, respectively. The dissolved oxygen was controlled manually adjusting the air flow, so that D.O. stayed above 50%, where 100% was calibrated at 7.5 mg O_2 per liter. 2F KOH base and 1F H_3PO_4 acid solutions were used by the pH controller to keep pH at the desired level, 5.1 $\pm$ .1 for all runs unless otherwise specified.

A.3 ANALYTICAL TECHNIQUES

A.3.1 CELL CONCENTRATION MEASUREMENT

Samples were taken every 20 minutes during the entire course of fermentation to measure cell concentration. The dry cell weight was measured by filtering the 20 ml sample through a Milipore filter (pore size: 0.65 μm) and drying the cake in a preweighed aluminum dish for 40 minutes at 110°C.

In order to minimize the delay, a first reading was taken after 20 minutes of drying time. This first estimate of cell concentration, which was overestimated from 0 to 3%, was fed back to the computer while the second reading after 40 minutes drying time, was logged as the true cell concentration.

Fifteen samples were taken and analyzed at the end of run # 8-a to obtain an estimate of the precision in cell concentration measurement. Analyzing the results, a standard deviation of 0.14 g/l was calculated at an average cell concentration of 6.30 g/l. Thus, an estimate of the standard error of measurement is 2.2%. It is noted that although the samples were dried for 40 minutes only, no additional error was introduced to the measurement. In Fig. (A-3) the cell concentration of 4 different samples versus drying time is shown. It is seen that after 40 minutes, all the non-chemically bound water is removed.

A.3.2 GLUCOSE CONCENTRATION MEASUREMENT

In several runs additional samples were taken to measure the limiting substrate concentration in the fermentor.

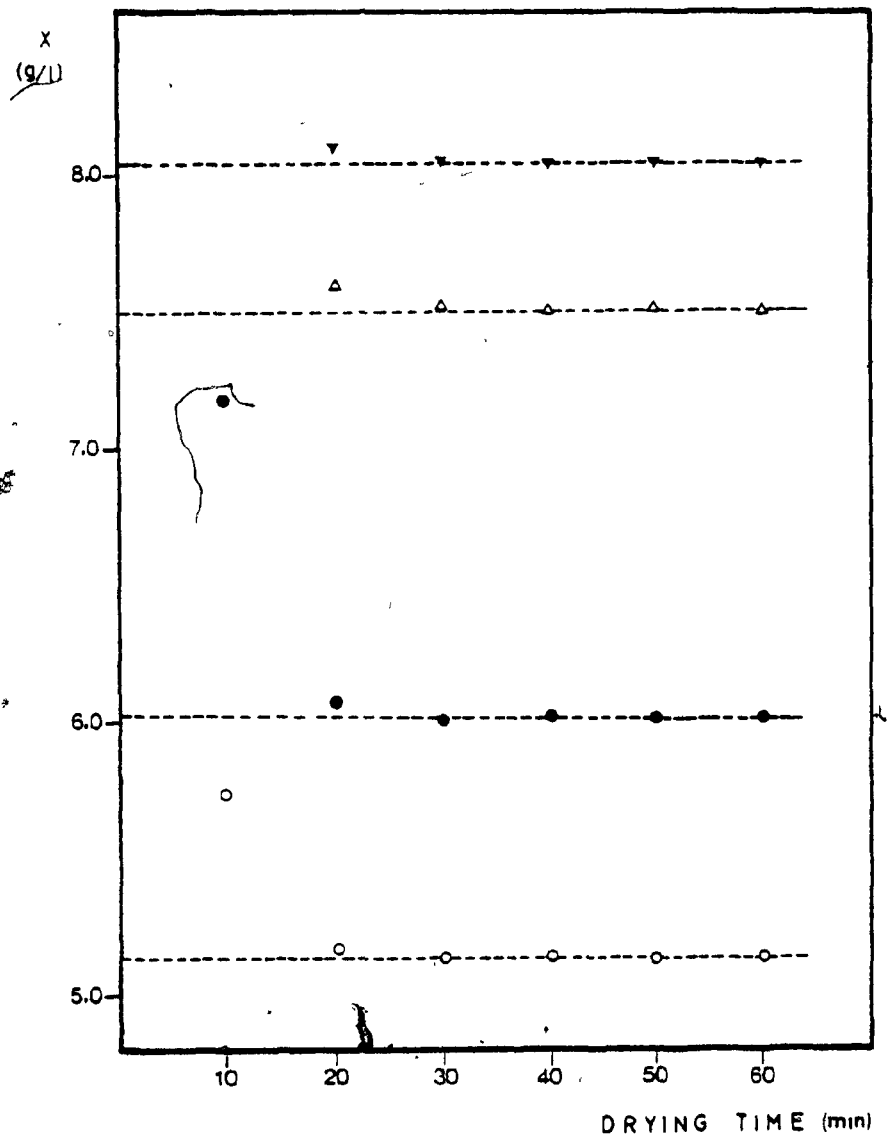

Fig. (A-3): Cell concentration versus drying time for different samples.

An enzymatic analysis was used, utilizing phosphorylation of glucose by hexokinase (HK) and ATP, followed by oxidization by glucose-6-phosphate dehydrogenase (G-6-PDH) with concomitant reduction of NAD^+ to NADH. The total amount of NADH formed, a direct measure of glucose concentration, was measured spectrophotometrically at 340 nm.

The standard error of measurement in the range of glucose concentration measured in this work is 4% [13].

The detailed procedure is as follows:

- Reconstitute reagent: Glucose HK 25-test vial add 80.0 ml distilled water. Swirl gently to dissolve.
- Zero measurement with 0.9% sodium chloride solution (physiological saline).
- Add 20 µl of sample to 3.0 ml 0.9% sodium chloride.
- Read and record sample blank absorbance (A_B) at 340 nm.
- Add 3.0 ml of reconstituted reagent to a cuvette.
- Read and record initial absorbance (A_I) of reagent at 340 nm.
- Add 20 µl of sample to reagent and mix gently.
- Wait 3 minutes, read and record final absorbance (A_F) at 340 nm.
- Calculate glucose concentration from:

$$s(mg/l) = (A_F - A_I - A_B) \times 4{,}370$$

(cuvette with a light path of 1 cm should be used.)

APPENDIX B

LIST OF THE PERFORMED EXPERIMENTS

LIST OF THE PERFORMED RUNS

Run #	Main Characteristic	Operational Conditions
1	Large positive step change in x_D	$x_0 = 5.80$ g/l, $\hat{\sigma} = 0.156$ hr^{-1} $\overline{s1} = 11.07$ g/l, $x_D = 7$ g/l ($t \geq 0$)
2	x_D and $\hat{\sigma}$ were kept constant to check whether the controller drifts off	$x_0 = 5.81$ g/l, $\hat{\sigma} = 0.176$ hr^{-1} $\overline{s1} = 10.69$ g/l, $x_D = 6$ g/l
3	Subsequent step changes in x_D	$x_0 = 5.34$ g/l, $\hat{\sigma} = 0.185$ hr^{-1} $\overline{s1} = \begin{vmatrix} 11.18 \text{ g/l}, \\ 13.03 \text{ g/l}, \\ 14.88 \text{ g/l}, \end{vmatrix}$ $x_D = \begin{vmatrix} 6 \text{ g/l}, & 0 \leq t < 4 \\ 7 \text{ g/l}, & 4 \leq t < 8 \\ 8 \text{ g/l}, & 8 \leq t \end{vmatrix}$
4-b	Large step change in σ	$x_0 = 5.82$ g/l, $x_D = 6$ g/l $\overline{s1} = 10.98$ g/l, $\hat{\sigma} = \begin{vmatrix} 0.185 \text{ hr}^{-1}, & 0 \leq t < 0.66 \\ 0.370 \text{ hr}^{-1}, & 0.66 \leq t \end{vmatrix}$
5	Subsequent step changes in θ	$x_0 = 5.68$ g/l, $\overline{s1} = 10.98$ g/l $x_D = 6$ g/l, $\hat{\sigma} = \begin{vmatrix} 0.190 \text{ hr}^{-1}, & 0 \leq t < 3.33 \\ 0.130 \text{ hr}^{-1}, & 3.33 \leq t < 4.66 \\ 0.190 \text{ hr}^{-1}, & 4.66 \leq t < 5.66 \\ 0.130 \text{ hr}^{-1}, & 5.66 \leq t < 6.66 \\ 0.228 \text{ hr}^{-1}, & 6.66 \leq t \end{vmatrix}$
6	Subsequent step changes in θ	$x_0 = 5.13$ g/l, $\overline{s1} = 10.07$ g/l $x_D = 5.5$ g/l, $\hat{\sigma} = \begin{vmatrix} 0.190 \text{ hr}^{-1}, & 0 \leq t < 2 \\ 0.130 \text{ hr}^{-1}, & 2 \leq t < 3.33 \\ 0.190 \text{ hr}^{-1}, & 3.33 \leq t < 4.66 \\ 0.130 \text{ hr}^{-1}, & 4.66 \leq t < 6 \\ 0.228 \text{ hr}^{-1}, & 6 \leq t \end{vmatrix}$

Run #	Main Characteristic	Operational Conditions
7	Negative step change in x_D	x_0 = 6.80 g/l, $\overline{s1}$ = 10.98 g/l $\hat{\sigma}$ = 0.185 hr^{-1}, x_D = 6 g/l ($t \geq 0$)
8-a	Negative step change in x_D	x_0 = 7.26 g/l, $\overline{s1}$ = 10.98 g/l $\hat{\sigma}$ = 0.185 hr^{-1}, x_D = 6 g/l ($t \geq 0$)
8-b	Step change in pH (disturbance response)	x_0 = 6.02 g/l, $\overline{s1}$ = 10.98 g/l $\hat{\sigma}$ = 0.185 hr^{-1}, x_D = 6 g/l, pH = 5.1 $0 \leq t < .66$ 3.6 $.66 \leq t$
9	Uncontrolled run	x_0 = 5.42 g/l, $\overline{s1}$ = 14.07 g/l D = 0.100 hr^{-1}

APPENDIX C

- tabulation of PROCON loops
- listing of PROCON loops
- typical output
- detail diagram of PROCON loop structure

TABLE C-I: TABULATION OF PROCON LOOPS

Loop #	Task	Label
1	Enter zero.	Zero
2	Pick up computer poll time (in seconds)	Poll-S
3	Convert poll time to minutes	Poll-M
5	Enter pH-filter tau	pH-Tau
6	Enter flowrate of pump-A when ON	K-FA
7	Enter flowrate of pump-B when ON	K-FB
8	Enter flowrate of pump-AC when ON	K-ACID
9	Enter flowrate of pump-BA when ON	K-BASE
10	Multiply by 100 the absolute difference between current x and the one of the previous cycle	SAMP-T
11	Set output = 1 when the output at loop 10 is greater than zero, else set output = 0	V-SAMP
15	Pick up from input channel 7 the pH measurement in mV	pH - mV
16	Convert pH measurement from mV to pH units	pH-CALC
17	Filter the pH measurement	pH FILT
18	Enter the initial volume	V-INIT
19	Calculate the total volume	TOTVOL
20	Enter x to the computer using the set-point command	X-DATA
21	Enter $\overline{s1}$	S0
22	Enter k_c	kc
23	Enter $\hat{\sigma}$	CONSRA
24	Enter s_D	SD
25	Enter x_D	xD
26	Enter s_A	SA

Loop #	Task	Label
27	Calculate s1 from the error: $x_D - x$	S1-CON
28	Intermediate calculation for s1MIN (F_{AMAX})	PROOFA
29	Intermediate calculation for s1MIN (F_{BMAX})	PROOFB
30	Calculate $F_{AMAX} + F_{ACID} + F_{BASE}$	FAM + FN
31	Calculate s1MIN (F_{AMAX}) and take the maximum of s1 and s1MIN (F_{AMAX})	S1MINA
32	Calculate s1MIN (F_{BMAX}) and take the maximum of s1MIN (F_{BMAX}) and the output of loop # 31	S1MINB
33	Calculate s1MAX and take the minimum of SAMAX and the output of loop # 32	S1MAX
34	Calculate $s1 - s_D$	S1-SD
35	Calculate $s_A - s1$	SA-S1
38	Calculate the flowrate of pump A	FEED-A
39	Calculate the flowrate of pump B	FEED-B
40	Calculate the flowrate of pump A for uncontrolled fed-batch	FA*
41	Calculate the flowrate of pump B for uncontrolled fed-batch	FB*
50	Manipulate the error in pH (P+I controller)	pH-CON
51	Calculate the flowrate of ACID	F-ACID
52	Calculate the flowrate of BASE	F-BASE
53	Calculate the total ml of acid used	V-ACID
54	Calculate the total ml of base used	V-BASE
70,71,72	Flow controller for pump A	
73,74,75	Flow controller for pump B	
76,77,78	Flow controller for pump AC	

LOOP #	Task	Label
79,80,81	Flow controller for pump BA	
82	Calculate the total grams of sugar fed	GR-SUG
83	Keep x of the previous cycle	x-CONC
90	Log periodically loops, 16,17,53,54,38,39, 82,19,83	
91	Log on demand loops 21,22,23,24,25,26	
92	Log periodically (every poll cycle) loops 15,16,17 (used for pH calibration curve)	
99	If set point is set equal to zero reset all accumulators	SWITCH

LISTING OF PROCON LOOPS

```
*
READY :LL
    1    2    3    5    6    7    8    9   10
   13   15   16   17   18   19   20   21   22
   23   24   25   26   27   28   29   30   31
   32   33   34   35   38   39   40   41   50
   51   52   53   74   70   71   72   73   74
   75   76   77   78   79   80   81   82   83
   90   91   92   99
*
READY :LI1
METHOD          5
M001=+    0.000
LIM CC          0
FORMAT         10          2
LABEL      ZERO
*
READY :LI2
METHOD          6
FROM            2       5198          0
LIM CC          0
FORMAT         10          2
LABEL      POLL-S
*
READY :LI3
METHOD          5
M003=+M002/  60.000
LIM CC          0
FORMAT         10          5
LABEL      POLL/M
*
READY :LI5
METHOD          5
M005=+    1.000
LIM CC          0
FORMAT         10          2
LABEL      PH-TAU
*
READY :LI6
METHOD          5
M006=+    3.932
LKM CC          0
FORMAT         10          3
LABEL      K-FA
*
```

```
*
READY :LI7
METHOD          5
M007=+  24.960
LIM CC          0
FORMAT         10          3
LABEL      K-FB
*
READY :LI8
METHOD          5
M008=+   2.535
LIM CC          0
FORMAT         10          3
LABEL      K-ACID
*
READY :LI9
METHOD          5
M009=+   2.586
LIM CC          0
FORMAT         10          3
LABEL      K-BASE
*
READY :LI10
METHOD          5
M010=+5020-M0837 100.000
LIM CC          0
FORMAT         10          4
LABEL      SAMP-T
*
READY :LI11
METHOD        1.0
STATUS          1          1          0
CTL RF          5          0
LOOPS           1         10
BAND        0.001
LIM CC          0
FORMAT         10          0
LABEL      V-SAMP
*
```

```
*
READY :LI15
METHOD          6
FROM           15          7          3
LIM CC          0
FORMAT         10          2
LABEL      PH-MV
*
READY :LI16
METHOD          5
M016=+M015/ 180.899+   7.419
LIM CC          0
FORMAT         10          2
LABEL      PH-CAL
*
READY :LI17
METHOD          5
M017=+M016-M017*M003/M005+M017
LIM CC          0
FORMAT         10          2
LABEL      PHFILT
*
READY :LI18
METHOD          5
M018=+   1.000-S099*5000.0
LIM CC          0
FORMAT         10          2
LABEL      V-INIT
*
READY :LI19
METHOD          5
M019=-M011*  25.000/M003+M072+M075+M078+M081*M003+M019*S099+M018
LIM CC          0
FORMAT         10          2
LABEL      TOTVOL
*
READY :LI20
METHOD          1
STATUS          1          0          0
CTL RF         70
LOOPS           1
GAINS       1.000
LIM CC          0
FORMAT         10          2
LABEL      X-DATA
*
```

```
*
READY :LI21
METHOD          5
M021=+   14.868
LIM CC          0
FORMAT         10          3
LABEL      SO
*
READY :LI22
METHOD          5
M022=+   25.000
LIM CC          0
FORMAT         10          2
LABEL      KC
*
READY :LI23
METHOD          5
M023=+    0.200
LIM CC          0
FORMAT         10          3
LABEL      CONSRA
*
READY :LI24
METHOD          5
M024=+    0.068
LIM CC          0
FORMAT         10          3
LABEL      SD
*
READY :LI25
METHOD          5
M025=+    7.000
LIM CC          0
FORMAT         10          2
LABEL      XD
*
READY :LI26
METHOD          5
M026=+  150.000
LIM CC          0
FORMAT         10          2
LABEL      SA
*
```

```
*
READY :LI27
METHOD          5
M027=+M025-S020*M022+M021
LIM CC          0
FORMAT         10          2
LABEL      SI-CON
*
READY :LI28
METHOD          5
M028=+M026*M006/M023/S020/M019*  60.000-    1.000
LIM CC          0
FORMAT         10          5
LABEL      PRODFA
*
READY :LI29
METHOD          5
M029=+M007*M026/M023/S020/M019*  60.000+    1.000
LIM CC          0
FORMAT         10          5
LABEL      PRODFB
*
READY :LI30
METHOD          5
M030=+M006+M051+M052
LIM CC          0
FORMAT         10          3
LABEL      FAM+FN
*
READY :LI31
METHOD          5
M031=+M024/M028+M024>M027
LIM CC          0
FORMAT         10          3
LABEL      SIMINA
*
READY :LI32
METHOD          5
M032=+M029-    1.000*M024+M026/M029>M031
LIM CC          0
FORMAT         10          3
LABEL      SIMINB
*
```

```
*
READY :LI33
METHOD          5
M033=+M026*M006/M030<M032
LIM CC          0
FORMAT         10          2
LABEL      S1MAX
*
READY :LI34
METHOD          5
M034=+M033-M024
LIM CC          0
FORMAT         10          2
LABEL      S1-SD
*
READY :LI35
METHOD          5
M035=+M026-M033
LIM CC          0
FORMAT         10          2
LABEL      SA-S1
*
READY :LI38
METHOD          5
M038=+M023*S020*M019/M026*M033/M034/  60.000
LIM CC          0
FORMAT         10          3
LABEL      FEED-A
*
READY :LI39
METHOD          5
M039=+M035/M033*M038
LIM CC          0
FORMAT         10          3
LABEL      FEED-B
*
READY :LI40
METHOD          5
M040=+M021/M026*M019/ 600.000
LIM CC          0
FORMAT         10          3
LABEL      FA*
*
```

```
*
READY :LI41
METHOD            5
M041=+M026-M021/M026*M019/ 600.000
LIM CC            0
FORMAT           10              3
LABEL       FB*
*
READY :LI50
METHOD            2
STATUS            1              0              3
CTL RF           79
LOOPS            16
GAINS         5.000    0.200000
LIM CC            0
FORMAT           10              2
LABEL       PH-CON
*
READY :LI51
METHOD            5
M051=-M050>     0.000<M008
LIM CC            0
FORMAT           10              3
LABEL       F-ACID
*
READY :LI52
METHOD            5
M052=+M050>     0.000<M009
LIM CC            0
FORMAT           10              3
LABEL       F-BASE
*
READY :LI53
METHOD            5
M053=+M078*M003+M053*S099
LIM CC            0
FORMAT           10              2
LABEL       V-ACID
*
```

```
*
READY :LI54
METHOD          5
M054=+L081*M003+M054*S099
LIM CC          0
FORMAT         10            2
LABEL      V-BASE
*
READY :LI70
METHOD          3
STATUS          1             1          5
CTL RF         71
LOOPS          72            40
GAINS       1.000   5.000000
LIM RG     50.000
LIM CC          0
FORMAT         10            3
LABEL      FA-CON
*
READY :LI71
METHOD         10
STATUS          1             1          0
CTL RF          0             0
LOOPS           1            70
BAND       -0.010
LIM CC          0
FORMAT         10            0
LABEL      PUMP-A
*
READY :LI72
METHOD          5
M072=+    1.000-M071*M006
LIM CC          0
FORMAT         10            3
LABEL      FBSIG1
*
READY :LI73
METHOD          3
STATUS          1             1          5
CTL RF         74
LOOPS          75            41
GAINS       1.000   5.000000
LIM RG    100.000
LIM CC          0
FORMAT         10            3
LABEL      FB-CON
*
```

```
*
READY :LI74
METHOD          10
STATUS           1            1          0
CTL RF           1            0
LOOPS            1           73
BAND        -0.010
LIM CC           0
FORMAT          10            0
LABEL       PUMP-B
*
READY :LI75
METHOD           5
M075=+    1.000-M074*M007
LIM CC           0
FORMAT          10            3
LABEL       FBSIG2
*
READY :LI76
METHOD           2
STATUS           1            1          3
CTL RF          77
LOOPS           78           51
GAINS        1.000    5.000000
LIM CC           0
FORMAT          10            2
LABEL       FACCON
*
READY :LI77
METHOD          10
STATUS           1            1          0
CTL RF           8            0
LOOPS            1           76
BAND         0.010
LIM CC           0
FORMAT          10            0
LABEL       PUMPAC
*
```

```
*
READY :LI83
METHOD          5
M083=+S020
LIM CC          0
FORMAT         10          2
LABEL      X-CONC
*
READY :LI90
METHOD          7
LFMT            0
TIMES     300.000       0.000
LOOPS     16    17    53    54    40    41    82    19    83
*
READY :LI91
METHOD          8
LFMT            0
LOOPS     21    22    23    24    25    26
*
READY :LI92
METHOD          7
LFMT            2
TIMES       6.000       0.000
LOOPS     15    16    17
*
READY :LI99
METHOD          1
STATUS          1          0          0
CTL RF         77
LOOPS           1
GAINS       1.000
LIM CC          0
FORMAT         10          2
LABEL      SWITCH
```

TYPICAL OUTPUT

```
TIME  014:00:00:45
M021     10.977   SO
M022      25.00   KC
M023      0.185   CONSRA
M024      0.068   SD
M025       6.00   XD
M026     150.00   SA
```

```
READY :SE20
TIME  014:01:16:56
S020        6.94   X-DATA:7.045

S020        7.04   X-DATA:EN
014:01:17:08 ENTERED
*
READY :FI.
#

TIME  014:01:20:00
M016        5.13   PH-CAL
M017        5.03   PHFILT
M053        2.19   V-ACID
M054        5.13   V-BASE
M038       1.021   FEED-A
M039      24.960   FEED-B
M082      10.870   GR-SUF
M019     6964.52   TOTVOL
M083        7.04   X-CONC
TIME  014:01:25:00
M016        5.02   PH-CAL
M017        5.04   PHFILT
M053        2.19   V-ACID
M054        6.45   V-BASE
M038       1.040   FEED-A
M039      24.960   FEED-B
M082      11.737   GR-SUS
M019     7095.61   TOTVOL
M083        7.04   X-CONC
```

```
*
READY :SE50
TKME  014:00:40:05
S050      5.100  PH-CON:3.60
S050      3.600  PH-CON:EN
014:00:40:21 ENTERED
*
READY :FI
#
```

```
READY :SE20
TIME  014:02:54:16
S020      5.61  X-DATA:5.665
S020      5.66  X-DATA:EN
014:02:54:30 ENTERED
*
READY :FI
#
TIME  014:02:55:13
M016      3.62  PH-CAL
M017      3.61  PHFILT
M053     13.15  V-ACID
M054      9.62  V-BASE
M038     0.758  FEED-A
M039     5.119  FEED-B
M082    18.755  GR-SUG
M019   6485.14  TOTVNL
M083      5.66  X-CONC
```

DETAILED LOOP STRUCTURE

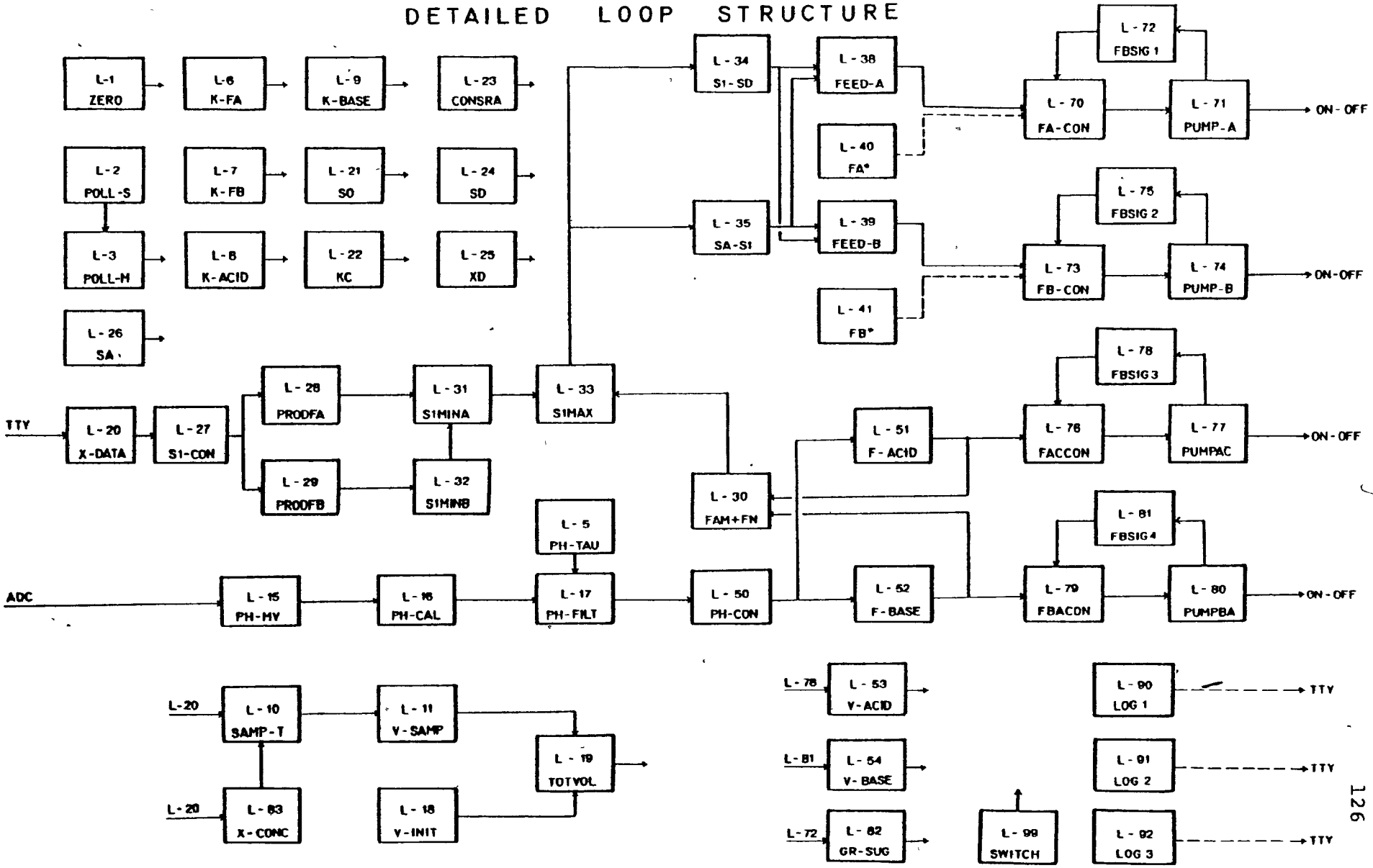

APPENDIX D

LISTING OF SIMULATION PROGRAMS

```
*GO
list simpr2
*IN PROGRESS
/LOAD VSBASIC
010  REM  NICK K. 15/7/78
020  REM
030  REM                    ****CONTROLLED  FED  BATCH
040  REM                    ****FERMENTATION (ACTUAL FLOWRATES
050  REM
060  DIM  W(10)
070  REM  INITIAL  STATE  AND  X-OLD
080  READ  X,S,V,T,X0
090  DATA  7.26,.080,5,0,7.25
100  REM  KINETIC  DATA
110  READ  K1,K2,Y1,M0
120  DATA  .30,.15,.57,0
130  REM  CONTROLLER KC,S0,SIGMA,XD,SD,FAMAX,FWMAX,SA
140  READ  G1,S0,G2,X9,S9,F8,F9,S8
150  DATA  25,10.98,.185,6,.068,.5,1.4976,150
160  REM  TIME INTERVAL-PRINT IN.-SAMPLING IN.- DELAY TIME-TEND
170  READ  T0,T3,T5,T6,T9
180  DATA  .0005,.33333,.33333,.33333,7
190  T2=T
200  T4=T
210  T8=T
220  REM  CALCULATE  DELAY  ARRAY  LENGTH
230  M1=INT(T6/T5/.999)+1
240  REM  INITIALIZE  DELAY  ARRAY  AND  POINTERS
250  FOR  I=1  TO  M1
260  W(I)=X
270  NEXT  I
280  W(1)=X0
290  N1=1
300  L1=M1
310  IF  T>=T2  THEN  GOSUB  680
320  IF  T>=T4  THEN  GOTO  370
330  IF  T>T9  THEN  GOTO  790
340  GOSUB  570
350  GOTO  310
360  REM                    ***CONTROLLER***
370  W(L1)=X
380  Z=W(N1)
390  S1=G1*(X9-Z)+S0
400  V=V-.025
410  IF  S1>S8  THEN  S1=S8
420  S5=S9*(1+1/(S8*F8/G2/Z/V-1))
430  IF  S1<S5  THEN  S1=S5
440  S6=S8-(S8-S9)*F9*S8/(G2*Z*V+F9*S8)
450  IF  S1<S6  THEN  S1=S6
```

```
460  F1=G2*Z*V*S1/S8/(S1-S9)
470  F2=F1*(S8-S1)/S1
480  F=F1+F2
490  REM  UPDATE  POINTERS
500  N1=N1+1
510  IF  N1.M1  THEN  N1=1
520  L1=L1+1
530  IF  L1.M1  THEN  L1=1
540  T4=T4+T5
550  GOTO  330
560  REM                    ****PROCESS****
570  M=K1*S/(K2+S)
580  Y=1/(1/Y1+M0/M)
590  D1=(M-F/V)*X
600  D2=F*(S1-S)/V-M*X/Y
610  D=F/V
620  X=X+D1*T0
630  S=S+D2*T0
640  V=V+F*T0
650  T=T+T0
660  RETURN
670  REM                    ****OUTPUT****
680  IF  T:T8  THEN  750
690  PRINT  USING  700,G2,X9,S9,S0,Y1
700:    SIGMA=.###   XD=##.##   SD=.###   S0=##.##   Y=.##
710  PRINT  USING  720, G1,T5,T6
720:    KC=###.#   T-SAMPL=.###(HOURS)    DELAY=.###(HOURS)
730  PRINT  USING  740
740:TIME    X       S     D    M    Y    F1    F2    S1     V
750  PRINT  USING  760 , T,X,S,D,M,Y,F1,F2,S1,V
760:##.## ##.### ##.### .### .### .### #,### #.### ###.## ##.## #.##
770  T2=T2+T3
780  RETURN
790  STOP
800  END
*END

*GO
```

```
list  errcon

*IN PROGRESS
/LOAD  WATS
C                       THIS  PROGRAM  CALCULATES  THE
C                       AUTOCORELLATIONS  AND  PARTIAL
C                       AUTOCORELLATIONS  OF  THE
C                       ERRORS . THE  ERROR(I)  IS
C                       CALCULATED  FROM  THE  OUTPUT
C                       OF  THE  S1-CONTROLLER
C
C
      DIMENSION  S1(100),FA(100),FB(100),ERROR(100)
      DATA  NOB/24/,NDIFF/1/,NL/12/
      DATA  GAIN/25./,S1OSS/12./
C                       READ  THE  DATA
C
      DO  100  I=1,NOB
      READ(5,90) FA(I),FB(I)
   90 FORMAT(10X,2F10.3)
  100 CONTINUE
C                       CALCULATE  GLUCOSE  CONC.  IN  THE  FEED
C
      DO  200  I=1,NOB
      S1(I)=150.*FA(I)/(FA(1)+FB(I))
  200 CONTINUE
C                       CALCULATE  THE  ERROR
C
      DO  300  I=1,NOB
      ERROR(I)=(S1(I)-S1OSS)/GAIN
  300 CONTINUE
C
C
      CALL  IDENT(ERROR,NOB,NL,NDIFF)
      STOP
      END
/INCLUDE  IDENT
*END

$GO
```

```
 /input
*/inc  errcon
 /inc  datar2
*/endrun

 *IN PROGRESS
 COMPILE =    0.98 SEC
```


AUTO AND PARTIAL CORRELATIONS OF ORIGINAL SERIES

I	AUTO	PARTIAL
1	0.429	0.429
2	0.134	-0.062
3	-0.151	-0.227
4	-0.157	0.002
5	-0.254	-0.193
6	-0.170	-0.027
7	-0.130	-0.057
8	0.122	0.175
9	0.288	0.190
10	0.244	-0.049
11	0.049	-0.083
12	0.015	0.090

APPROX. 95 PERCENT CONF. LIMIT ON CORRELATIONS = 0.408

STANDARD DEVIATION OF SERIES = 0.1461134E 00

CHI-SQUARED STATISTIC = 16.14 BASED ON 12 DEGREES OF FREEDOM

AUTO AND PARTIAL CORRELATIONS OF FIRST DIFFERENCES OF SERIES

I	AUTO	PARTIAL
1	-0.257	-0.257
2	-0.055	-0.130
3	-0.198	-0.269
4	0.113	-0.037
5	-0.145	-0.205
6	0.042	-0.122
7	-0.225	-0.351
8	0.076	-0.289
9	0.182	-0.040
10	0.126	0.005
11	-0.203	-0.210
12	0.094	-0.057

APPROX. 95 PERCENT CONF. LIMIT ON CORRELATIONS = 0.417.

STANDARD DEVIATION OF SERIES = 0.1570390E 00

CHI-SQUARED STATISTIC = 9.75 BASED ON 12 DEGREES OF FREEDOM

```
EXEC =    0.27 SEC
*END
```

APPENDIX E

PLOTS OF EXPERIMENTAL DATA

NOTE ON THE ESTIMATION OF THE OVERALL YIELD

The following graphs were used to determine the overall yield, Y, as already discussed in section 4.3 Previous workers [17], [11] have shown that the effect of maintenance requirements on the overall yield can be represented by:

$$\frac{1}{Y} = \frac{1}{Y_G} + \frac{m}{\mu}$$

In the following graphs it appears that the overall yield remained constant unless inhibition occurred or changes in $\hat{\sigma}$. This can be explained with the fact that the control system substrate concentration and therefore the specific growth rate, was kept constant and assuming constant Y_G and m for a given set of culture conditions, the overall yield is expected to have remained constant.

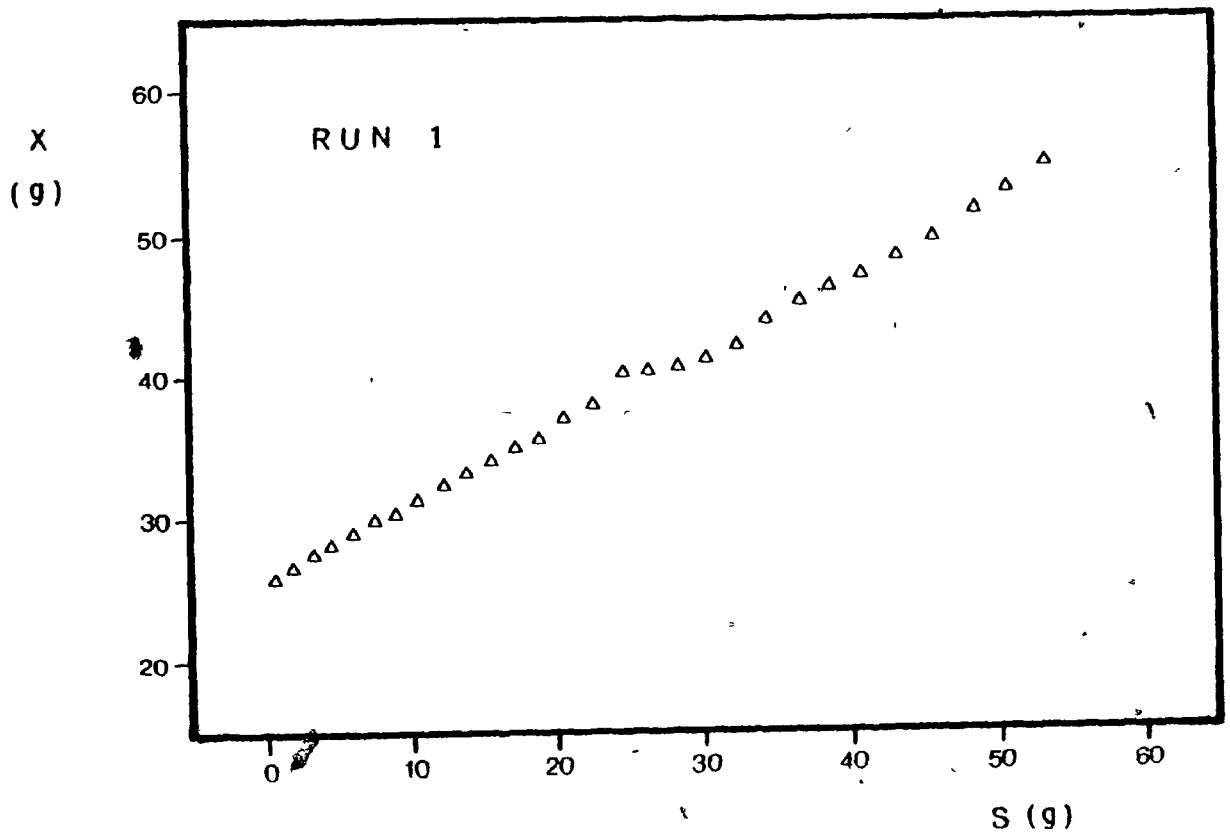

Fig. (E-1): Run # 1, total biomass versus total glucose fed.

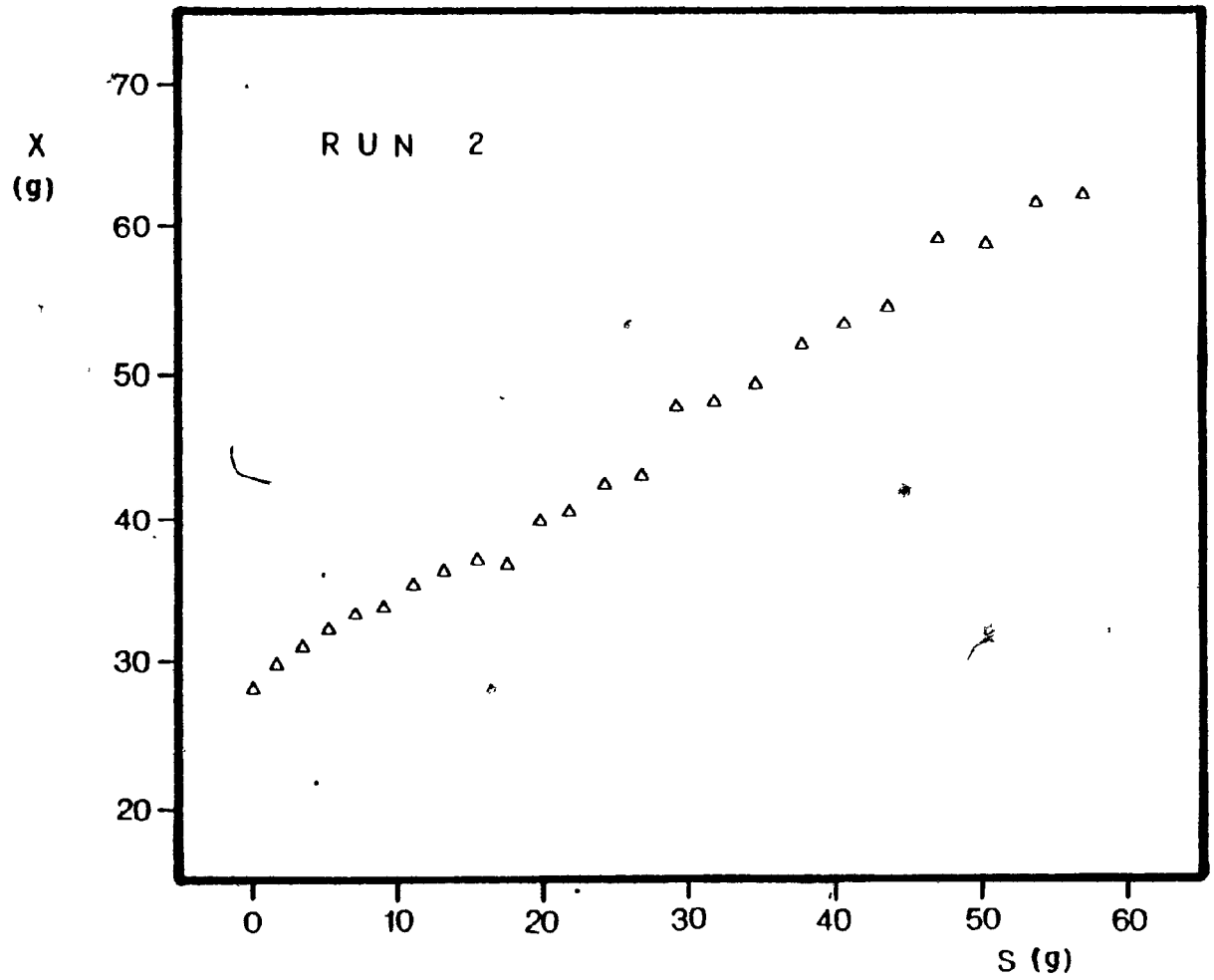

Fig. (E-2): Run # 2, total biomass versus total glucose fed.

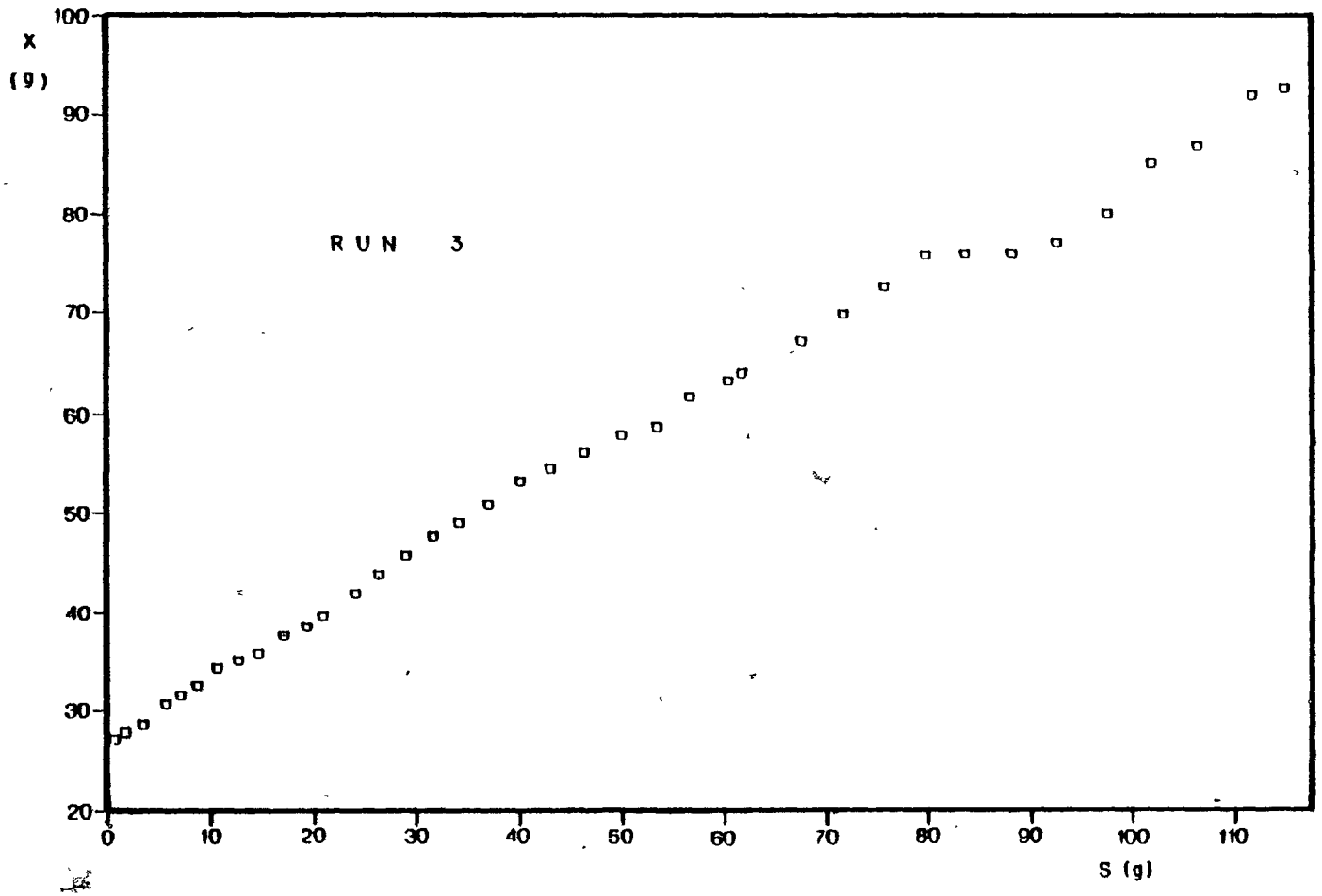

Fig. (E-3): Run # 3, total biomass versus total glucose fed.

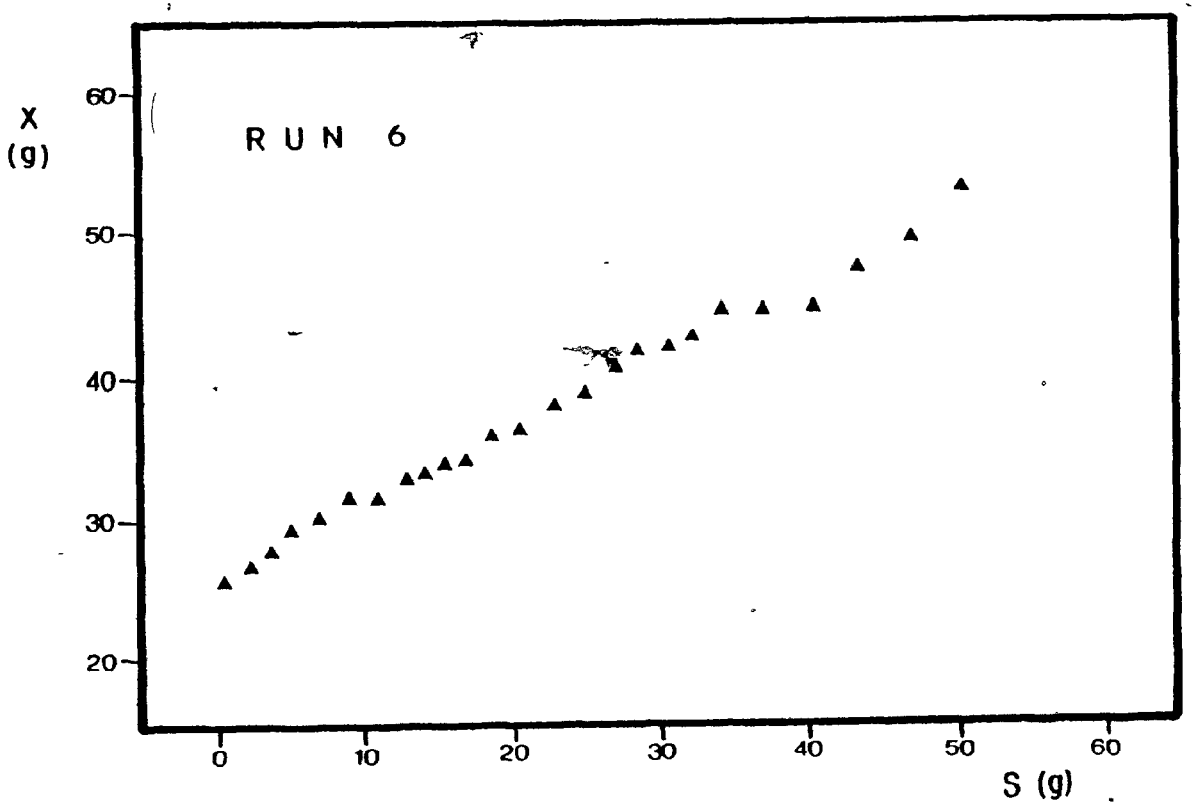

Fig. (E-4): Run # 6, total biomass versus total glucose fed.

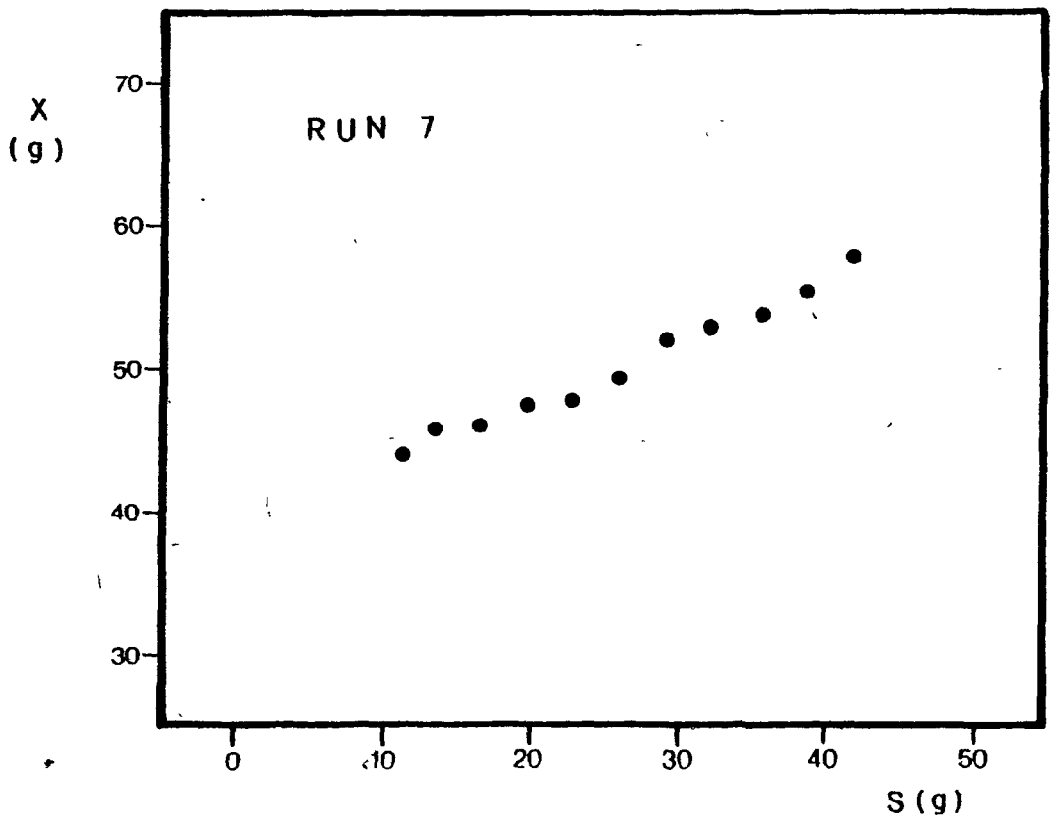

Fig. (E-5): Run # 7, total biomass versus total glucose fed.

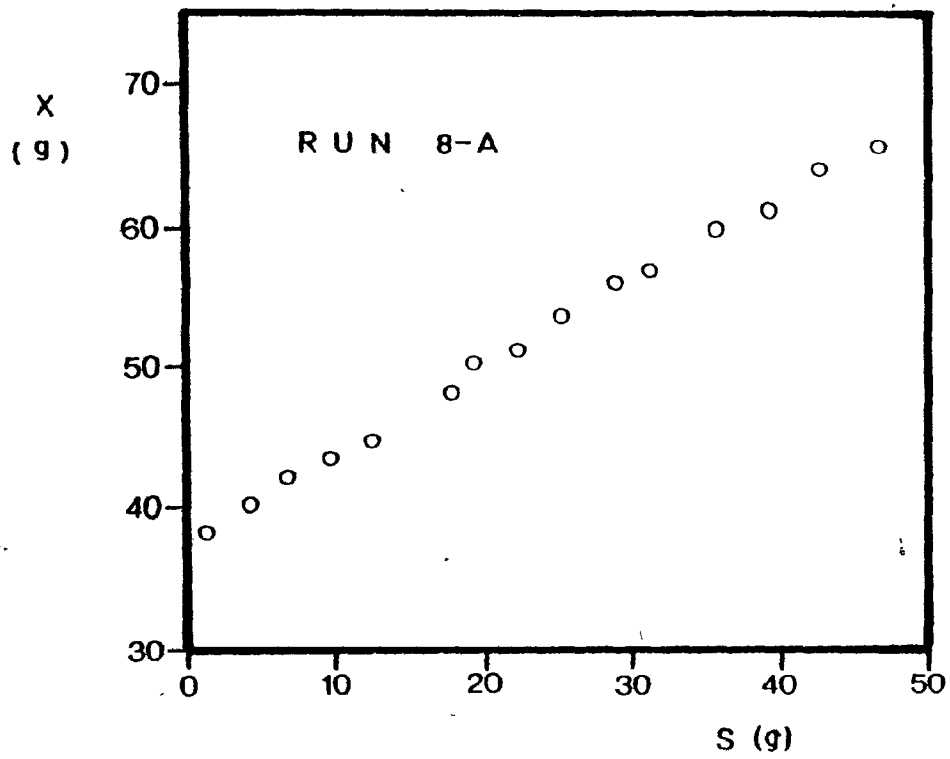

Fig. (E-6): Run # 8-a, total biomass versus total glucose fed.

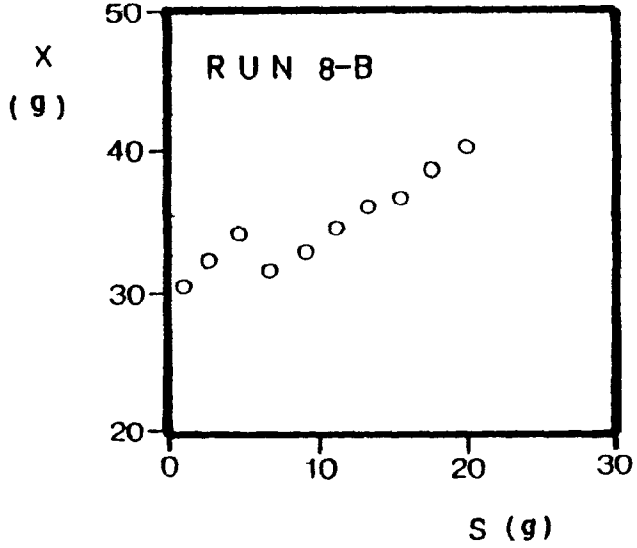

Fig. (E-7): Run # 8-b, total biomass versus total glucose fed.

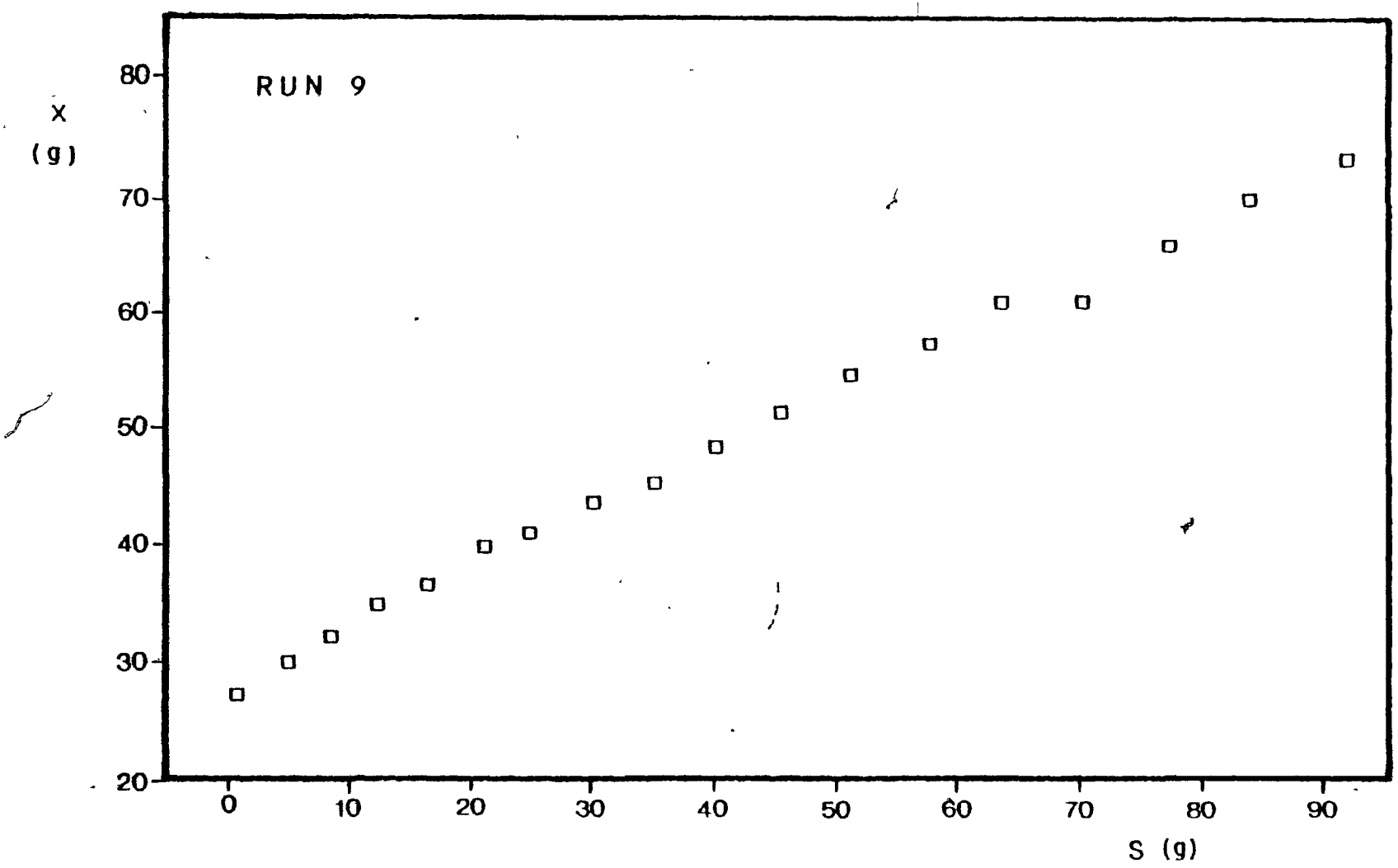

Fig. (E-8): Run # 9, total biomass versus total glucose fed.

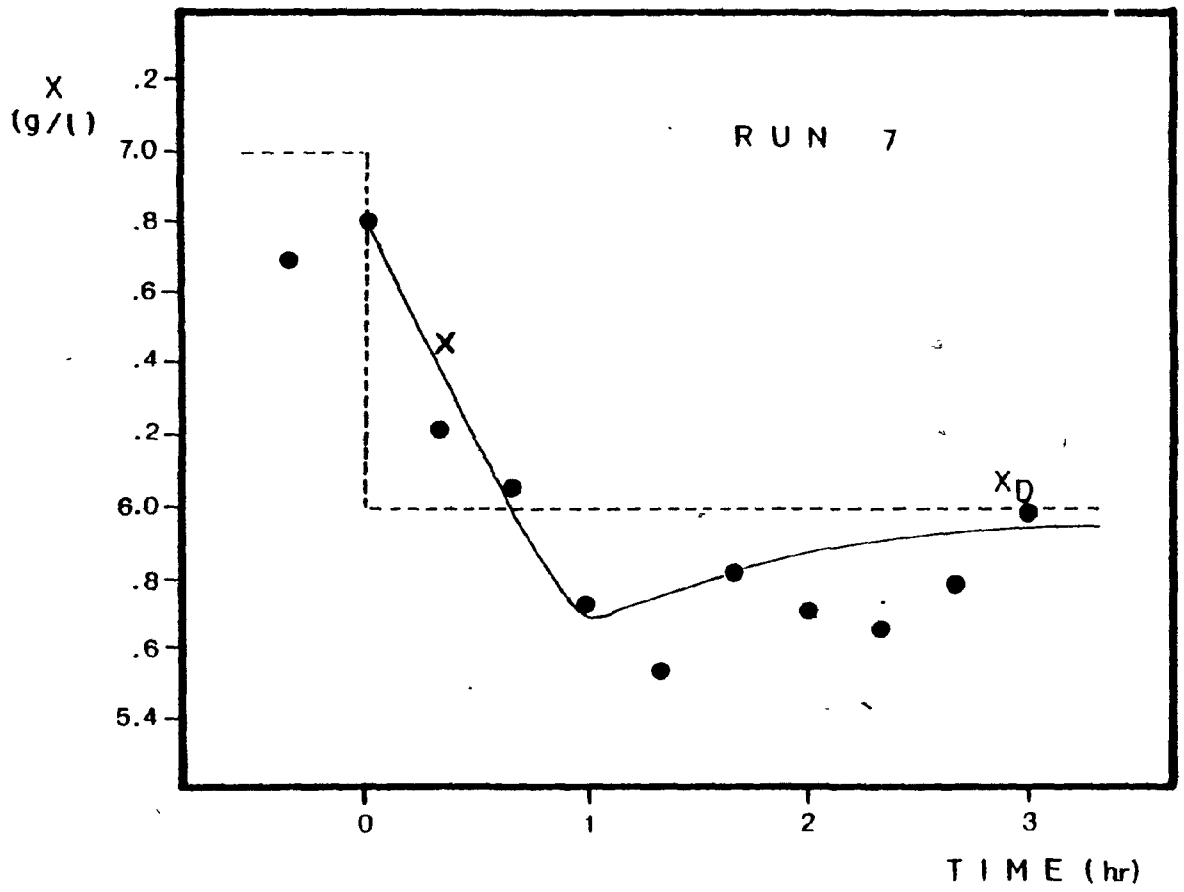

Fig. (E-9): Run # 7, x versus time (—— simulation, ● x-data).

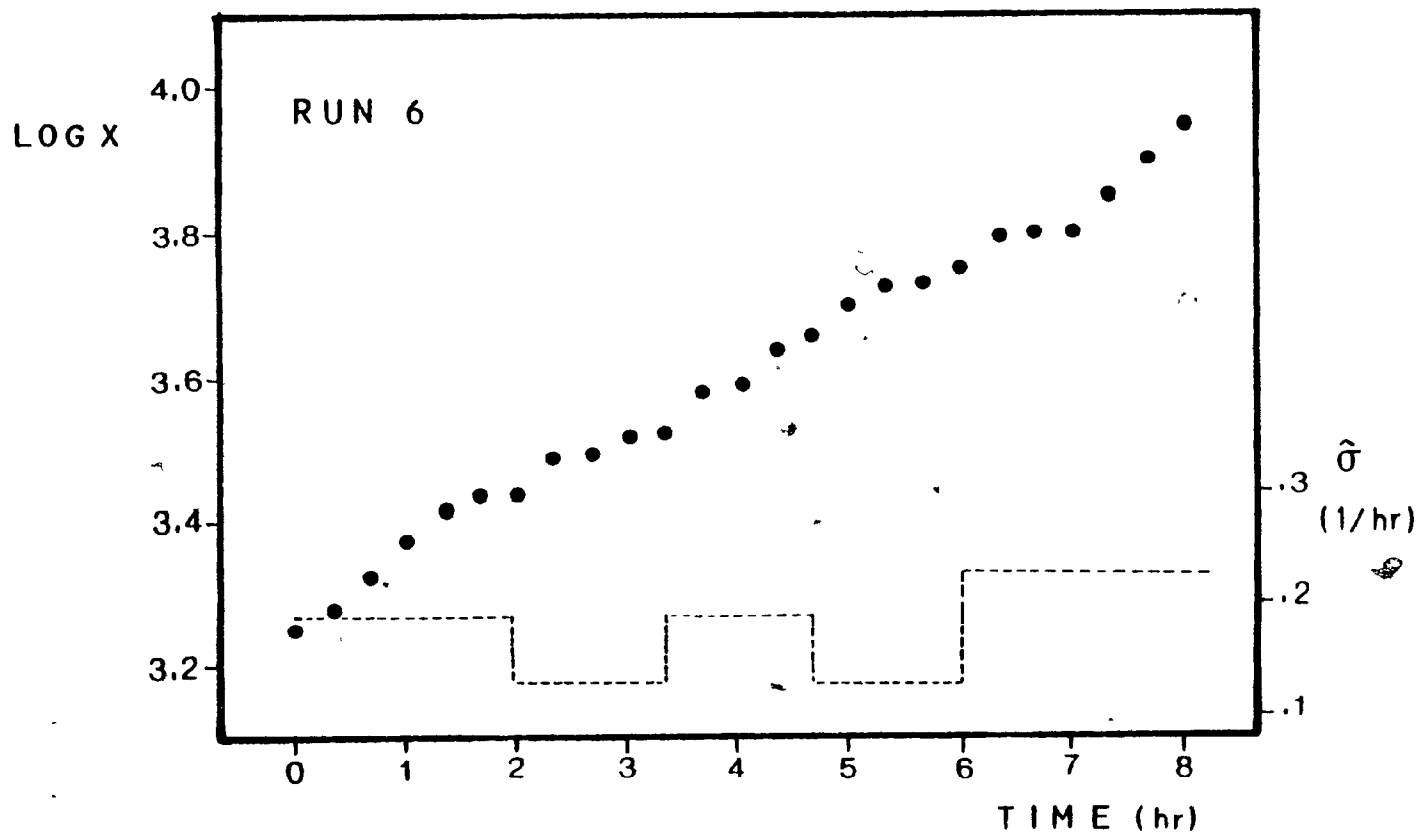

Fig. (E-10): Run # 6, ln X versus time.